

การพัฒนาวิธีการตรวจวัดซัลโฟนาไมด์โดยใช้คอลัมน์มอดอลิตร์ร่วมกับการตรวจวัดแบบแอมเพอโรเมตรี

นางสาว หฤทัย แสงจรัสวิชัย

ศูนย์วิทยทรัพยากร  
จุฬาลงกรณ์มหาวิทยาลัย

วิทยานิพนธ์นี้เป็นส่วนหนึ่งของการศึกษาตามหลักสูตรปริญญาวิทยาศาสตรมหาบัณฑิต

สาขาวิชาเคมี ภาควิชาเคมี

คณะวิทยาศาสตร์ จุฬาลงกรณ์มหาวิทยาลัย

ปีการศึกษา 2551

ลิขสิทธิ์ของจุฬาลงกรณ์มหาวิทยาลัย

METHOD DEVELOPMENT FOR THE DETERMINATION OF SULFONAMIDES  
USING A MONOLITHIC COLUMN COUPLED WITH AMPEROMETRIC  
DETECTION



Miss Haruthai Sangjarusvichai

ศูนย์วิทยทรัพยากร  
จุฬาลงกรณ์มหาวิทยาลัย

A Thesis Submitted in Partial Fulfillment of the Requirements  
for the Degree of Master of Science Program in Chemistry

Department of Chemistry

Faculty of Science

Chulalongkorn University

Academic Year 2008

Copyright of Chulalongkorn University



หยุดยั้ง แสงจรัลวิชัย : การพัฒนาวิธีการตรวจวัดซัลโฟนาไมด์โดยใช้คอลัมน์มอนอลิต  
 ร่วมกับการตรวจวัดแบบแอมเพอโรเมตรี. (METHOD DEVELOPMENT FOR THE  
 DETERMINATION OF SULFONAMIDES USING A MONOLITHIC COLUMN  
 COUPLED WITH AMPEROMETRIC DETECTION) อ.ที่ปรึกษาวิทยานิพนธ์หลัก :  
 รศ. ดร.อรรวรรณ ชัยลภากุล, 104 หน้า.

งานวิจัยนี้ได้ศึกษาลักษณะทางเคมีไฟฟ้าของสารซัลโฟนาไมด์ที่ขั้วไฟฟ้าเพชรที่โดปด้วย  
 โบรอนโดยใช้การตรวจวัดแบบไซคลิกโวลแทมเมตรี โดยทำการเปรียบเทียบการทดลองที่ใช้  
 ขั้วไฟฟ้ากลาสสิคาร์บอน จากการทดลองพบว่าขั้วไฟฟ้าเพชรที่โดปด้วยโบรอนให้ผลของไซคลิกโวล  
 แทมโมแกรมที่ชัดเจน และมีสัญญาณกระแสสูงกว่าที่ได้รับจากขั้วไฟฟ้ากลาสสิคาร์บอน ดังนั้น  
 ในงานวิจัยนี้จึงใช้ขั้วไฟฟ้าที่โดปด้วยโบรอนในการหาสภาวะที่เหมาะสมสำหรับระบบไฮเพอร์  
 ฟอร์มานซีลิควิดโครมาโทกราฟีร่วมกับการตรวจวัดทางเคมีไฟฟ้า วิธีที่เสนอนี้ทำการพัฒนาโดย  
 ลดระยะเวลาการวิเคราะห์โดยใช้คอลัมน์มอนอลิตร่วมกับการตรวจวัดแบบแอมเพอโรเมตรีสำหรับ  
 ตรวจวัดสารซัลโฟนาไมด์ทั้ง 7 ชนิด (ซัลฟาควินิดีน, ซัลฟาไดเอซอิน, ซัลฟาเมทาซีน, ซัลฟามอนอ  
 เมททอกซีน, ซัลฟาเมททอกซาโซล, ซัลฟาไดเมททอกซีน และ ซัลฟาควินอซาลีน) จาก  
 คุณลักษณะของคอลัมน์มอนอลิตให้การแยกที่รวดเร็ว ความดันด้านกลับต่ำ และมีประสิทธิภาพ  
 ในการแยกสารสูงเมื่อเปรียบเทียบกับแพคคอลัมน์ คอลัมน์มอนอลิต (100 มม. x 4.6 มม.)  
 นำมาใช้ในการแยกสารซัลโฟนาไมด์ซึ่งใช้ระยะเวลาในการวิเคราะห์น้อยกว่า 8 นาที ที่อัตราเร็ว  
 1.5 มิลลิเมตรต่อนาที จากการศึกษาไฮโดรไดนามิกโวลแทมเมตรีทำให้ทราบค่าศักย์ไฟฟ้าที่  
 เหมาะสมสำหรับการตรวจวัดสารซัลโฟนาไมด์ที่ 1.2 โวลต์ เทียบกับซิลเวอร์/ซิลเวอร์คลอไรด์ วิธีนี้  
 นำไปประยุกต์ใช้ในการตรวจวัดสารซัลโฟนาไมด์ในกึ่ง ค่าการคืนกลับของสารซัลโฟนาไมด์ในกึ่ง  
 ที่ระดับความเข้มข้น 1.5, 5, และ 10 ไมโครกรัมต่อกรัม อยู่ในช่วง 81.7 % ถึง 97.5 % ค่า  
 เบี่ยงเบนมาตรฐานสัมพัทธ์อยู่ในช่วง 1.0 % ถึง 4.6% ผลการวิเคราะห์ด้วยวิธีที่พัฒนาขึ้นให้ผล  
 การทดลองสอดคล้องกับเทคนิคไฮเพอร์ฟอร์มานซีลิควิดโครมาโทกราฟีร่วมกับการตรวจวัด  
 แมสสเปกโทรเมตรี ดังนั้นวิธีที่เสนอนี้สามารถใช้หาสารซัลโฟนาไมด์ที่ปนเปื้อนในอาหารได้ และ  
 เป็นวิธีที่รวดเร็ว มีการเลือกจำเพาะ และ ตอบสนองได้ดี

ภาควิชา.....เคมี..... ลายมือชื่อนิสิต..... ทักษิณ แสงจรัลวิชัย.....  
 สาขาวิชา.....เคมี..... ลายมือชื่ออ.ที่ปรึกษาวิทยานิพนธ์หลัก..... อรรวรรณ ชัยลภากุล.....  
 ปีการศึกษา..... 2551.....

## 4972558723 : MAJOR CHEMISTRY

KEYWORDS : SULFONAMIDE/ MONOLITHIC COLUMN/  
AMPEROMETRY/ BORON-DOPED DIAMOND ELECTRODE

HARUTHAI SANGJARUSVICHAI : METHOD DEVELOPMENT FOR  
THE DETERMINATION OF SULFONAMIDES USING A  
MONOLITHIC COLUMN COUPLED WITH AMPEROMETRIC  
DETECTION. ADVISOR: ASSOC. PROF. ORAWON CHAILAPAKUL,  
Ph.D., 104 pp.

Sulfonamides (SAs) were electrochemically investigated at boron-doped diamond (BDD) electrode using cyclic voltammetry. Comparison experiments were carried out using glassy carbon (GC) electrodes. It was found that the BDD electrode provided well-resolved oxidative irreversible cyclic voltammograms and higher current signals when compared to GC electrode. Thus, BDD electrode was used to optimize conditions for the HPLC-EC system. The proposed method was improved by reducing the analysis time using a monolithic column coupled with amperometric detection to determine 7 sulfonamides (sulfaguanidine, sulfadiazine, sulfamethazine, sulfamonomethoxine, sulfamethoxazole, sulfadimethoxine and sulfaquinoxaline). Because of its rapid separation, low back-pressure and high separation efficiency compared to a particle-packed column, a monolithic column (100 mm x 4.6 mm) was used for sulfonamide separation. Chromatographic separation was performed in less than 8 min at flow rate of 1.5 mL min<sup>-1</sup>. The optimal detection potential using hydrodynamic voltammetry was found to be 1.2 V versus Ag/AgCl. The method was applied to determine sulfonamides in shrimp. The recoveries of sulfonamides in spiked shrimp samples at 1.5, 5 and 10 µg g<sup>-1</sup> were in the range of 81.7 % to 97.5 % with a relative standard deviation (R.S.D) between 1.0 % and 4.6 %. This methodology produced results that were highly correlated with HPLC-MS data. Therefore, the proposed method can be used for the rapid, selective and sensitive evaluation of sulfonamides in contaminated food.

Department : Chemistry

Student's Signature: Haruthai Sangjarusvichai

Field of Study : Chemistry

Advisor's Signature: Orawon Chailapakul

Academic Year : 2008

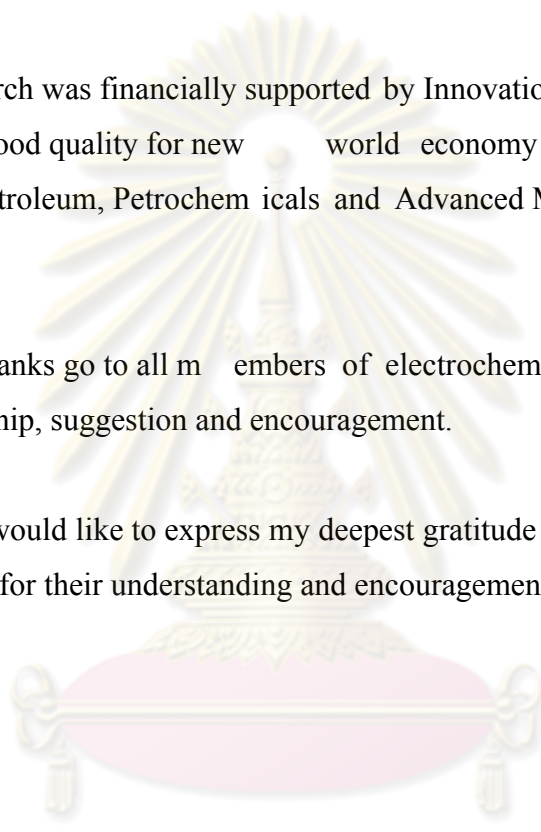
## ACKNOWLEDGEMENTS

First of all, I would like to address my appreciation to my advisor, Associate Professor Dr. Orawon Chailapakul for her suggestions and encouragement throughout the course of this research. My grateful acknowledgement is sincerely made to the thesis committee who gave their valuable comments, advice and corrections of this thesis.

This research was financially supported by Innovation for the improvement of food safety and food quality for new world economy project, and Center of Excellence for Petroleum, Petrochemicals and Advanced Materials, Chulalongkorn University.

Special thanks go to all members of electrochemical Research Group for wonderful friendship, suggestion and encouragement.

Finally, I would like to express my deepest gratitude and sincerest thank to my parent and family for their understanding and encouragement throughout three years.



ศูนย์วิจัยทรัพยากร  
จุฬาลงกรณ์มหาวิทยาลัย

# CONTENTS

	<b>PAGE</b>
<b>ABSTRACT (THAI)</b> .....	iv
<b>ABSTRACT (ENGLISH)</b> .....	v
<b>ACKNOWLEDGEMENTS</b> .....	vi
<b>CONTENTS</b> .....	vii
<b>LIST OF TABLES</b> .....	xi
<b>LIST OF FIGURES</b> .....	xii
<b>LIST OF ABBREVIATIONS</b> .....	xviii
<b>CHAPTER I INTRODUCTION</b> .....	1
1.1 Introduction and literature reviews.....	1
1.2 Research objective.....	4
1.3 Scope of research .....	4
<b>CHAPTER II THEORY</b> .....	5
2.1 High performance liquid chromatography (HPLC).....	5
2.1.1 Types of HPLC.....	6
2.1.1.1 High performance partition chromatography.....	6
2.1.1.2 High performance adsorption chromatography.....	6
2.1.1.3 High performance ion exchange chromatography.....	7
2.1.1.4 High performance size exclusion chromatography.....	7
2.1.2 Instrumentation.....	9
2.1.2.1 Mobile phase reservoir.....	9
2.1.2.2 Pump.....	10
2.1.2.3 Injector.....	11
2.1.2.4 Column.....	12
2.1.2.5 Polymer-based monolithic column.....	13
2.1.2.5.1 Synthesis approaches and characterization.....	13
2.1.2.6 Silica-based monolithic column.....	14

2.1.2.6.1 Formation processes and pore structure control of silica monoliths.....	14
2.1.2.7 Detectors.....	16
2.1.2.8 Flow cell.....	18
2.1.2.8.1 Flow cell for spectroscopy.....	18
2.1.2.8.2 Flow cell for electrochemistry.....	18
2.2 Electroanalytical chemistry .....	20
2.2.1 Mass transport.....	21
2.2.1.1 Diffusion.....	21
2.2.1.2 Migration.....	21
2.2.1.3 Convection.....	21
2.2.2 Voltammetry.....	22
2.2.3 Cyclic voltammetry.....	23
2.2.4 Amperometry.....	26
2.3 Sample preparation.....	27
2.3.1 Solid-phase extraction.....	28
2.3.1.1 Mode of solid-phase extraction.....	29
2.3.1.1.1 Reversed phase.....	29
2.3.1.1.2 Normal phase.....	29
2.3.1.1.3 Ion exchange.....	29
2.3.1.1.4 Mixed mode.....	30
2.3.1.2 Step of solid-phase extraction.....	31
<b>CHAPTER III EXPERIMENTAL.....</b>	<b>34</b>
3.1 Chemical and reagents.....	34
3.2 Instruments and equipment.....	34
3.3 Preparation of chemical solution.....	36
3.3.1 Preparation of solution for cyclic voltammetry.....	36
3.3.1.1 Supporting electrolyte.....	36
3.3.1.2 Stock standard solution.....	36
3.3.1.3 Working standard solution.....	37

3.3.2 Preparation of solution in HPLC-EC.....	37
3.3.2.1 Mobile phase.....	37
3.3.2.2 Stock standard solution.....	38
3.3.3 Preparation of solution for sample preparation.....	38
3.3.3.1 Na <sub>2</sub> EDTA-McIlvaine's buffer solution.....	38
3.4 Procedure.....	39
3.4.1 Cyclic voltammetry.....	39
3.4.1.1 pH dependence.....	39
3.4.1.2 Comparison between BDD and GC electrode.....	39
3.4.1.3 The scan rate dependence.....	40
3.4.1.4 The concentration dependence.....	40
3.4.2 High performance liquid chromatography-electrochemical detection.....	40
3.4.2.1 Flow rate of mobile phase.....	41
3.4.2.2 Optimum potential of amperometry.....	41
3.4.2.3 Linearity.....	42
3.4.2.4 Limit of detection and limit of quantitation.....	42
3.4.3 Sample preparation.....	42
3.4.3.1 pH dependence of Na <sub>2</sub> EDTA-McIlvaine's buffer solution.....	42
3.4.3.2 Comparison of SPE.....	43
3.4.3.3 Sample preparation of shrimp.....	43
3.4.3.4 Accuracy and precision.....	44
3.4.3.5 Comparison of methods between the HPLC-EC and HPLC-EC.....	44
<b>CHAPTER IV RESULTS AND DISCUSSION.....</b>	<b>45</b>
4.1 Cyclic voltammetric investigation.....	45
4.1.1 The electrochemical characteristics.....	45
4.1.2 pH dependence.....	47
4.1.3 Comparison between BDD and GC electrode.....	48

	<b>PAGE</b>
4.1.4 The scan rate dependence study.....	53
4.1.5 The concentration dependence study.....	61
4.2 High performance liquid chromatography-electrochemical detection.....	68
4.2.1 Optimal potential of amperometry.....	68
4.2.2 Optimal Flow rate of mobile phase.....	70
4.2.3 Optimal conditions of HPLC-EC.....	72
4.2.4 Comparison column between particles packed column and monolithic column.....	74
4.2.5 Calibration and linearity.....	76
4.2.6 LOD and LOQ.....	78
4.3 Application to real sample.....	78
4.3.1 pH of extracting solution.....	78
4.3.2 Comparison SPE.....	79
4.3.3 Determination of SAs in shrimp.....	80
4.3.4 Method accuracy and precision.....	82
4.3.5 Comparison of methods between the HPLC-EC and HPLC-MS	85
<b>CHAPTER V CONCLUSIONS.....</b>	<b>88</b>
5.1 Conclusions.....	88
5.2 Suggestion for further work.....	89
<b>REFERENCES.....</b>	<b>90</b>
<b>APPENDICES.....</b>	<b>96</b>
APPENDIX A The Scan Rate Dependence Study at GC Electrode.....	97
APPENDIX B Results for various volume of methanol in elute step of solid- phase extraction.....	102
APPENDIX C Precision and accuracy.....	103
<b>VITAE.....</b>	<b>104</b>

## LIST OF TABLES

<b>TABLE</b>	<b>PAGE</b>
2.1 Performance of HPLC detectors.....	17
3.1 Recipes of phosphate buffer preparation.....	36
3.2 Composition of each concentration for seven SAs in a 3 mL electrochemical cell of cyclic voltammetry.....	37
3.3 The weight ratios of disodium hydrogen phosphate dehydrate and citric acid.....	38
4.1 The electrochemical data obtained from cyclic voltammograms of 0.1 mM seven SAs in phosphate buffer solution pH 3 at the BDD and GC electrode. The scan rate was 50 mV s <sup>-1</sup> .....	53
4.2 The HPLC-EC conditions for the detection of seven SAs.....	72
4.3 Calibration characteristics of SG, SDZ, SMZ, SMM, SMX, SDM and SQ by optimal conditions of HPLC-EC at BDD electrode.....	76
4.4 LOD and LOQ of seven standard SAs at BDD electrode.....	78
4.5 Intra-day precisions and recoveries of spiked level 1.5, 5, and 10.0 µg mL <sup>-1</sup> by proposed method.....	83
4.6 Inter-day precisions and recoveries of spiked level 1.5, 5, and 10.0 µg mL <sup>-1</sup> by propose method.....	84
4.7 Comparisons results of two methods in shrimp sample.....	86
4.8 <i>t</i> -test values of comparison two method.....	87
A1 Linear equation of relation between current response and scan rate at GC electrode of 0.1 mM SAs.....	101
C1 Acceptable RSD values according to AOAC International.....	103
C2 Acceptable recovery percentages as a function of the analyte concentration.....	103

## LIST OF FIGURES

FIGURE		PAGE
1.1	Chemical structures of the studied sulfonamides.....	4
2.1	Types of liquid chromatography.....	5
2.2	Schematic representation of the four modes of liquid chromatography.....	8
2.3	Components of a typical HPLC instrument.....	9
2.4	Schematic diagram of a loop injector in the (A) load and (B) inject positions.....	11
2.5	Reaction of bonded stationary phase.....	12
2.6	(A) Nucleation and growth (diffusion limited) of silica-based monoliths (B) Spinodal decomposition (spontaneous) of silica-based monoliths.....	15
2.7	SEM photographs for the bimodal pore structure of silica-based monolithic column.....	16
2.8	Schematic diagrams of flow cell detectors for HPLC using (A) UV/Vis absorption spectrophotometric cell and (B) Thin-layer amperometric cell.....	19
2.9	Typical excitation signals for voltammetry.....	23
2.10	Waveform for cyclic voltammetry.....	25
2.11	Cyclic voltammograms of (A) 1mM O <sub>2</sub> in acetonitrile with 0.10 M (C <sub>2</sub> H <sub>5</sub> ) <sub>4</sub> N <sup>+</sup> ClO <sub>4</sub> <sup>-</sup> electrolyte and (B) 0.060 mM 2-nitropropane in acetonitrile with 0.10 M (n-C <sub>7</sub> H <sub>15</sub> ) <sub>4</sub> N <sup>+</sup> ClO <sub>4</sub> <sup>-</sup> electrolyte.....	26
2.12	A typical waveform employed in amperometry.....	27
2.13	Anatomy of a cartridge SPE.....	28
2.14	Mixed-mode SPE.....	30
2.15	Structure of solid-phase extraction.....	31
2.16	Steps of solid-phase extraction.....	33
3.1	A thin-layer flow cell.....	41
4.1	Cyclic voltammogram of 0.1 mM seven SAs in phosphate buffer solution (pH 3) at BDD electrode. The scan rate was 50 mV s <sup>-1</sup> .	46

<b>FIGURE</b>	<b>PAGE</b>
4.2 The current of 0.1 mM seven SAs in phosphate buffer solution pH 2.5, 3.0, 4.0, 5.0, 6.0, 7.0, and 7.2, scan rate 50 mV s <sup>-1</sup> using BDD electrode.....	47
4.3 Cyclic voltammogram of phosphate buffer solution (pH 3) at BDD and GC electrode. The scan rate was 50 mV s <sup>-1</sup> .....	48
4.4 Cyclic voltammogram of 0.1 mM SG in phosphate buffer solution pH 3 at (A) BDD and (B) GC electrode. The scan rate was 50 mV s <sup>-1</sup> .....	49
4.5 Cyclic voltammogram of 0.1 mM SDZ in phosphate buffer solution pH 3 at (A) BDD and (B) GC electrode. The scan rate was 50 mV s <sup>-1</sup> .....	50
4.6 Cyclic voltammogram of 0.1 mM SMZ in phosphate buffer solution pH 3 at (A) BDD and (B) GC electrode. The scan rate was 50 mV s <sup>-1</sup> .....	50
4.7 Cyclic voltammogram of 0.1 mM SMM in phosphate buffer solution pH 3 at (A) BDD and (B) GC electrode. The scan rate was 50 mV s <sup>-1</sup> .....	51
4.8 Cyclic voltammogram of 0.1 mM SMX in phosphate buffer solution pH 3 at (A) BDD and (B) GC electrode. The scan rate was 50 mV s <sup>-1</sup> .....	51
4.9 Cyclic voltammogram of 0.1 mM SDM in phosphate buffer solution pH 3 at (A) BDD and (B) GC electrode. The scan rate was 50 mV s <sup>-1</sup> .....	52
4.10 Cyclic voltammogram of 0.1 mM SQ in phosphate buffer solution pH 3 at (A) BDD and (B) GC electrode. The scan rate was 50 mV s <sup>-1</sup> .....	52
4.11 Cyclic voltammogram of 0.1 mM SG in phosphate buffer solution pH 3 at BDD electrode. The scan rate was varied from 25 to 200 mV s <sup>-1</sup> . The relationship of the current signal to the square root of the current signal to the square root of the scan rate is shown in inset.....	54

<b>FIGURE</b>	<b>PAGE</b>	
4.12	Cyclic voltammogram of 0.1 mM SDZ in phosphate buffer solution pH 3 at BDD electrode. The scan rate was varied from 25 to 200 $\text{mV s}^{-1}$ . The relationship of the current signal to the square root of the current signal to the square root of the scan rate is shown in inset.....	55
4.13	Cyclic voltammogram of 0.1 mM SMZ in phosphate buffer solution pH 3 at BDD electrode. The scan rate was varied from 25 to 200 $\text{mV s}^{-1}$ . The relationship of the current signal to the square root of the current signal to the square root of the scan rate is shown in inset.....	56
4.14	Cyclic voltammogram of 0.1 mM SMM in phosphate buffer solution pH 3 at BDD electrode. The scan rate was varied from 25 to 200 $\text{mV s}^{-1}$ . The relationship of the current signal to the square root of the current signal to the square root of the scan rate is shown in inset.....	57
4.15	Cyclic voltammogram of 0.1 mM SMX in phosphate buffer solution pH 3 at BDD electrode. The scan rate was varied from 25 to 200 $\text{mV s}^{-1}$ . The relationship of the current signal to the square root of the current signal to the square root of the scan rate is shown in inset.....	58
4.16	Cyclic voltammogram of 0.1 mM SDM in phosphate buffer solution pH 3 at BDD electrode. The scan rate was varied from 25 to 200 $\text{mV s}^{-1}$ . The relationship of the current signal to the square root of the current signal to the square root of the scan rate is shown in inset.....	59
4.17	Cyclic voltammogram of 0.1 mM SQ in phosphate buffer solution pH 3 at BDD electrode. The scan rate was varied from 25 to 200 $\text{mV s}^{-1}$ . The relationship of the current signal to the square root of the current signal to the square root of the scan rate is shown in inset.....	60

<b>FIGURE</b>	<b>PAGE</b>
4.18 Cyclic voltammogram of SG in phosphate buffer solution pH 3 at BDD electrode. The concentration was increased from 0.02 to 0.10 mM. The relationship of the current signal to concentration is shown the in inset.....	61
4.19 Cyclic voltammogram of SDZ in phosphate buffer solution pH 3 at BDD electrode. The concentration was increased from 0.02 to 0.10 mM. The relationship of the current signal to concentration is shown the in inset.....	62
4.20 Cyclic voltammogram of SMZ in phosphate buffer solution pH 3 at BDD electrode. The concentration was increased from 0.02 to 0.10 mM. The relationship of the current signal to concentration is shown the in inset.....	63
4.21 Cyclic voltammogram of SMM in phosphate buffer solution pH 3 at BDD electrode. The concentration was increased from 0.02 to 0.10 mM. The relationship of the current signal to concentration is shown the in inset.....	64
4.22 Cyclic voltammogram of SMX in phosphate buffer solution pH 3 at BDD electrode. The concentration was increased from 0.02 to 0.10 mM. The relationship of the current signal to concentration is shown the in inset.....	65
4.23 Cyclic voltammogram of SDM in phosphate buffer solution pH 3 at BDD electrode. The concentration was increased from 0.02 to 0.10 mM. The relationship of the current signal to concentration is shown the in inset.....	66
4.24 Cyclic voltammogram of SQ in phosphate buffer solution pH 3 at BDD electrode. The concentration was increased from 0.02 to 0.10 mM. The relationship of the current signal to concentration is shown the in inset.....	67

4.25	Hydrodynamic voltammetric results for a $10 \mu\text{g mL}^{-1}$ mixture of seven SAs at BDD electrode. (A) (■) : SG, (*) : SDZ, (▲) : SMZ, (○) : SMM, (◇) : SMX, (▽) : SDM, (×) : SQ, (●) : background; (B) hydrodynamic voltammogram of signal-to-background ratios. The mobile phase was phosphate buffer (0.05 M, pH 3), acetonitrile and ethanol in the ratio of 80:15:5 (v/v/v). The injection volume was $20 \mu\text{L}$ , and the flow rate was $1.5 \text{ mL min}^{-1}$ .....	69
4.26	HPLC-EC chromatograms of a $10 \mu\text{g mL}^{-1}$ mixture of seven standard SAs at various flow rate of mobile phase.....	71
4.27	HPLC-EC chromatogram of a $10 \mu\text{g mL}^{-1}$ mixture of seven standard SAs separated on a monolithic column at flow rate $1.5 \text{ mL min}^{-1}$ . The detection potential was 1.2 V vs. Ag/AgCl using a BDD electrode.....	73
4.28	HPLC-EC chromatogram of a $10 \mu\text{g mL}^{-1}$ mixture of seven standard SAs separated on (A) a particles packed column and (B) monolithic column at flow rate 1.0, $1.5 \text{ mL min}^{-1}$ , respectively. The detection potential was 1.2 V vs. Ag/AgCl using a BDD electrode.....	75
4.29	Linearity of seven standard SAs by HPLC-EC using BDD electrode.....	77
4.30	Recoveries obtained of a $10 \mu\text{g mL}^{-1}$ standard mixture of seven SAs using C18 and Oasis HLB cartridges.....	80
4.31	HPLC-EC chromatogram of (A) a shrimp sample spiked with $10 \mu\text{g mL}^{-1}$ of standard mixture of seven SAs; (B) a blank shrimp sample separated on a monolithic column (100 mm x 4.6 mm i.d.) at flow rate $1.5 \text{ mL min}^{-1}$ . The detection potential was 1.2 V vs. Ag/AgCl using a BDD electrode.....	81
A1	Cyclic voltammogram of 0.1 mM SG in phosphate buffer solution (pH 3) at the GC electrode. The scan rate was from 25 to $200 \text{ mV s}^{-1}$ .....	97

<b>FIGURE</b>	<b>PAGE</b>
A2	Cyclic voltammogram of 0.1 mM SDZ in phosphate buffer solution (pH 3) at the GC electrode. The scan rate was from 25 to 200 mV s <sup>-1</sup> ..... 98
A3	Cyclic voltammogram of 0.1 mM SMZ in phosphate buffer solution (pH 3) at the GC electrode. The scan rate was from 25 to 200 mV s <sup>-1</sup> ..... 98
A4	Cyclic voltammogram of 0.1 mM SMM in phosphate buffer solution (pH 3) at the GC electrode. The scan rate was from 25 to 200 mV s <sup>-1</sup> ..... 99
A5	Cyclic voltammogram of 0.1 mM SMX in phosphate buffer solution (pH 3) at the GC electrode. The scan rate was from 25 to 200 mV s <sup>-1</sup> ..... 99
A6	Cyclic voltammogram of 0.1 mM SDM in phosphate buffer solution (pH 3) at the GC electrode. The scan rate was from 25 to 200 mV s <sup>-1</sup> ..... 100
A7	Cyclic voltammogram of 0.1 mM SQ in phosphate buffer solution (pH 3) at the GC electrode. The scan rate was from 25 to 200 mV s <sup>-1</sup> ..... 100
B1	Volume of methanol in elute step by using 10 µg mL <sup>-1</sup> seven standard mixture of SA for loading step at Oasis HLB SPE..... 102

## LIST OF ABBREVIATIONS

BDD	boron-doped diamond electrode
°C	degree Celsius
CE	capillary electrophoresis
CV	cyclic voltammetry
$E$	potential
$E^0$	formal reduction potential
$E_{1/2}$	half-wave potential
EC	electrochemical
ELISA	enzyme-linked immunosorbent assay
$E_{pa}$	anodic peak potential
$E_{pc}$	cathodic peak potential
EU	European Union
GC	glassy carbon electrode
HPLC	high performance chromatography
L	liter
LLE	liquid-liquid extraction
M	molar
mL	milliliter
min	minute
MRL	maximum residue limit
MS	mass spectrometry
MSPD	matrix solid-phase dispersion
$n$	number of electron
$i$	current
$I_p$	peak current
$R^2$	correlation coefficient
SA	sulfonamide
S/B	signal to background ratio
SDM	sulfadimethoxine
SDZ	sulfadiazine
SG	sulfaguanidine

SMM	sulfamonomethoxine
SMX	sulfamethoxazole
SMZ	sulfamethazine
SPE	solid-phase extraction
SPME	solid-phase microextraction
SQ	sulfaquinoxaline
t	time
TLC	thin-layer chromatography
V	volt
v/v	volume by volume
$\mu\text{A}$	microampere
$\mu\text{L}$	microliter
v	scan rate



ศูนย์วิทยทรัพยากร  
จุฬาลงกรณ์มหาวิทยาลัย

# CHAPTER I

## INTRODUCTION

### 1.1 Introduction and Literature Reviews

Currently, sulfonamides (SAs) were widely used as broad-spectrum synthetic antibiotics due to their low cost. They were used for therapeutic, prophylactic and growth-promoting purposes in animals. Drugs consisting of SAs can be employed to prevent and treat various diseases and infections in the urinary, digestive, and respiratory tracts not only in humans but also in animals. The use of SAs can cause residual problems in meat because of excessive or uncontrolled dosages to animals before sales to consumers. The hazardous SAs can cause allergic reactions and antibiotic resistance, and be carcinogenic in humans [1, 2]. The European Union (EU) has set a maximum residue limit (MRL) of 100 ng g<sup>-1</sup> for SA residues in original animal food [3]. In addition, each country has set different limits for antibiotic residues in food. In Thailand, shrimp is one of the top ten exports sent to other countries. To overcome the limitations of trade based on SAs residues, a rapid, accurate, selective and sensitive method for the quantification of SAs in shrimp is necessary. Several methods have been developed for the determination of residual SAs including thin-layer chromatography (TLC), high-performance liquid chromatography (HPLC), high-performance liquid chromatography-mass spectrometry (HPLC/MS) [4-11], gas chromatography (GC), gas chromatography-mass spectrometry (GC/MS), capillary electrophoresis (CE) [12, 13] and the enzyme-linked immunosorbent assay (ELISA) [14]. The common method used for the separation of sulfonamides is HPLC coupled with ultraviolet (UV) [15-22] and fluorescent detectors [1, 23], which exhibited high sensitivity and selectivity. However, there is a high cost for the equipment and laboratories and a requirement for significant labor and analytical resources, which can potentially cause substantial delays in obtaining results. The electrochemical (EC) detector [24, 25] is an alternative method for SA determination that has the benefits of simplicity, speed, sensitivity and low cost.

The conventional column employed for the separation of these analytes is particle-packed, which has disadvantages, such as high flow resistance, high back-pressure and particle splitting at elevated flow rates. These drawbacks can lead to non-reproducibility, low separation efficiency and reduced sample throughput [26]. Recently, the monolithic column was discovered and verified as an alternative material for a conventional column. This column was classified according to its base, such as a polymer-based or silica-based monolithic column [27, 28]. The polymer-based monolithic column was prepared by a polymerization process of a monomer [29]. The excellent properties of the polymer-based monolithic columns were suitable for large molecule separation and can be used over a wider pH range than the silica-based monolithic columns. However, these polymer-based columns were easily swollen or shrunk in organic solvent. The silica-based monolithic column is prepared by the sol-gel process [30] and was used for the separation of small or medium molecules. The advantage of this column over the polymer-based monolithic column was that it provided a high tolerance for organic solvent, which led to a longer lifetime. Therefore, in this work, we selected a silica-based monolithic column for the separation of analytes. Both classical monolithic columns had pore sizes that were controlled by porogenic solvents such as polyethylene glycol. The characteristic of monolithic columns were single piece, through-pore and cross-linked skeletons. The silica-based monolithic column had small-sized skeleton and bimodal pores (both macropores and mesopores in one structure). The mesopores had an average diameter of 13 nm, and large macropores had an average diameter of 2  $\mu\text{m}$ . The total porosity in a silica single piece is more than 80 % with a lower back-pressure than a particle-packed column, even at high flow rates, the separation can be performed by silica-based monolithic column with a shorter analysis time and higher sample throughput. Because of this strong performance, the monolithic column was applied for the separation of several analytes in food [31-34], cosmetics [35], pharmaceuticals [36, 37] and environmental samples [38].

A critical problem for the determination of residual sulfonamides in animal tissues and environmental was the matrix. Therefore, sample extraction techniques were required before analysis. The sample preparation techniques have been reported for SAs consisting of liquid-liquid extraction (LLE) [19, 24], matrix solid-phase dispersion (MSPD) [39], solid-phase microextraction (SPME) [20] and solid-phase

extraction (SPE) [1, 4, 6-10, 21]. SPE was used for simultaneous extraction and cleanup analytes. The advantages of SPE were selective, simple and short time-consumption. Among the SPE materials reported, Oasis HLB was attractive. It was a hydrophilic-lipophilic balanced sorbent in SPE that was composed of two monomers (N-vinylpyrrolidone and divinylbenzene). This material has exhibited excellent retention capacity for a wider polarity of analytes [4, 10].

In this work, a method for the determination of sulfonamides in shrimp samples by monolithic column couple with amperometric detection using a boron-doped diamond thin film electrode has been developed. It is one part on the use of a diamond electrode for sulfonamide quantification in 'real world' contaminated samples. The analytical figures with limits of detection in the low ppb range, good sensitivity, excellent response precision and stability were observed. The proposed method has provided a rapid, highly sensitive and accurate method by exploiting a monolithic column coupled with a diamond electrode and validated it through a comparison measurement using HPLC-MS. The methodology was applied to determine residual sulfonamides (sulfaguanidine (SG), sulfadiazine (SDZ), sulfamethazine (SMZ), sulfamonomethoxine (SMM), sulfamethoxazole (SMX), sulfadimethoxine (SDM) and sulfaquinoxaline (SQ)) in fresh shrimp using Oasis HLB cartridges for sample extraction. The structures of the seven sulfonamides were presented in Figure 1.1.

ศูนย์วิทยทรัพยากร  
จุฬาลงกรณ์มหาวิทยาลัย

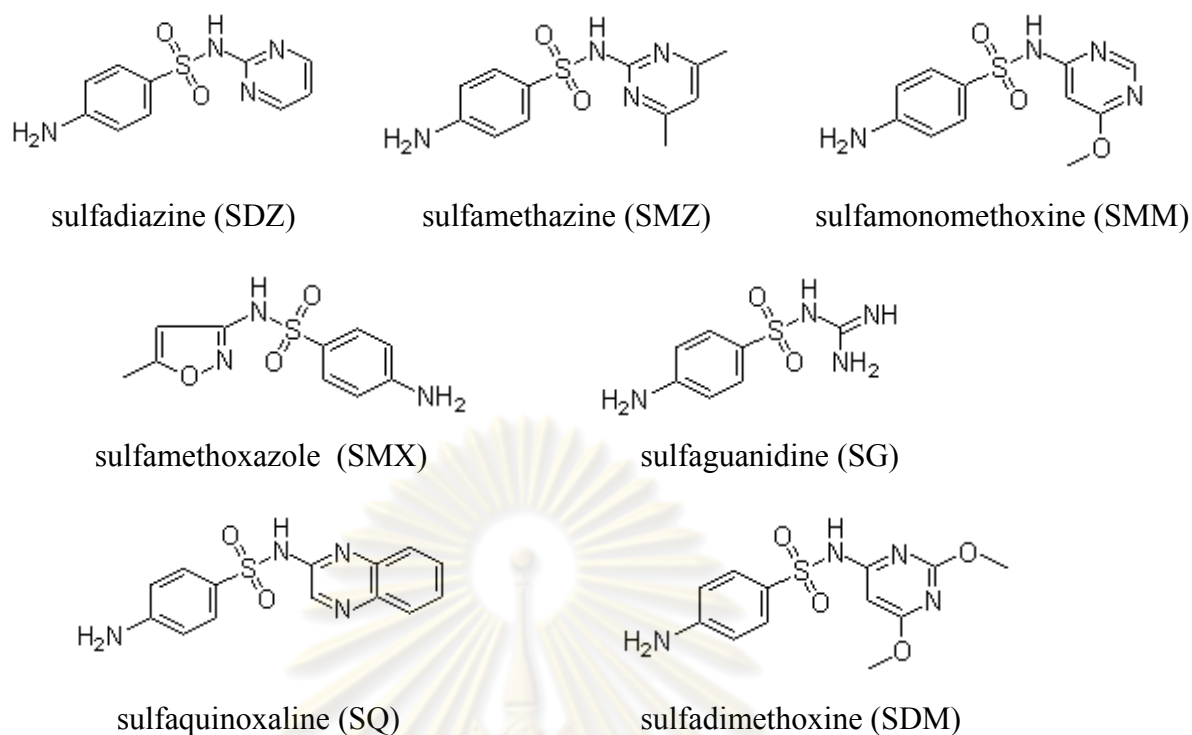


**Figure 1.1** Chemical structures of the studied sulfonamides.

## 1.2 Research Objective

The target of this research is to develop a method with rapidity, accuracy, and low detection limit for the determination of seven SAs contaminated in shrimp using the monolithic column coupled with amperometric BDD detector.

## 1.3 Scope of Research

The monolithic column coupled with amperometric detection using boron-doped diamond electrode was used for separation and detection of seven SAs. The effect of pH of mobile phase and extraction solution, flow rate of mobile phase, detection potential, linearity, limit of detection, and limit of quantitation were studied in detail.

## CHAPTER II

### THEORY

#### 2.1 High Performance Liquid Chromatography (HPLC) [40, 41]

High performance liquid chromatography is widely used for separation of two or more compounds in a mixture by distributing themselves between two phases: (a) a stationary phase, which can be a solid or liquid supported on a solid; and (b) a mobile phase, which is liquid and flows continuously around the stationary phase. The separation of individual component results primarily from differences in their affinity for the stationary phase. Figure 2.1 showed the four most widely used types of HPLC. These methods include: (1) partition or liquid-liquid chromatography; (2) adsorption or liquid-solid chromatography; (3) ion exchange chromatography; and (4) two types of size exclusion chromatography; including gel permeation chromatography and gel filtration chromatography.

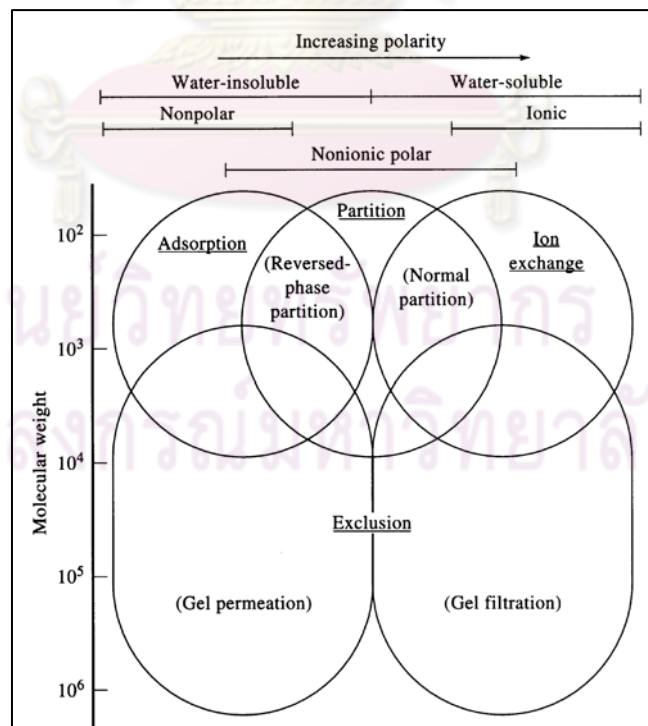


**Figure 2.1** Types of liquid chromatography.

### 2.1.1 Types of HPLC [42]

The schematic of the four modes of liquid chromatography are demonstrated in Figure 2.2.

#### 2.1.1.1 High Performance Partition Chromatography

Partition chromatography (Figure 2.2 (B)) has become the most widely used of all liquid chromatographic procedures. This technique can be subdivided into liquid-liquid and liquid bonded-phase chromatography. The difference between the two types is that the stationary phase is held on the supported particles of the packing. For liquid-liquid, the retention is controlled by physical adsorption, while bonded-phase; covalent bonds are involved. Early partition chromatography was exclusively liquid-liquid. Presently, bonded-phase packings were also predominated because of their greater stability. There are two types based on the relative polarities of the mobile and stationary phase. Firstly, they were based upon highly polar stationary phases and a relatively nonpolar solvent was used as mobile phase. For historic reasons, this type of chromatography is so called normal-phase chromatography. Secondly, they were reversed-phase chromatography, which consisted of nonpolar stationary phase and polar solvent mobile phase.

#### 2.1.1.2 High Performance Adsorption Chromatography

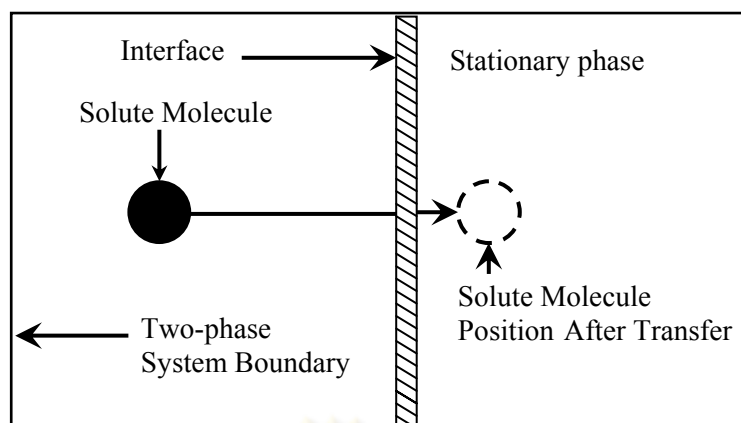
Adsorption chromatography (Figure 2.2 (C)), often referred to as liquid-solid chromatography, is based on interactions between the solute and fixed active sites on a solid adsorbent used as the stationary phase. The adsorbent can be packed in a column or spread on a plate. The adsorbent is generally an active, porous solid with a large surface area, such as silica gel, alumina or charcoal. The active sites, such as silanol groups of silica gel generally interacted with the polar functional groups of compounds to be separated. The nonpolar portion of a molecule showed only a minor influence on the separation.

### **2.1.1.3 High Performance Ion Exchange Chromatography**

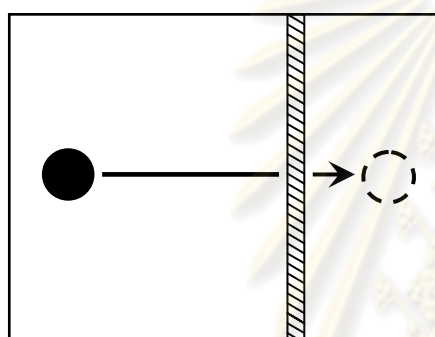
Ion exchange Chromatography, depicted in Figure 2.2 (D), is based on the affinity of ions in solution to the oppositely charged ions on the stationary phase. Ion exchange packing consisted of a porous solid phase, usually a resin, onto which ionic groups are chemically bonded. The mobile phase is usually a buffered aqueous solution containing a counter ion whose charge is opposite to that of the surface groups on stationary phase. Anyhow, they had same charge as the solute which is in charge equilibrium with the resin in the form of an ion pair. Competition between the solute and the counter ion for the ionic site governs the chromatographic retention. Ion-exchange chromatography has found to be useful for the application in inorganic chemistry for separating metallic ions, and in biological systems for separating water soluble ionic compounds such as proteins, nucleotides and amino acid.

### **2.1.1.4 High Performance Size Exclusion Chromatography**

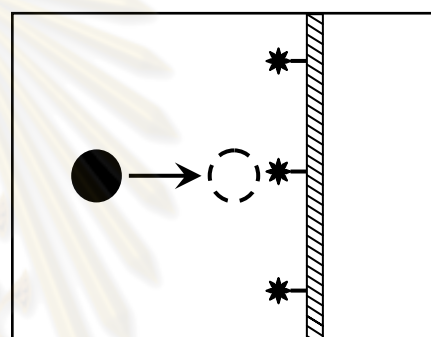
The mechanism of size exclusion chromatography, also classified to gel permeation or gel filtration chromatography, is shown in Figure 2.2 (E). Here, the stationary phase should be chemically inert. Size exclusion chromatography involves the selective diffusion of solute molecules into and out of mobile phase filled pores in a three dimensional network, which may be a gel or porous inorganic solid. The degree of retention depends on the size of the solvated solute molecule relative to the size of the pore. Small molecules will be permeated into the smaller pores, intermediate sized molecules will be permeated only part of the pores and be excluded from other, and the very large molecules will be completely excluded. The larger molecules will be traveled faster through the stationary phase and eluted from the column first. Thus, size exclusion chromatography is especially useful in separation of high molecular weight organic compound and biopolymers from smaller molecules.



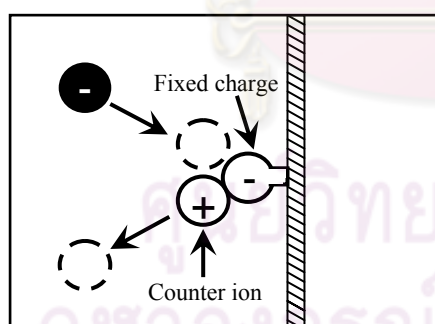
A. Transfer of solute to a Generalized Stationary Phase



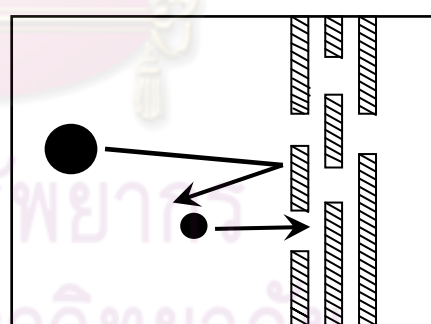
B. Liquid-Liquid



C. Liquid-Solid



D. Ion-Exchange



E. Exclusion

**Figure 2.2** Schematic representation of the four modes of liquid chromatography

### 2.1.2 Instrumentation [40, 43]

HPLC is frequently used in biochemistry and analytical chemistry to separate, identify, and quantify compounds. HPLC utilizes a column that holds chromatographic packing material (stationary phase), a pump that moves the mobile phase through the column, and a detector that shows the retention times of the molecules. The variation of retention times depend on the interaction between target analyte, the stationary phase, and the solvent used. Figure 2.3 depicted a diagram of important components for a typical HPLC instrument.

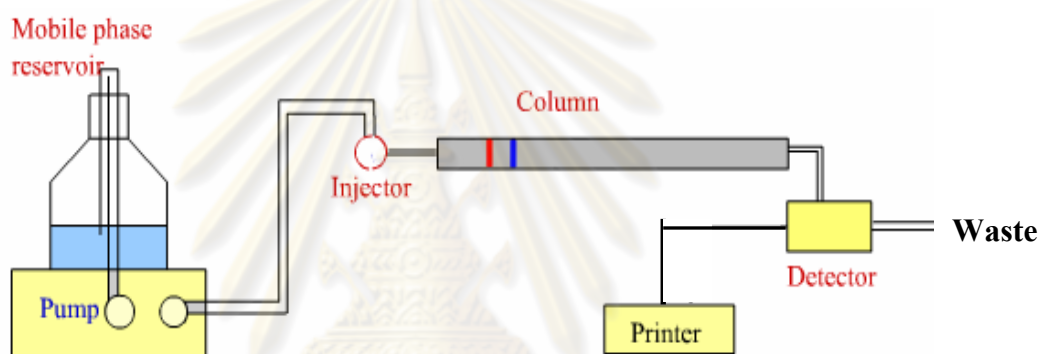


**Figure 2.3** Components of a typical HPLC instrument

#### 2.1.2.1 Mobile Phase Reservoir

The reservoirs are a storage container made of material resistant to chemical attack by the mobile phase. In most common size bottles are 1 or 2 liter glass reservoirs. Mobile phase is often necessary to remove dissolved air before the mobile phase is fed to the pump. This procedure is called mobile phase degassing. Degassing can be achieved by helium dispersion, applying vacuum to the mobile phase, ultrasonication, or heating. Therefore, degassing mobile phase prior used is preferred. The bubbles cause the operation of HPLC pumps unreliable, leading to fluctuations in flow rate. Bubbles can also get trapped in the detector flow cell, causing problems with this module as well.

The mobile phase used a single solvent or a solvent mixture of constant composition is isocratic elution. In gradient elution, two (and sometimes more) solvent systems that significantly different in polarity are used. The ratio of the two solvents is varied in a preprogrammed way during the separation, sometimes continuously and sometimes in a series of steps.

### 2.1.2.2 Pump

The requirements for liquid chromatographic pumps included (1) ability to generate pressures of up to 6,000 psi, (2) pulse-free output, (3) flow rates ranging from 0.1 to 10 mL min<sup>-1</sup>, (4) flow reproducibility of 0.5 % relative or better, and (5) resistance to corrosion of solvents. The types of pumps used in liquid chromatography can be divided into two categories according to the mechanism of dispensing the mobile phase: constant volume pump (e.g. reciprocating pump and syringe pump) and constant pressure pumps (e.g. pneumatic pump)

Syringe pumps employ solvent displacement by a mechanically controlled piston advancing at a constant rate in a fixed volume chamber (250-500 mL capacity). The pump output is relatively pulse free, very high pressure can be obtained, and gradient and flow programming are quite straightforward. The disadvantages of this pump are high cost, limited solvent reservoir capacity and problems with solvent compressibility.

The reciprocating pump is the most widely used. This device consists of a small cylindrical chamber that is filled and then emptied by back-and-forth motion of a piston. The pumping motion produces a pulsed flow that must be subsequently damped. Advantages of reciprocating pump include small internal volume, high output pressure (up to 10,000 psi), ready adaptability to gradient elution, and constant flow rates, which are largely independent of column back-pressure and solvent viscosity. Most modern commercial chromatographs employed a reciprocating pump.

Some instruments use a pneumatic pump, which it consists of a solvent container housed in vessel that can be pressurized by a compressed gas. This pump is inexpensive and pulse-free. The limit of solvent capacity and pressure output are major disadvantages and the pumping rates depend on solvent viscosity. In addition, they can not adapt to gradient elution.

### 2.1.2.3 Injector

The most commonly used sample injector in HPLC is the loop injector. A six-port, high-pressure, external loop injector and its basic operating principle are illustrated in Figure 2.4. In the load position, sample is forced through the loop by a syringe. Once the loop is completely filled, the valve core is rotated either manually or by an automatic air-operated or electrically operated actuator. The chromatographic pump then forces mobile phase through the loop and displaces the load to the column. To refill the loop, the core is rotated in the opposite direction.

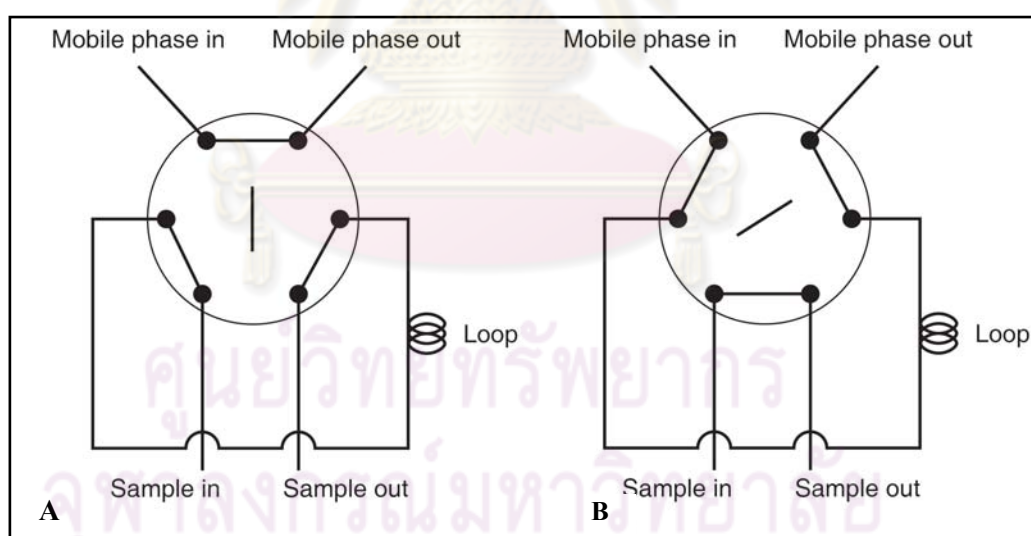


**Figure 2.4** Schematic diagram of a loop injector in the (A) load and (B) inject positions

### 2.1.2.4 Columns

Typically, there are two types of columns: an analytical column and a guard column. The guard column is placed before the analytical column to protect it from contamination. Guard columns usually contain the same particulate packing material as same as the analytical column, but they are significantly shorter and less expensive. Analytical columns, the conventional columns are particle packed column. The most widely used type of particle packed column is bonded-phase packings. Bonded-phase packings are a liquid film coated on a packing material consisting of 3–10  $\mu\text{m}$  porous silica particles. The stationary phase may be partially soluble in the mobile phase, causing it to “bleed” from the column over time. To prevent lossing of stationary phase, it is covalently bound to the silica particles. Bonded stationary phases are attached by reacting the silica particles with an organochlorosilane. The general form is  $\text{Si}(\text{CH}_3)_2\text{RCl}$ , where R is an alkyl or substituted alkyl group.

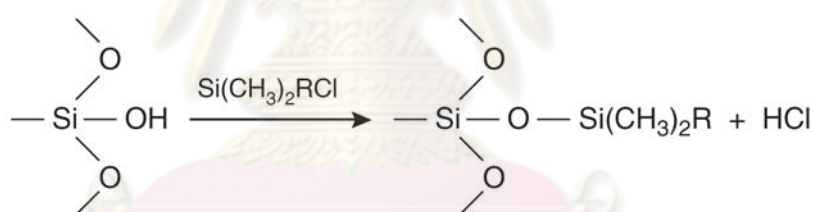


**Figure 2.5** Reaction of Bonded stationary phase

The disadvantages of particle packed column are high flow resistance, high back-pressure and particle splitting at elevated flow rates. These drawbacks can lead to non-reproducibility, low separation efficiency and reduced sample throughput.

Recently, the monolithic column was discovered and verified as an alternative material instead of using a conventional column. Monolithic column is classified according to its base, such as a polymer- or silica-based monolithic column. The polymer-based monolithic column is prepared by a polymerization process of a monomer. The excellent properties of the polymer-based monolithic columns are suitable for large molecule separation and can be used over a wider pH range than the silica-based monolithic columns. However, these polymer-based columns are easily swollen or shrunk in organic solvent. The silica-based monolithic column is prepared by the sol-gel process and is used for the separation of small or medium molecules. The advantage of this column over the polymer-based monolithic column is that it provides a high tolerance for organic solvent, which leads to a longer lifetime.

#### **2.1.2.5 Polymer-Based Monolithic Columns [27]**

##### **2.1.2.5.1 Synthesis Approaches and Characterization**

To synthesize an organic monolith, a mixture of monomers, co-monomer, initiator, crosslinker and porogenic solvents is poured in to a mold. The porogen acts as an emulsifier, creating the porous structure. The mixture is either heated or treated with UV light to initiate polymerization. The resulting monolith is washed to remove any remaining monomer or porogen and subsequently functionalized. The interstices generate a macroporous system with pore diameters in excess of 100 nm. The reported specific surface area is much smaller than those of monolithic silicas ( $<50 \text{ m}^2 \text{ g}^{-1}$ ). The pore size depends on the solvent and the swelling properties of the material. One major advantage of polymeric monoliths over silica monoliths is the fact that the surface functionality can be generated and controlled by the use of appropriate co-monomers. Thus hydrophobic, hydrophilic, polar and charged surfaces can be obtained. Also polymeric monoliths are manufactured in a wide variety of column formats as thin membranes, disks, capillary columns and large bore preparative columns.

### 2.1.2.6 Silica-Based Monolithic Columns

#### 2.1.2.6.1 Formation Processes and Pore Structure Control of Silica Monoliths

The starting silica sources are tetramethoxysilane, tetraethoxysilane or *n*-alkyltrialkoxysilanes which are subjected to acid catalyzed hydrolysis and condensation in presence of water soluble polymers such as polyethyleneglycols and polyacrylic acid and surfactants as additives. The multicomponent solution converts into a sol–gel system by a nucleation and growth mechanism in which small fractions of a finely dispersed phase grow in size (see Figure 2.6 (A)) being limited by a thermally activated diffusion process. A second process, called spinodal decomposition, takes place leading to a co-continuous domain structure, which remains stable over an extended period of time (see Figure 2.6 (B)). The gel morphology is controlled by the kinetics of two competitive processes: the domain coarsening and the structure freezing by the sol–gel transition. The resulting gels are aged and a solvent exchange is performed to tailor the pore structure. The macroporous gel domains are filled with the polymer, which has been burned out by calcination after drying. The mesopore structure and mesopore size is adjusted by hydrothermal treatment conditions. In this way the process enables to generate two continuous pore systems and to adjust and control the pore size, and porosity of macropores and mesopores independently. The manufacturing process of monolithic silica rods with 4.6mm I.D. comprises the following consecutive steps: preparation of the starting sol, phase separation and gelation, aging and drying. After drying the rods are cladded with poly (ether ether ketone) (PEEK). Surface functionalization is performed in situ. The product is called Chromolith Performance and marketed by Merck, Darmstadt, Germany.

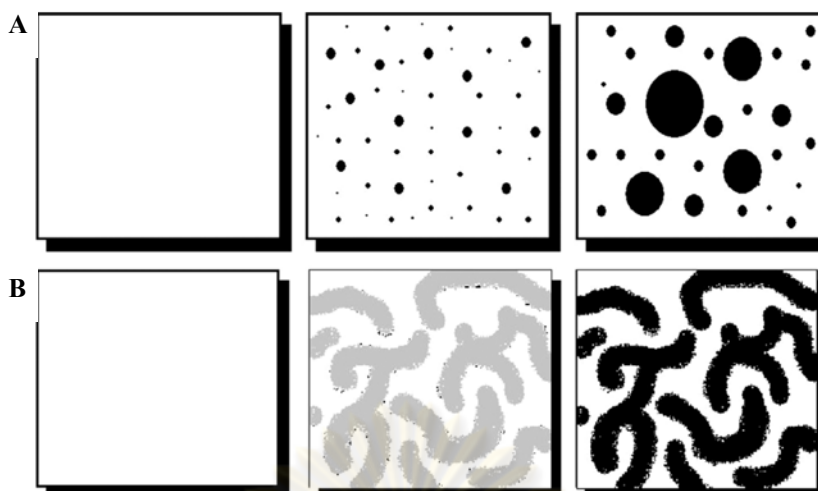


**Figure 2.6** (A) Nucleation and growth (diffusion limited) of silica-based monoliths (B) Spinoidal decomposition (spontaneous) of silica-based monoliths

The bimodal pore structure of a Chromolith column is characterized by a distinct bimodal pore structure: macropores of 2  $\mu\text{m}$  in diameter and mesopores with an average pore diameter of approximately 13 nm. The total porosity of the monolithic column amounts to 80% and higher, the larger proportion accounts for the macropores. The mesopores generate a specific surface area of approximately 300  $\text{m}^2 \text{g}^{-1}$ . Silica monoliths (rods) of 4.6 mm. I.D. size were characterized by the classical pore structure analysis such as nitrogen sorption at 77 K, mercury intrusion, scanning electron microscopy (SEM) and transmission electron microscopy (TEM). SEM photographs for the bimodal pore structure of silica-based monolithic column are illustrated in Figure 2.7. As a result the mesopore volume and macropore volume distribution were assessed to detect the size of diffusive pore and the size of flow through pores.

Characteristics of monolithic columns have single piece, through-pore, high porosity, and cross-linked skeletons. Advantageous of monolithic column are a lower back-pressure than a particle-packed column, even at high flow rates, the separation can be performed in monolithic column with a shorter analysis time and high sample throughput.

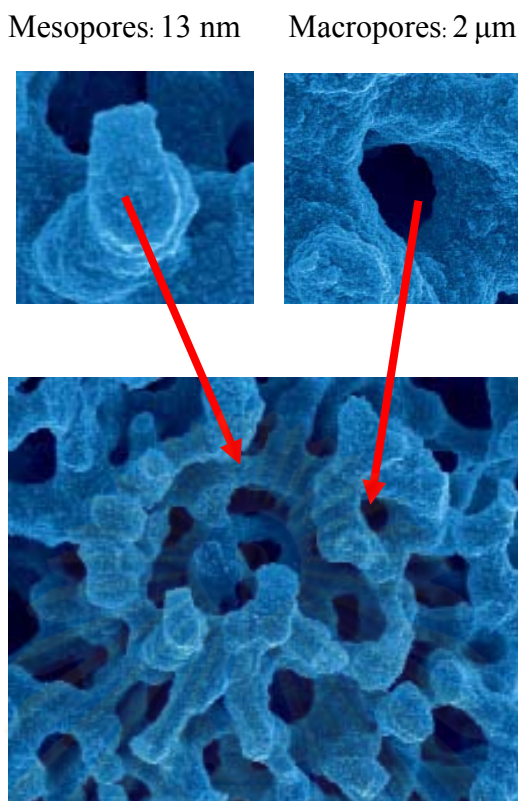


**Figure 2.7** SEM photographs for the bimodal pore structure of silica-based monolithic column

#### 2.1.2.7 Detectors

The detector measures the signal corresponding to the concentration of sample bands that they moved from the analytical column and pass through the detector flow cell. An ideal detector of any type was sensitive to low concentrations of analyte, provided linear response, and did not broaden the eluted peaks. It was also insensitive to changes in temperature and solvent composition. To prevent peak broadening, the detector volume should be less than 20% of the volume of the chromatographic band. Gas bubbles in the detector create noise, so mobile phase must be degassed beforehand. Table 2.1 listed some of common detectors and their properties. The popular detectors are spectroscopic detectors and electrochemical detectors.

Spectroscopic detector, the most popular HPLC detectors are based on spectroscopic measurements, including UV/Vis absorption, and fluorescence.

Electrochemical detector, another common group of HPLC detectors are those based on electrochemical measurements such as amperometry, voltammetry, coulometry, and conductivity.

**Table 2.1** Performance of HPLC detectors\*

HPLC Detector	Commercially Available	Mass LOD <sup>+</sup> (typical)	Linear Range ‡ (decades)
Absorbance	Yes	10 pg	3-4
Fluorescence	Yes	10 fg	5
Electrochemical	Yes	100 pg	4-5
Refractive index	Yes	1 ng	3
Conductivity	Yes	100 pg-1 ng	5
Mass spectrometry	Yes	< 1 pg	5
FTIR	Yes	1 µg	3
Light scattering	Yes	1 µg	5
Optical activity	No	1 ng	4
Element selective	No	1 ng	4-5
Photoionization	No	< 1 pg	4

\* From manufacturer's literature; *Hand book of Instrumental Techniques for Analytical Chemistry*, F. Settle, Ed. Upper Saddle River, NJ: Prentice-Hall, 1997; E. S. Yeung and R. E. Synovec, *Anal. Chem.*, 1986, 58,1237A.

+ Mass LODs (limits of detection) are dependent on compound, instrument, and HPLC conditions, but those given are typical values with commercial systems when available.

‡ Typical values from the sources above.

### **2.1.2.8 Flow Cell**

#### **2.1.2.8.1 Flow Cell for Spectroscopy [43]**

The Z flow cell for HPLC using a UV/Vis spectrophotometer as a detector is showed in Figure 2.8 (A). Careful consideration must be given to the design of the detector flow cell as it forms an integral part of both the chromatographic and optical systems. A compromise between the need to miniaturize the cell volume to reduce extracolumn band broadening and the desire to employ long path lengths to increase sample delectability must be made. The Z-cell design was used to minimize stagnant flow regions in the cell and to reduce peak tailing.

#### **2.1.2.7.2 Flow Cell for Electrochemistry [44]**

The thin-layer amperometric flow cell showed in Figure 2.8 (B). The thin-layer channel is defined by a gasket held between a stainless-steel block and a polymeric block. The stainless-steel block is the auxiliary electrode and provides a compartment for the reference electrode. The polymeric block contains the working electrode. This design and, in fact, nearly all cell designs incorporate three electrodes: working, auxiliary, and reference. The potential selected by the user is applied between the reference and working electrodes while the current is passed between the auxiliary and working electrodes. Detection occurs at the working electrode in the thin-layer region. Electrodes of the same or different materials may be interchanged by simply swapping the working electrode half of the thin-layer cell. Carbon pastes, glassy carbon, mercury on gold, platinum, and silver have all been used. This design allows easy collection of solute bands without appreciable dispersion. The cell volume can also be reduced for microbore LC to less than 300 nL by simple gasket changes.

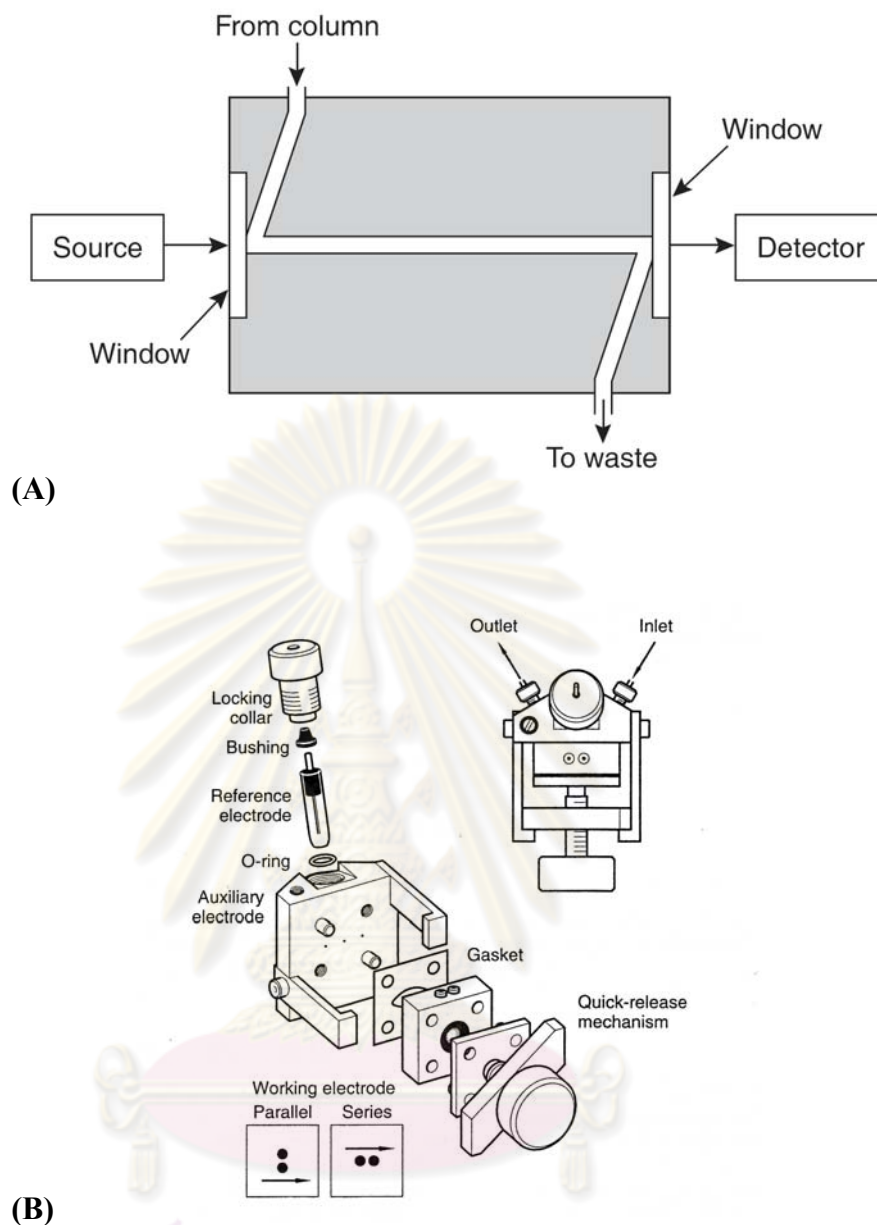


**Figure 2.8** Schematic diagrams of flow cell detectors for HPLC using (A) UV/Vis absorption spectrophotometric cell and (B) Thin-layer amperometric cell

## 2.2 Electroanalytical chemistry (EC)

Electrochemistry encompasses chemical and physical processes that involve the transfer of charge. There are two categories of electrochemical processes, potentiometric and electrolytic methods, that are applied to quantitative measurements. Potentiometry is the field of electroanalytical chemistry in which potential is measured under the conditions of no current flow. The measured potential may then be used to determine the analytical quantity of interest, generally the concentration of some component of the analyte solution. Unlike potentiometry, where the free energy contained within the system generates the analytical signal, electrolytic methods are an area of electroanalytical chemistry in which an external source of energy is supplied to drive an electrochemical reaction which would not normally occur. The externally applied driving force is either an applied potential or current. When potential is applied, the resultant current is the analytical signal; and when current is applied, the resultant potential is the analytical signal. Techniques which utilize applied potential are typically referred to as voltammetric methods while those with applied current are referred to as galvanostatic methods. Unlike potentiometric measurements, which employ only two electrodes, voltammetric measurements utilize a three electrode electrochemical cell. The use of three electrodes (working, auxiliary, and reference) along with the potentiostat instrument allows accurate application of potential functions and the measurement of the resultant current. The different voltammetric techniques are distinguished from each other primarily by the potential function that is applied to the working electrode to drive the reaction, and by the material used as the working electrode. Some voltammetric techniques used in this work such as cyclic voltammetry, hydrodynamic voltammetry, and amperometric detection are considered respectively.

## 2.2.1 Mass transport [40]

Reactants or charges are transported to the surface of an electrode by three mechanisms: (1) diffusion, (2) migration, and (3) convection. Products are removed from electrode surfaces in the same ways.

### 2.2.1.1 Diffusion

When there is a concentration difference between two regions of a solution, ions or molecules move from the more concentrated region to the more dilute. This process is called diffusion and ultimately leads to a disappearance of the concentration gradient. The rate of diffusion is directly proportional to the concentration difference.

### 2.2.1.2 Migration

The electrostatic process by which ions move under the influence of an electric field is called migration. The rate at which ions migrate to or away from an electrode surface generally increases as the electrode potential increases. This charge movement constitutes a current, which also increases with potential. Migration causes anion to be attracted to the positive electrode and cations to the negative electrode. Migration of analyte species can be minimized by having a high concentration of an inert electrolyte, called a supporting electrolyte, present in the cell. The current in the cell is then primarily due to charges carried by ions from the supporting electrolyte.

### 2.2.1.3 Convection

Reactants can also be transferred to or from an electrode by mechanical means. Forced convection, such as stirring or agitation, tends to decrease the thickness of the diffusion layer at the surface of an electrode and thus decrease concentration polarization.

### 2.2.2 Voltammetry [42, 45, 46]

Voltammetry comprises a group of the electroanalytical methods in which information about the analyte is derived from the measurement of current as a function of applied potential. It is based on the measurement of a current that develops in an electrochemical cell under conditions of complete concentration of polarization of working electrode. In the presence of the electroactive (reducible or oxidizable) species, a current will be recorded when the applied potential becomes sufficiently negative or positive for it to electrolyze. The recording result is called a voltammogram. The potential excitation signal is imposed on an electrochemical cell containing an electrode. Three waveforms of most common excitation signals used in voltammetry are shown in Figure 2.9. The classical voltammetric excitation signal is a linear scan shown in Figure 2.9(a). The potential applied to the cell of this excitation increases linearly as a function of time. The two pulse excitation signals are shown in Figure 2.9(b) and 2.9(c). The current responses of the pulse type are measured at various times during the lifetime of these pulses.

Voltammetry is widely used for the fundamental studies of oxidation and reduction processes in various media, adsorption process on electrode surfaces, and electron transfer mechanisms at electrode surfaces. In the mid-1960s, several major modifications of classical voltammetric techniques were developed that enhanced the sensitivity and selectivity of the method.

ศูนย์วิทยทรัพยากร  
จุฬาลงกรณ์มหาวิทยาลัย

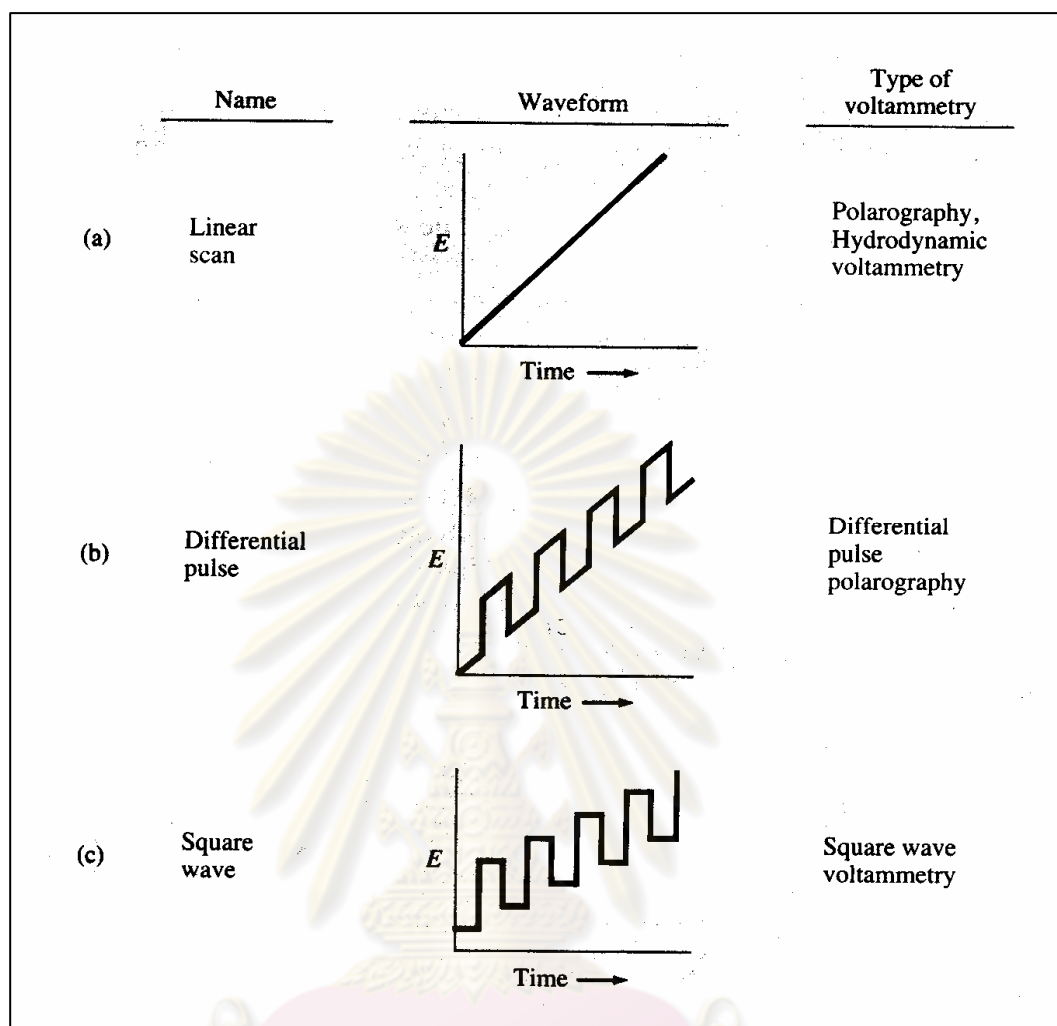


**Figure 2.9** Typical excitation signals for voltammetry

### 2.2.3 Cyclic voltammetry [47]

Cyclic voltammetry (CV) is an important and widely used electroanalytical technique. Although CV is infrequently used for quantitative analysis, it finds wide applicability in study of oxidation/reduction reaction, the detection of reaction intermediates, and the observation of follow-up reaction of products formed at electrodes. In CV apply the triangular waveform in Figure 2.10 to the working electrode. After the application of a linear voltage ramp between times  $t_0$  and  $t_1$  (typically a few seconds), the ramp is reversed to bring the potential back to its initial value at time  $t_2$ . The cycle may be repeated many times.

The initial portion of the cyclic voltammogram in Figure 2.11, beginning at  $t_0$ , exhibits a cathodic wave. Instead of leveling off at the top of the wave, current decreases at more negative potential because analyte becomes depleted near the electrode. Diffusion is too slow to replenish analyte near the electrode. At the time of peak voltage ( $t_1$ ) in Figure 2.11, the cathodic current has decayed to a small value. After  $t_1$ , the potential is reversed and, eventually, reduced product near the electrode is oxidized, thereby giving rise to an anodic wave. Finally, as the reduced product is depleted, the anodic current decays back toward its initial value at  $t_2$ .

Figure 2.11 (A) illustrates a reversible reaction that is fast enough to maintain equilibrium concentrations of reactant and product at the electrode surface. The anodic peak and cathodic peak currents have equal magnitudes in a reversible process, and

$$E_{pa} - E_{pc} = \frac{2.303RT}{nF} = \frac{60.0}{n} (mV) \quad (\text{at } 25^\circ\text{C})$$

Where  $E_{pa}$  and  $E_{pc}$  are the potentials at which the anodic peak and cathodic peak currents are observed and  $n$  is the number of electrons in the half-reaction. The half-wave potential,  $E_{1/2}$ , lies midway between the two peak potentials.

The formal reduction potential ( $E^0$ ) reversible reaction is given by

$$E^0 = \frac{E_{pc} + E_{pa}}{2}$$

For an irreversible reaction, the cathodic and anodic peaks are drawn out and more separated (Figure 2.11 (B)). At the limit of irreversibility, where the oxidation is very slow, no anodic peak is seen.

For a reversible reaction, the peak current ( $I_p$ , amperes) for the forward sweep of the first cycle is proportional to the concentration of analyte and the square root of sweep rate:

$$I_p = (2.686 \times 10^5) n^{3/2} ACD^{1/2} \nu^{1/2} \quad (\text{at } 25^\circ\text{C})$$

Where  $n$  is the number of electrons in the half-reaction,  $A$  is the area of the electrode ( $\text{cm}^2$ ),  $C$  is the concentration ( $\text{mol}/\text{cm}^3$ ),  $D$  is the diffusion coefficient of the electroactive species ( $\text{cm}^2/\text{s}$ ), and  $v$  is sweep rate ( $\text{V}/\text{s}$ ). The faster the sweep rate, the greater the peak current, as long as the reaction remains reversible. If the electroactive species is adsorbed on the electrode, the peak current is proportion to  $v$  rather than  $\sqrt{v}$ .

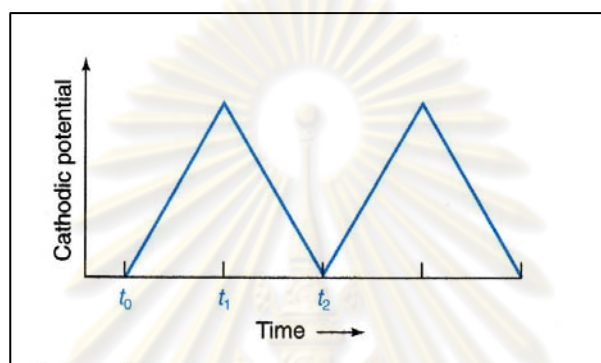


**Figure 2.10** Waveform for cyclic voltammetry, Corresponding times are indicated in Figure 2.11

ศูนย์วิทยทรัพยากร  
จุฬาลงกรณ์มหาวิทยาลัย

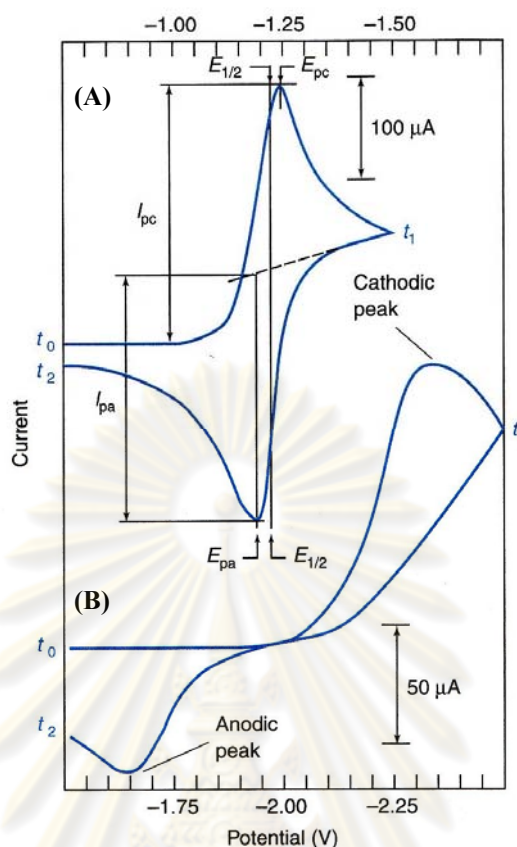


**Figure 2.11** Cyclic voltammograms of (A) 1mM  $\text{O}_2$  in acetonitrile with 0.10 M  $(\text{C}_2\text{H}_5)_4\text{N}^+\text{ClO}_4^-$  electrolyte and (B) 0.060 mM 2-nitropropane in acetonitrile with 0.10 M  $(n\text{-C}_7\text{H}_{15})_4\text{N}^+\text{ClO}_4^-$  electrolyte.

#### 2.2.4 Amperometry [48]

Amperometric detection was the measurement of current at a fixed potential. Either an oxidation or reduction was forced to occur by judicious selection of the potential applied to an electrode by a controlling potentiostat. A typical waveform of amperometry is shown in Figure 2.12. The electrode acts as an oxidizing or reducing agent of variable power. In order to use amperometric measurements effectively, it was important to recognize that electrochemical detection was a surface technique, which means molecules not adjacent to the electrode must be moved to the surface to react.

Amperometry had an advantage over most analytical detection techniques in that it involved a direct conversion of chemical information to an electrical signal without the use of optical or magnetic carriers. If a reduction takes place, electrons flow from the electrode to the molecule in a heterogeneous transfer; conversely, an oxidation was the transfer of electrons in the opposite direction. Under steady-state conditions, the current measured was contributed from three sources: the background electrolyte, the electrode material itself, and the analyte.

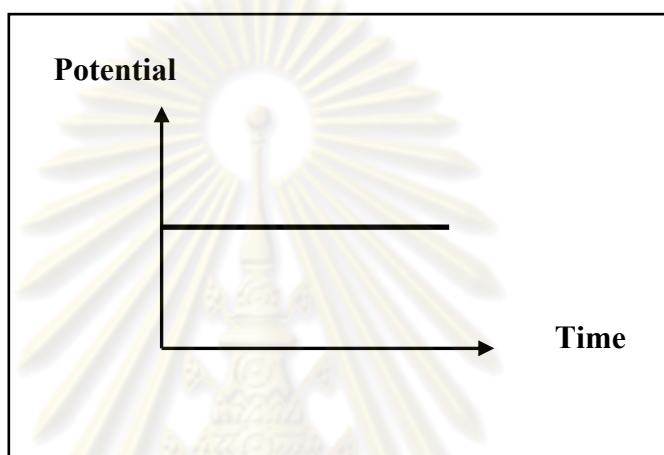


**Figure 2.12** A typical waveform employed in amperometry

### 2.3 Sample Preparation [49]

Sample preparation was a technique used to clean-up a sample before analyzing and/or to concentrate a sample to improve its detection. The important problem of analysis was interferences that led to the low sensitivity as well. Sample preparation is usually needed to eliminate interferences and to increase the sensitivity. Samples consisted of two distinct parts, the analytes and matrix. The analytes were the compounds of interest that must be analyzed, while the matrix was the remainder of the sample, which did not require analysis. Sample preparation may include dissolving the sample, extracting analyte from a complex matrix, concentrating a dilute analyte to a level that can be measured, chemically converting analyte into a detectable form, and removing interfering species. The purpose of sample preparation was to have a processed sample that led to better analytical results compared to those of the initial sample.

### 2.3.1 Solid-Phase Extraction (SPE) [50, 51]

Solid-phase extraction is a technique of sample preparation that concentrates and purifies analytes from solution by sorption onto a disposable solid-phase cartridge, followed by elution of the analyte with an appropriate solvent for analysis. SPE techniques have been developed to replace the traditional liquid-liquid extraction method. The solid-phase cartridge is shown in Figure 2.13. The mechanisms of retention include reversed phase, normal phase, and ion exchange. SPE techniques provided a way to perform sample preparation quickly, use less solvent, isolate analytes from large volumes of samples with minimal or no evaporation losses, and provide good reproducible results.

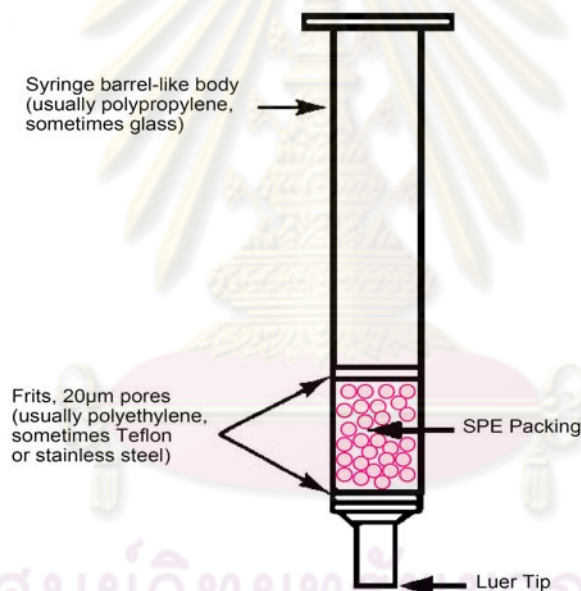


**Figure 2.13** Anatomy of a cartridge SPE

### **2.3.1.1 Mode of solid-phase extraction [47-48]**

#### **2.3.1.1.1 Reversed phase**

The interested analytes are usually moderate to non-polar. The hydrophobic interactions are non-polar interactions, Van-Der Waals or dispersion forces. The secondary interaction between silica-based and analytes present. The endcapping is useful to reduce these interactions. However, secondary interaction may be useful in the extraction of highly polar compounds or matrices. Reversed-phase sorbents are packed with more hydrophobic material. The aqueous sample is commonly analyzed by reversed phase SPE. The reversed phase sorbents are non-polar functionalized such as C-18, C-8, C-2, cyclohexyl and phenyl functional groups and bonded to the silica or polymeric sorbent.

#### **2.3.1.1.2 Normal phase**

Normal phase SPE refers to the sorption of an analyte by a polar surface. It is a standard type of separation. The mechanism is polar interaction such as hydrogen bonding, dipole-dipole interaction,  $\pi$ - $\pi$  interaction and induced dipole-dipole interaction. Polar-functionalized bonded silica (LC-CN, LC-NH<sub>2</sub>, and LC-Alumina) are typically used in normal phase conditions. For example, silica base is extremely hydrophilic. This material adsorbs polar compounds from non-polar matrix and elutes compounds with a more polar organic solvent than the original sample matrix.

#### **2.3.1.1.3 Ion exchange**

Ion exchange can be used for compounds that are changed in solution. The hydrophobic ion exchange is capable of exchanging both a cations and anions with free cation or anion functional groups. Strong cation-exchange sorbent consists of interaction sites like sulfonic acid groups and weak cation-exchange sites like carboxylic acidic groups. Strong anion-exchange sorbents would be quaternary amine, primary, and secondary. Tertiary amines refer to weak ion exchange. The secondary non-polar interaction with non-polar portions can be provided. A decrease in the

balance of pH, ionic strength, and organic content may be necessary for elution of interested analyte from these sorbents. The strong sites are always shown as an exchange site at any pH. Weak sites present are only at pH levels greater or less than the pKa. It has found many applications, for example, it is used for natural products, protein, cellulose, and trace enrichment.

#### 2.3.1.1.4 Mixed mode

The deliberate use of two different function groups on the same sorbent is called “mixed-mode SPE”. This sorbents are useful for complex samples that differ in polarity and ionization. Mixed-mode sorbent contains co-bonded ion exchange and alkyl group cartridge. Two different functional groups eliminate the complex sample matrix. The initial hydrophobic interaction is a function of the chain length, with shorter chains (C-4) being retained less than longer chains (C-18). An example of the mixed-mode is shown in figure, with reversed phase (hydrocarbon) and cation-exchange site of the sorbent (amino functional group).

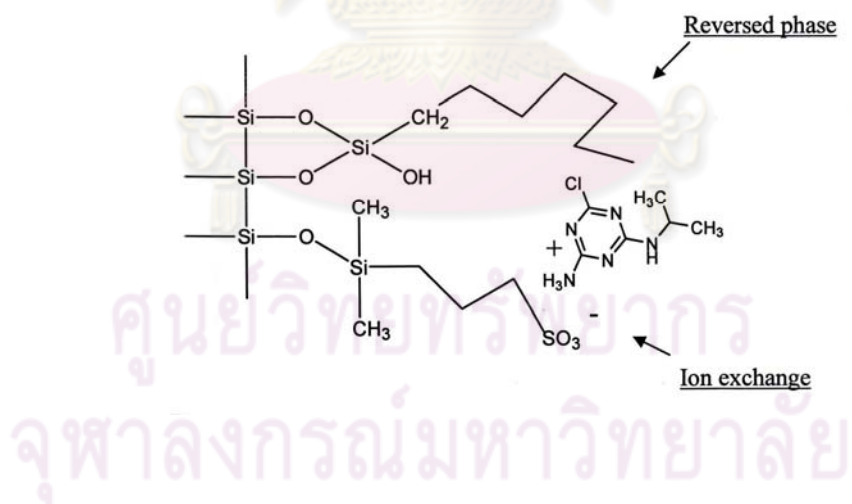


**Figure 2.14** Mixed-mode SPE

In current, Oasis HLB cartridges are interested for sample preparation. It is a hydrophilic-lipophilic balanced sorbent in SPE that is composed of two monomers (N-vinylpyrrolidone and divinylbenzene). This material has exhibited excellent retention capacity for a wider polarity of analytes. Figure 2.15 shows structure of Oasis HLB cartridges

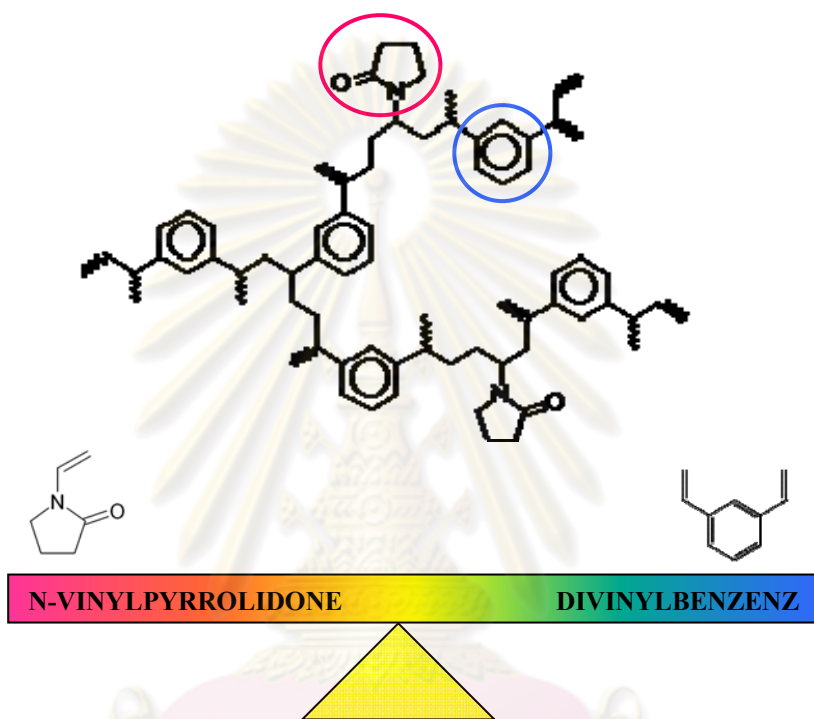


**Figure 2.15** Structure of Oasis HLB cartridges

### 2.3.1.2 Step of solid-phase extraction [52]

Four steps of SPE process, which comprised of conditioning, loading, washing, and eluting are illustrated in Figure 2.16.

Conditioning step is the first of the solid-phase sorbent (step 1). This simply means that a solvent is passed through the sorbent to wet the packing material and to solvate the functional groups of the sorbent. Furthermore, the air present in the column is removed and the void spaces are filled with solvent. Typically the

conditioning solvent is methanol, which is then followed by water or an aqueous buffer. The methanol followed by water or buffer activates the column in order for the sorption mechanism to work properly for aqueous samples. Care must be taken not allow the bonded-silica packing or the polymeric sorbent to go dry. In fact, if the sorbent dries for more than several minutes under vacuum, the sorbent must be reconditioned. If it is not reconditioned, the mechanism of sorption will not work effectively and recoveries will be poor for the analyte.

In the next step, the sample and analyte are applied to the column (step 2). This is the retention or loading step. Depending on the type of sample, from 1 mL to 1 L of sample may be applied to the column either by gravity feed, pumping, aspirated by vacuum, or by an automated system. It is important that the mechanism of retention holds the analyte on the column while the sample is added. The mechanisms of retention include van der Waals (also called non-polar, hydrophobic, partitioning, or reversed-phase) interaction, hydrogen bonding, dipole-dipole forces, size exclusion, and cation and anion exchange). This retention step is the digital step, or “on/off mechanism”, of solid-phase extraction. During this retention step, the analyte is concentrated on the sorbent. Some of the matrix components may also be retained and others may pass through, which gives some purification of the analyte.

In the washing step, this step is to rinse the column of interferences and to retain the analyte (step3). This rinse will remove the sample matrix from the interstitial spaces of the column, while retaining the analyte. If the sample matrix was aqueous, an aqueous buffer or a water-organic-solvent mixture may be used. If the sample was dissolved in an organic solvent, the rinse solvent could be the same solvent.

In the last step, step 4 is to elute the analyte from the sorbent with an appropriate solvent that is specifically chosen to disrupt the analyte-sorbent interaction, resulting in elution of the analyte. The eluting solvent should remove as little as possible of the other substances sorbed on the column. This is the basic method of solid-phase extraction. There is an alternate method where the interferences are sorbed and the analyte passes through the column. The analyte is collected and assayed directly.

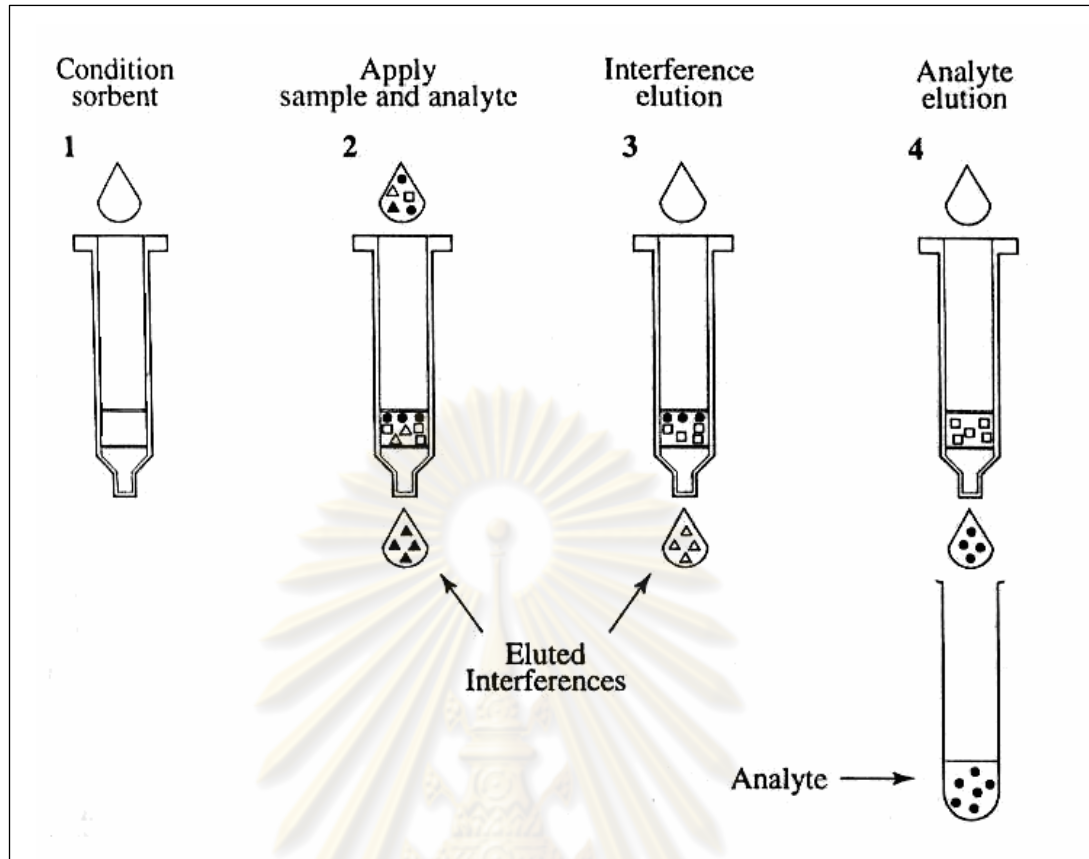


Figure 2.16 Steps of solid-phase extraction

ศูนย์วิทยทรัพยากร  
จุฬาลงกรณ์มหาวิทยาลัย

## CHAPTER III

### EXPERIMENTAL

#### 3.1 Chemical and Reagents

- 3.1.1 Sulfaguanidine (ICN Biomedical Inc)
- 3.1.2 Sulfadiazine (Sigma-Aldrich)
- 3.1.3 Sulfamethazine (Sigma-Aldrich)
- 3.1.4 Sulfamonomethoxine (Sigma-Aldrich)
- 3.1.5 Sulfamethoxazole (Sigma-Aldrich)
- 3.1.6 Sulfadimethoxine (Sigma-Aldrich)
- 3.1.7 Sulfaquinoxaline (Sigma-Aldrich)
- 3.1.8 Potassium dihydrogen orthophosphate (BDH)
- 3.1.9 di-sodium hydrogen phosphate dihydrate (Merck)
- 3.1.10 Citric acid (Carlo Erba)
- 3.1.11 Sodium hydroxide (Merck)
- 3.1.12 Ethylenediaminetetraacetic acid disodium salt dehydrate (Sigma-Aldrich)
- 3.1.13 Ethanol (HPLC Grade, Merck)
- 3.1.14 Methanol (HPLC Grade, Merck)
- 3.1.15 Acetonitrile (HPLC Grade, Merck)
- 3.1.16 ortho-phosphoric acid 85% (Merck)
- 3.1.17 A standard buffer solution pH 4 and pH 7 (Metrohm)

#### 3.2 Instruments and Equipment

- 3.2.1 Autolab potentiostat 100 (Eco-chemic, Netherland)
- 3.2.2 HPLC compact pump model 2250 (Bischoff, Germany)
- 3.2.3 Rheodyne injection valve, Model 7125 (Altech), with a 20  $\mu$ L stainless steel injection loop (0.5 mm. i.d.)
- 3.2.4 RP-18e monolithic column silica base Chromolith® Performance (100 mm x 4.6 mm i.d., Merck)

- 3.2.5 RP-18e monolithic column silica base Chromolith® guard cartridge kit (5 mm x 4.6 mm i.d., Merck)
- 3.2.6 Electrochemical flow cell (Bioanalytical System Inc., USA)
- 3.2.7 Teflon cell gasket (Bioanalytical System Inc.)
- 3.2.8 PEEK tubing (0.25 mm. i.d.) and connecting (Upchurch)
- 3.2.9 Teflon tubing (1/10 inch i.d., Upchurch)
- 3.2.10 Silver/silver chloride (Ag/AgCl) electrode (Bioanalytical System Inc., USA)
- 3.2.11 Platinum wire (Bioanalytical System Inc., USA)
- 3.2.12 Boron-doped diamond (BDD) electrode (Toyo Kohan Co., Ltd., Japan)
- 3.2.13 Glassy carbon (GC) electrode (Bioanalytical System Inc.. USA)
- 3.2.14 Stainless steel electrode (Bioanalytical System Inc.. USA)
- 3.2.15 Polishing set of 0.3 and 1 micron alumina powder (Metrohm)
- 3.2.16 Oasis HLB SPE cartridges 200 mg, 6 mL (Water, USA)
- 3.2.17 12 position vacuum manifold system (Phenomenex, USA)
- 3.2.18 Mobile phase filter set included 300 mL glass reservoir, glass membrane holder, 1000 mL flask and metal clip (Millipore, USA)
- 3.2.19 Milli Q water system (Millipore, USA,  $R \geq 18.2 \text{ M}\Omega\text{cm}$ )
- 3.2.20 pH meter (Metrohm 744 pH meter, Metrohm, Switzerland)
- 3.2.21 Analytical balance (Mettler AT 200, Mettler, Switzerland)
- 3.2.22 Ultrasonic bath (ULTRASONIK 28H, ESP Chemicals, Inc., USA)
- 3.2.23 Centrifuge, CENTAURA 2 (Sanyo, U.K)
- 3.2.24 Vortex mixer (Mixer Uzusio LMS. Co. Ltd., Japan)
- 3.2.25 Nitrogen evaporator model 112 (Organomation Associates Inc., USA).
- 3.2.26 Autopipette and tips (Eppendorf, Germany)
- 3.2.27 Filters membrane (0.2  $\mu\text{M}$ , 47 mm, Whatman)
- 3.2.28 Nylon Syringe filters (0.45  $\mu\text{m}$ , 13 mm ([www.vertichrom.com](http://www.vertichrom.com)))
- 3.2.29 Beaker 10, 25, 50, 100, 250, 500 and 1,000 mL
- 3.2.30 Volumetric flask 5,10, 25, 50, 500 and 1,000 mL

### 3.3 Preparation of Chemical Solution

#### 3.3.1 Preparation of Solution for Cyclic Voltammetry

##### 3.3.1.1 Supporting Electrolyte

The phosphate buffer solutions (pH 5-7.2) were prepared from weight the ratio of 0.05 M potassium dihydrogen orthophosphate and 0.05 M disodium hydrogen orthophosphate in 100 mL volumetric flask. The Milli Q water was used to adjust the volume to 100 mL. The recipes of each pH solution were shown in Table 3.1.

**Table 3.1** Recipes of phosphate buffer preparation.

pH	Potassium dihydrogen phosphate (g)	Di-sodium hydrogen phosphate (g)
5	0.891	0.0094
6	0.798	0.1304
7	0.371	0.6896
7.2	0.2659	0.8270

The phosphate buffer solutions at pH 2.5, 3 and 4 were prepared by weighting potassium dihydrogen phosphate 0.8982 g, dissolved with MilliQ water and after that transferred into a 100 mL volumetric flask and the volume was adjusted to 100 mL with MilliQ water. Each pH of the phosphate buffer solutions were adjusted by phosphoric acid to make the pH ranging from 2.5 to 4.

##### 3.3.1.2 Stock Standard Solution

Each stock standard solution (10 mM) of seven SAs was prepared by weighing SG 0.011 g, SDZ 0.013 g, SMZ 0.014 g, SMM 0.014 g, SMX 0.013 g, SDM 0.016 g, and SQ 0.016 g, dissolved each SAs with 50 % acetonitrile, and after that transferred into a 5 mL volumetric flask and the volume was adjusted to 5 mL with 50 % acetonitrile. All of the stock standard solutions were stored at 4 °C in amber glass.

### 3.3.1.3 Working Standard Solution

The volume of electrochemical cell for cyclic voltammetry is 3 mL. The concentrations for cyclic voltammetry were prepared by pipetting of each stock standard solution 10 mM into a 3 mL electrochemical cell. The concentration and volumes required for preparations are shown in Table 3.2.

**Table 3.2** Composition of each concentration for seven SAs in a 3 mL electrochemical cell of cyclic voltammetry

Final concentration of each SA standard solution (mM)	Concentration of Each SA stock solutions (mM)	Volume of stock solution ( $\mu\text{L}$ )	Volume of supporting electrolyte ( $\mu\text{L}$ )
0.02	10	6	2994
0.04	10	12	2988
0.06	10	18	2982
0.08	10	24	2976
0.10	10	30	2970

### 3.3.2 Preparation of Solution for HPLC-EC

#### 3.3.2.1 Mobile phase

The mobile phase for HPLC condition consisted of the phosphate buffer solution, acetonitrile and ethanol in the ratio of 80: 15: 5 (v/v/v). The phosphate buffer solution of pH 3 was prepared daily by 0.05 M potassium dihydrogen phosphate that adjusted pH by phosphoric acid. The phosphate buffer solution was filtered through a 0.45  $\mu\text{m}$  Nylon membrane filter and degas by ultrasonic bath.

### 3.3.2.2 Stock Standard Solution

A stock standard solution ( $500 \mu\text{g mL}^{-1}$ ) of each SAs was prepared by dissolving 5 mg of SA in 10 mL of an acetonitrile: Milli Q water (50: 50; v/v) solution in a volumetric flask and stored at  $4^\circ\text{C}$  in the dark.

A stock standard solution of seven SAs mixture ( $500 \mu\text{g mL}^{-1}$ ) was prepared by dissolving 5 mg of SG, SDZ, SMZ, SMM, SMX, SDM and SQ in 10 mL of an acetonitrile: Milli Q water (50: 50; v/v) solution in a volumetric flask and stored at  $4^\circ\text{C}$  in the dark.

The mixed working standard solution was prepared by suitable dilution of the stock standard solution with the mobile phase.

### 3.3.3 Preparation of Solution for Sample Preparation

#### 3.3.3.1 $\text{Na}_2\text{EDTA}$ -McIlvaine's Buffer Solution

$\text{Na}_2\text{EDTA}$ -McIlvaine buffer was the extraction solution. The pH range from 3 to 7 of  $\text{Na}_2\text{EDTA}$ -McIlvaine buffer was prepared by mixing of disodium hydrogen phosphate dihydrate, citric acid and 0.186 g of  $\text{Na}_2\text{EDTA}$  in 50 mL volumetric flask by using Milli Q water for dissolution. The weight ratios of disodium hydrogen phosphate dehydrate and citric acid were shown in Table 3.3.

**Table 3.3** The weight ratios of disodium hydrogen phosphate dehydrate and citric acid

pH	$\text{Na}_2\text{HPO}_4$ (g)	Citric acid (g)
3	0.844	0.351
4	0.651	0.676
5	0.515	0.908
7	0.1996	1.442

## 3.4 Procedure

### 3.4.1 Cyclic Voltammetry

Electrochemical measurements were performed in a single compartment three-electrode glass cell, with a volume of 3 mL. The BDD electrode was pressed against a smooth ground joint at the bottom of the cell, and isolated by placing the backside of the Si substrate onto a brass plate. The GC electrode was also used as a working electrode in a comparison study. A platinum wire and Ag/AgCl electrode with a salt bridge were used as the counter and reference electrodes, respectively. Cyclic voltammetry was carried out by an Autolab Potentiostat 100. The electrochemical equipment was housed in a faradaic cage to reduce electronic noise.

#### 3.4.1.1 pH Dependency

The pH of phosphate buffer solutions at 2.5, 3, 4, 5, 6, 7, and 7.2 were used to study the effect of electrochemical reaction of 0.1 mM SG, SDZ, SMZ, SMM, SMX, SDM and SQ. These experiments were performed to obtain the optimal pH for SAs detection. The potential was scanned from 0.6 V to 1.3 V at scan rate of 50 mV s<sup>-1</sup>.

#### 3.4.1.2 Comparison between BDD and GC electrode

The BDD and GC electrode was used to study the electrochemical reaction of SDZ. The 0.1 mM SDZ was investigated by cyclic voltammetry. The phosphate buffer solution at pH 3 was used as electrolyte. The potential was scanned from 0.6 V to 1.3 V for both electrodes. The scan rate of 50 mV s<sup>-1</sup> was used. The results obtained from cyclic voltammograms for both electrodes were compared.

### 3.4.1.3 The Scan Rate Dependence

The effect of the scan rate on the electrochemical behaviors of SAs was investigated by variation of the scan rate using cyclic voltammetry. The phosphate buffer solution (pH 3) and 0.1 mM SG, SDZ, SMZ, SMM, SMX, SDM and SQ were used in these experiments. The potential was scanned from 0.6 V to 1.3 V at a scan rate of 25, 50, 100, 150 and 200  $\text{mV s}^{-1}$ . The peak currents obtained from cyclic voltammogram at each scan rate were plotted as a function of the square root of the scan rate.

### 3.4.1.4 The Concentration Dependence

The variation of SAs concentration was investigated by cyclic voltammetry. The 0.02, 0.04, 0.06, 0.08 and 0.10 mM of seven SAs standard were studied on the electrochemical behaviors at BDD electrode. The potential was scanned from 0.6 V to 1.3 V at a scan rate of 50  $\text{mV s}^{-1}$ . The peak currents obtained from cyclic voltammogram at each concentration were plotted as a function of concentration.

## 3.4.2 High Performance Liquid Chromatography-Electrochemical Detection

The thin-layer flow cell consisted of three electrodes: a BDD working electrode, an Ag/AgCl reference electrode and a stainless steel tube counter electrode. The geometric area of the BDD electrode in the flow cell was estimated to be 0.37  $\text{cm}^2$  by using a 1 mm-thick silicon rubber gasket as a spacer. Figure 3.1 shows the thin-layer flow cell. The experiment was performed in a copper faradaic cage for reducing the electronic noise. An Autolab Potentiostat 100 was used for amperometric controlling and signals processing.

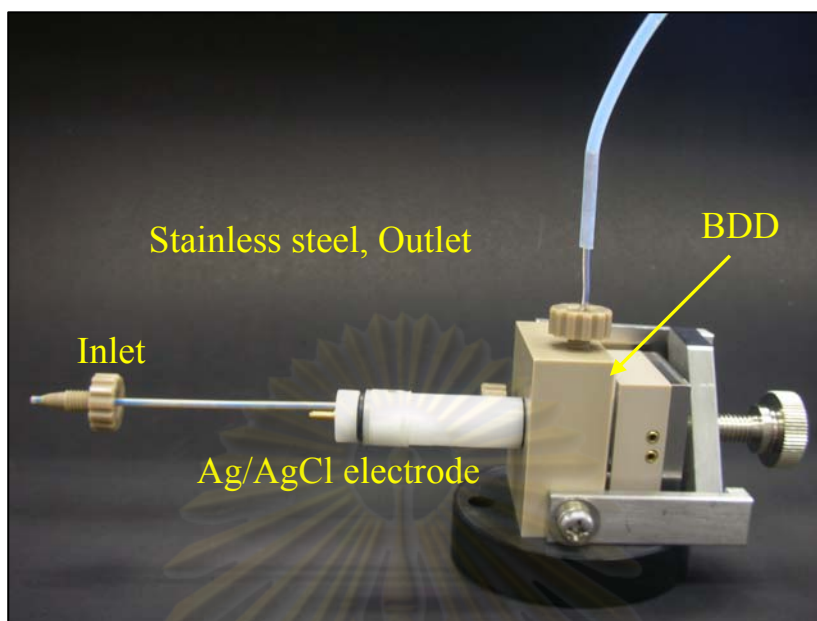


**Figure 3.1** A thin-layer flow cell

#### 3.4.2.1 Flow Rate of Mobile Phase

The flow rate of mobile phase for carrying SAs to the electrochemical flow cell was studied in the range from 0.5 to 2.0 ml min<sup>-1</sup>. The peak areas for three injections of 10 µg mL<sup>-1</sup> of mixture SAs standard were measured for each flow rates. The results obtained to use in HPLC-EC for separation and determination of SAs.

#### 3.4.2.2 Optimum Potential of Amperometry

Hydrodynamic voltammetry was employed to optimize the detection potential for SA detection before use in amperometric determination. The detection potential ranging from 1.0 V to 1.3 V versus Ag/AgCl was investigated at BDD electrode. The data were obtained by recording the background current at each potential and then injecting a series of three replicate of 20 µl of 10 µg mL<sup>-1</sup> SA solutions, respectively. The peak current after each injection was recorded, together with the corresponding background current. These data were plotted as a function of applied potential to obtain hydrodynamic voltammograms.

### 3.4.2.3 Linearity

The concentration range from 0.01 to 120  $\mu\text{g mL}^{-1}$  of the mixed standard solution of SAs was injected in three replicates of each concentration on optimal conditions of HPLC-EC at BDD electrode. The results were used to plot the calibration curve and to obtain the linear range.

### 3.4.2.4 Limit of Detection (LOD) and Limit of Quantitation (LOQ)

The calibration of the peak areas against concentrations generated linear functions for all of the analytes within a range between 0.01 and 120  $\mu\text{g mL}^{-1}$ . The slope of the linearity to obtain from section 3.4.2.3 was used to calculate of the limits of detection (LOD) and limits of quantitation (LOQ). The LOD and LOQ were calculated from  $3S_{bl}/S$  and  $10S_{bl}/S$ , where  $S_{bl}$  is the standard deviation of the blank measurement ( $n=10$ ) and  $S$  is the sensitivity of the method or the slope of the linearity.

## 3.4.3 Sample Preparation

The proposed method was applied to real samples. The real samples were fresh shrimp in local supermarket. The standard addition method was used to determine the amount of SAs in the real sample. The developed method was compared to Laboratory Center for Food and Agricultural Products Company Limited (LCFA) by using LC-MS.

### 3.4.3.1 pH Dependence of $\text{Na}_2\text{EDTA}$ -McIlvaine's Buffer Solution

The optimal pH of the  $\text{Na}_2\text{EDTA}$ -McIlvaine buffer solution for extraction of seven SA residues in shrimp was studied over the range of pH 3 to 7.

### 3.4.3.2 Comparison of SPE

The comparison between the C18 and Oasis HLB SPE cartridges was investigated. The conditions of the use of SPE procedure were 5 mL of methanol, equilibrated with 5 mL of Milli-Q water and 5 mL of Na<sub>2</sub>EDTA-McIlvaine buffer solution, pH 4. Then, 10 mL of a 10 µg ml<sup>-1</sup> SA standard mixture solution, prepared in a Na<sub>2</sub>EDTA-McIlvaine buffer solution, was loaded and 7 mL of methanol was used to elute the SAs from the SPE cartridge. The eluted fraction was dried under a gentle stream of nitrogen and reconstituted with 10 mL of the mobile phase. That injected into HPLC-EC system. The peak area obtained from both SPE cartridges was used for comparison.

### 3.4.3.3 Sample Preparation of Shrimp

Shrimp were purchased from a local supermarket. Two grams of a homogeneous shrimp sample was placed in a 20 mL-amber glass bottle, and 10 mL of Na<sub>2</sub>EDTA-McIlvaine's buffer solution was added into the bottle. The mixture was well mixed on a vortex mixer for 5 min at high speed. Then, the mixture was placed in an ultrasonic water bath following centrifugation at 3500 rpm for 10 min. The collected supernatant was continually extracted and cleaned up with 200 mg Oasis HLB SPE cartridges connected to a 12-position vacuum manifold system.

For the solid phase extraction, the SPE cartridges were conditioned with 5 mL of methanol and equilibrated with 5 mL of Milli-Q water, 5 mL of Na<sub>2</sub>EDTA-McIlvaine buffer solution. The supernatant was loaded on Oasis HLB cartridges. During this step, the SA compounds are retained on the cartridges. The SA compounds were eluted with 7 mL of methanol at a flow rate of 1 mL min<sup>-1</sup>. The eluted fraction was evaporated under a gentle stream of nitrogen and reconstituted with 10 mL of the mobile phase. The solution was filtered through a 0.45 µm nylon membrane filter before injection into the HPLC-EC system.

#### 3.4.3.4 Accuracy and Precision

For intra-day precision, the repeatability of analysis of spiked sample was studied in one day. For inter-day precision, the repeat ability of analysis of spiked sample was studied on different days. The concentration of 1.5, 5 and 10  $\mu\text{g mL}^{-1}$  was used to spike in the sample. Each level was injected in triplicate. The precision is assessed in terms of the relative standard deviation (%RSD), using the following formula:

$$\%RSD = \frac{\text{standard deviation}}{\text{Mean}} \times 100$$

The accuracy is assessed in terms of percent recovery (% recovery), using the following formula:

$$\% \text{ recovery} = \frac{\text{spike}_{\text{matrix}}}{\text{spike}_{\text{blank}}} \times 100$$

Recovery is then calculated as the percentage of the measured spike of the matrix sample relative to the measured spike of the blank control or the amount of spike added to the sample.

#### 3.4.3.5 Comparison of Methods between the HPLC-EC and HPLC-MS

The optimal conditions of HPLC-EC were applied to determine SAs in shrimp. The blank shrimp, and spiked 5, 10  $\mu\text{g mL}^{-1}$  was detected. The results of the proposed method were compared to those obtained by HPLC-MS from Laboratory Center for Food and Agricultural Products Company Limited.

## CHAPTER IV

### RESULTS AND DISCUSSION

#### 4.1 Cyclic Voltammetric Investigation

The cyclic voltammetry was used to investigate the electrochemical behavior of SG, SDZ, SMZ, SMM, SMX, SDM and SQ. This technique is very useful for studying electrochemical characteristic of seven SAs. The Ag/AgCl as reference electrode, platinum wire as counter electrode and BDD or GC electrode as working electrode were used for cyclic voltammetry. The results obtained from cyclic voltammetry were found to be suitable as condition for using in HPLC-EC such as pH of phosphate buffer solution, the range of potential detection and working electrode type.

##### 4.1.1 The Electrochemical Characteristics of SAs

Figure 4.1 showed irreversible oxidation peak of 0.1 mM SG, SDZ, SMZ, SMM, SMX, SDM and SQ in phosphate buffer solution (pH 3) at BDD electrode. The response obtained was observed on the positive scan from 0.6 to 1.3 V versus Ag/AgCl at a scan rate of 50 mV s<sup>-1</sup>. The BDD exhibited a well-defined irreversible oxidation peak of SAs at ~ 1.0 V.

ศูนย์วิทยทรัพยากร  
จุฬาลงกรณ์มหาวิทยาลัย

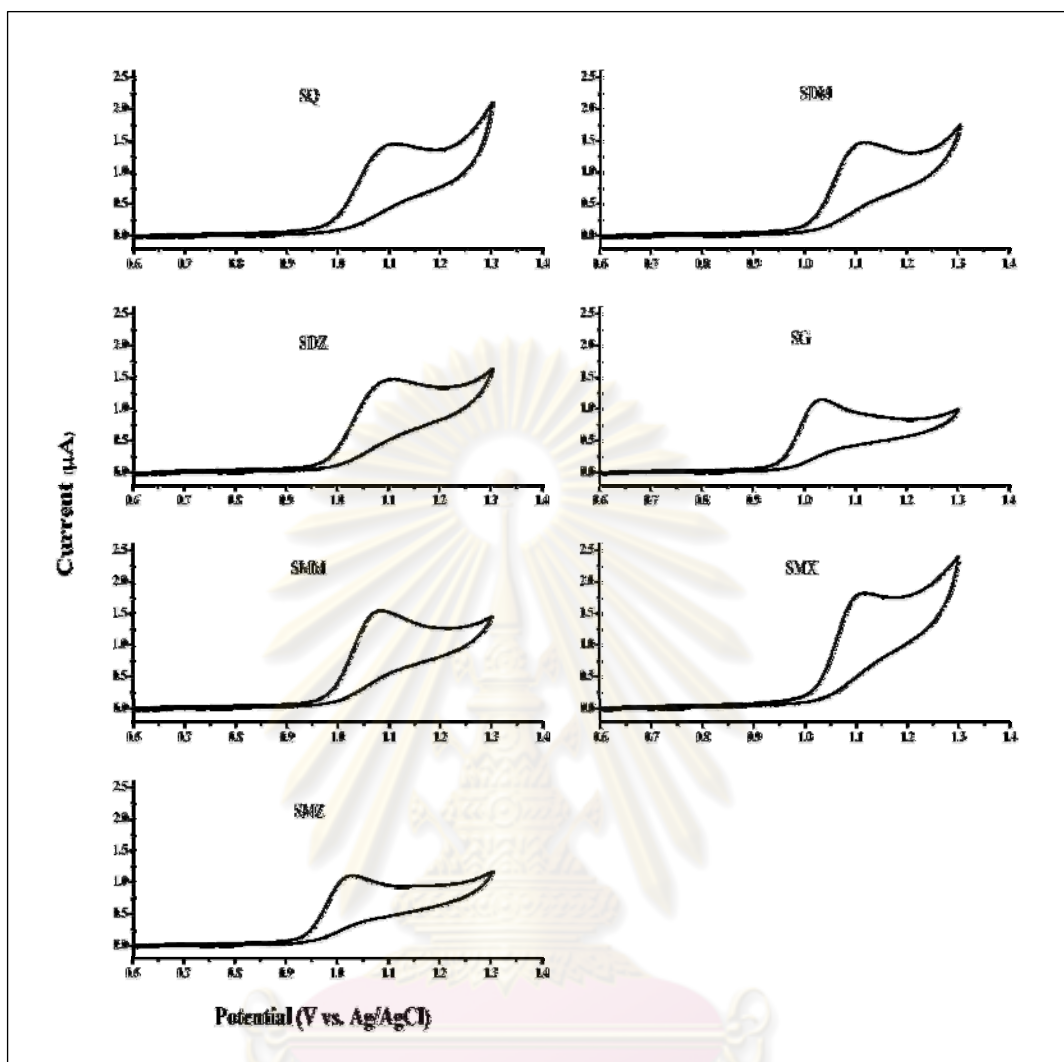


**Figure 4.1** Cyclic voltammogram of 0.1 mM seven SAs in phosphate buffer solution (pH 3) at BDD electrode. The scan rate was  $50 \text{ mV s}^{-1}$ .

จุฬาลงกรณ์มหาวิทยาลัย

### 4.1.2 pH Dependence

The influence of pH on the electrochemical oxidation of 0.1 mM SG, SDZ, SMZ, SMM, SMX, SDM and SQ was investigated by cyclic voltammetry using BDD electrode. A phosphate buffer solution was employed as a supporting electrolyte. The optimal pH of phosphate buffer was studied at pH 2.5, 3, 4, 5, 6, 7, and 7.2. The relationships between current of seven SAs and buffer pH were shown in Figure 4.2. The phosphate buffer at pH 3 was selected as optimal solution for all analytes because this pH provided low background current and also gave the best precision. Therefore, this pH was set for all subsequent work.

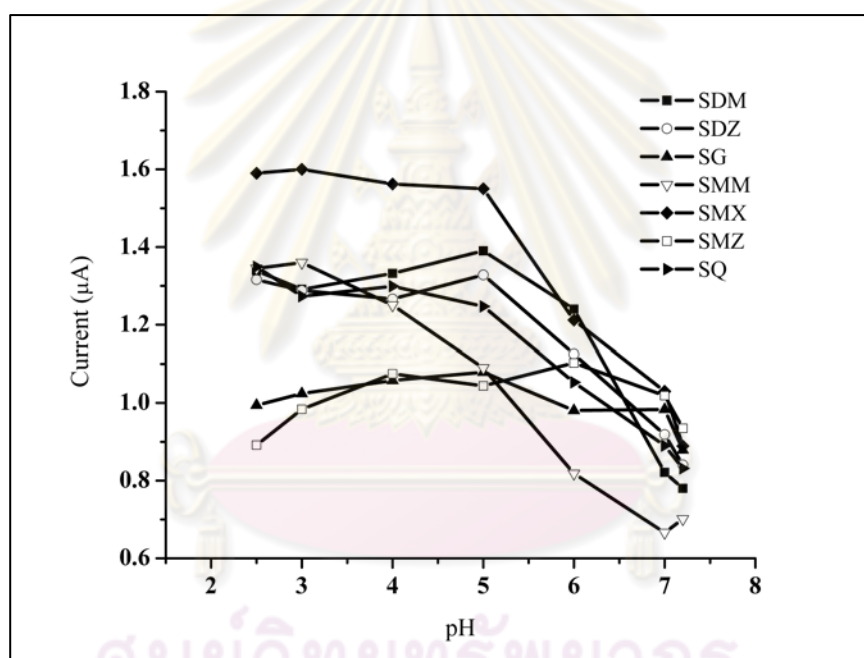


**Figure 4.2** The current of 0.1 mM seven SAs in phosphate buffer solution pH 2.5, 3.0, 4.0, 5.0, 6.0, 7.0 and 7.2, scan rate  $50 \text{ mV s}^{-1}$  using BDD electrode

### 4.1.3 Comparison between BDD and GC electrode

The background current obtained from BDD electrode was compared to those of GC electrode in phosphate buffer solution (pH 3) by cyclic voltammetry. Cyclic voltammograms of phosphate buffer solution (pH 3) at BDD and GC electrode were shown in Figure 4.3. It was observed that the background current for the BDD electrode was seven times lower than the GC electrode. The significant reason for explanation this result was that the relative absence of electroactive carbon-oxygen functionalities on the hydrogen terminated diamond surface as compared with glassy carbon.

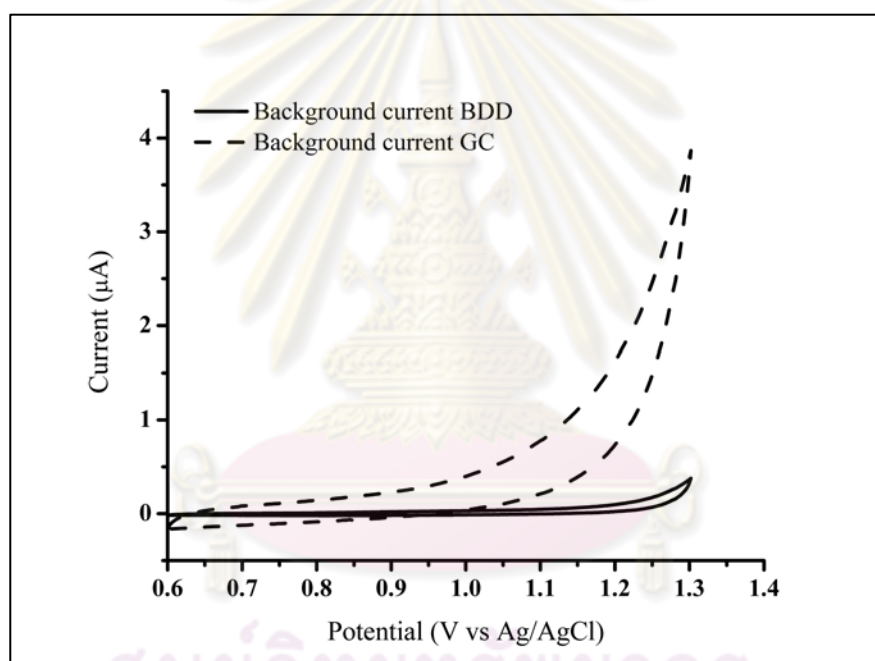


**Figure 4.3** Cyclic voltammogram of phosphate buffer solution (pH 3) at BDD and GC electrode. The scan rate was  $50 \text{ mV s}^{-1}$ .

The comparison of the voltammetric data of 0.1 mM SG, SDZ, SMZ, SMM, SMX, SDM and SQ obtained for BDD and GC electrode were shown in figure 4.4, 4.5, 4.6, 4.7, 4.8, 4.9 and 4.10, respectively at the BDD and GC electrode. It was found that the peak current of seven SAs at the BDD electrode is higher than the peak current at the GC electrode. Thus, the use of the BDD electrode for studying the electrochemical oxidation of seven SAs was more sensitive than the use of GC electrode.

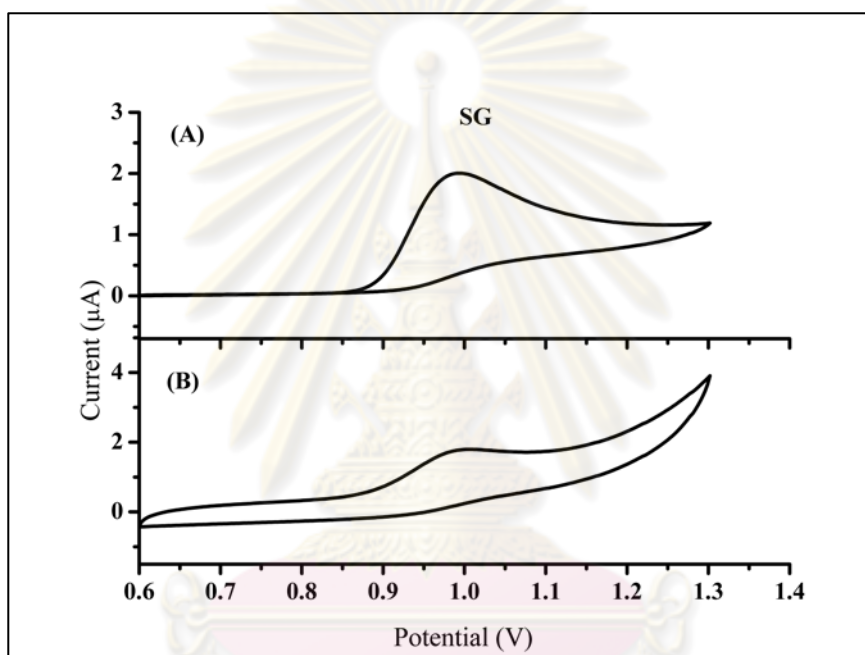


**Figure 4.4** Cyclic voltammogram of 0.1 mM SG in phosphate buffer solution pH 3 at (A) BDD and (B) GC electrode. The scan rate was 50 mV s<sup>-1</sup>.

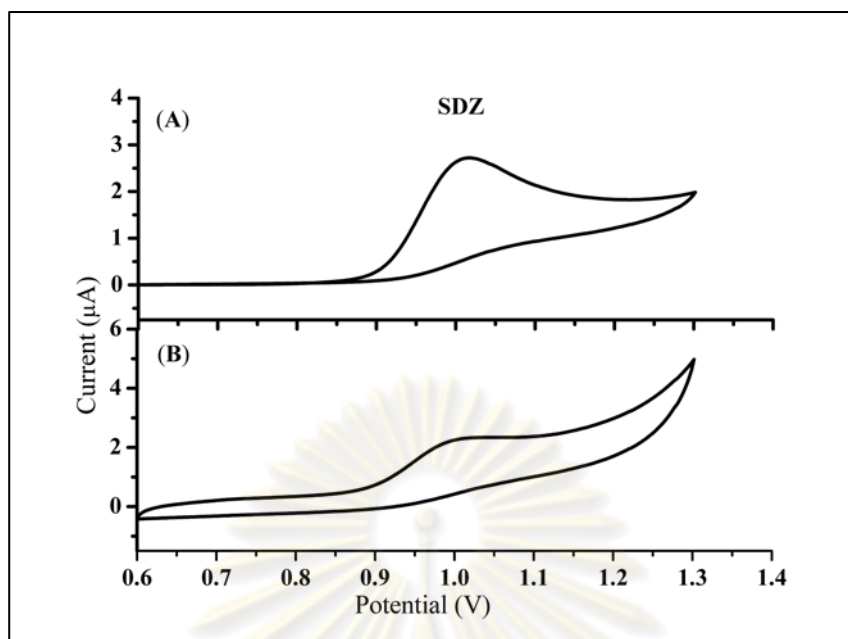


**Figure 4.5** Cyclic voltammogram of 0.1 mM SDZ in phosphate buffer solution pH 3 at (A) BDD and (B) GC electrode. The scan rate was  $50 \text{ mV s}^{-1}$ .

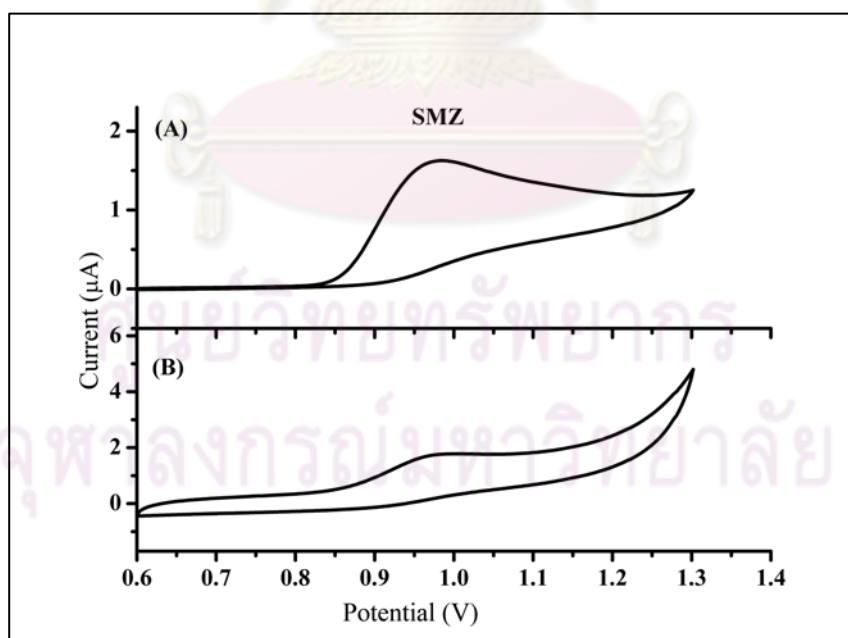


**Figure 4.6** Cyclic voltammogram of 0.1 mM SMZ in phosphate buffer solution pH 3 at (A) BDD and (B) GC electrode. The scan rate was  $50 \text{ mV s}^{-1}$ .

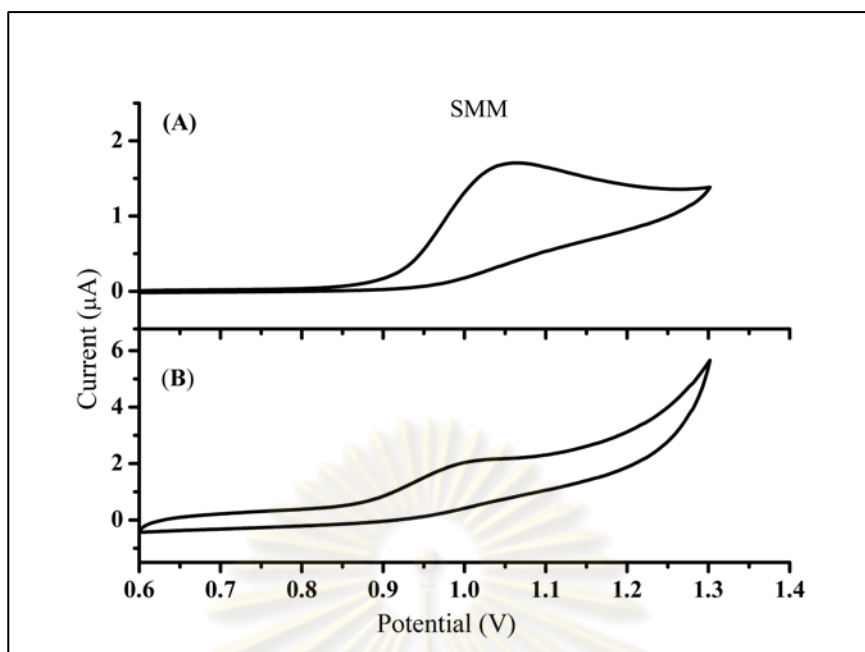


**Figure 4.7** Cyclic voltammogram of 0.1 mM SMM in phosphate buffer solution pH 3 at (A) BDD and (B) GC electrode. The scan rate was  $50 \text{ mV s}^{-1}$ .

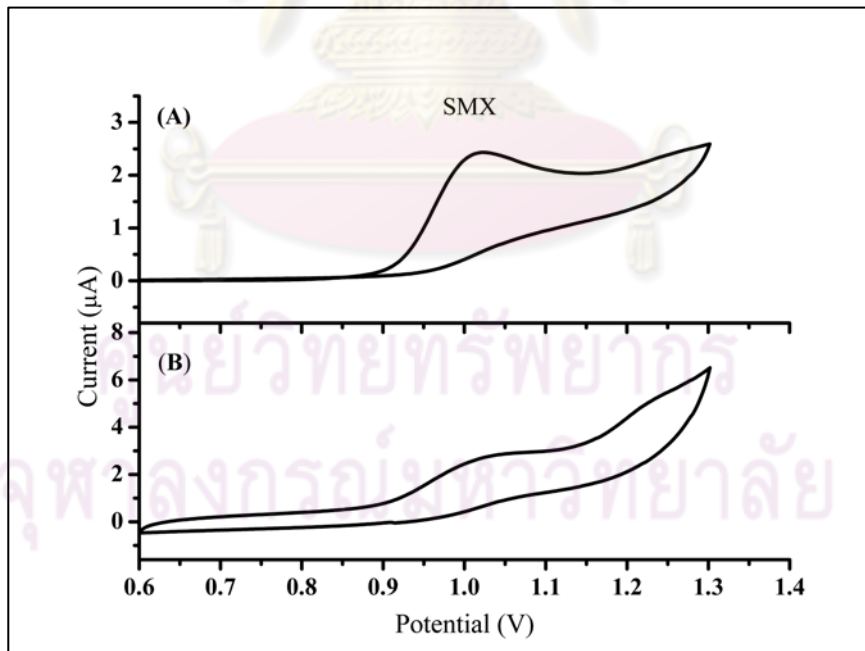


**Figure 4.8** Cyclic voltammogram of 0.1 mM SMX in phosphate buffer solution pH 3 at (A) BDD and (B) GC electrode. The scan rate was  $50 \text{ mV s}^{-1}$ .

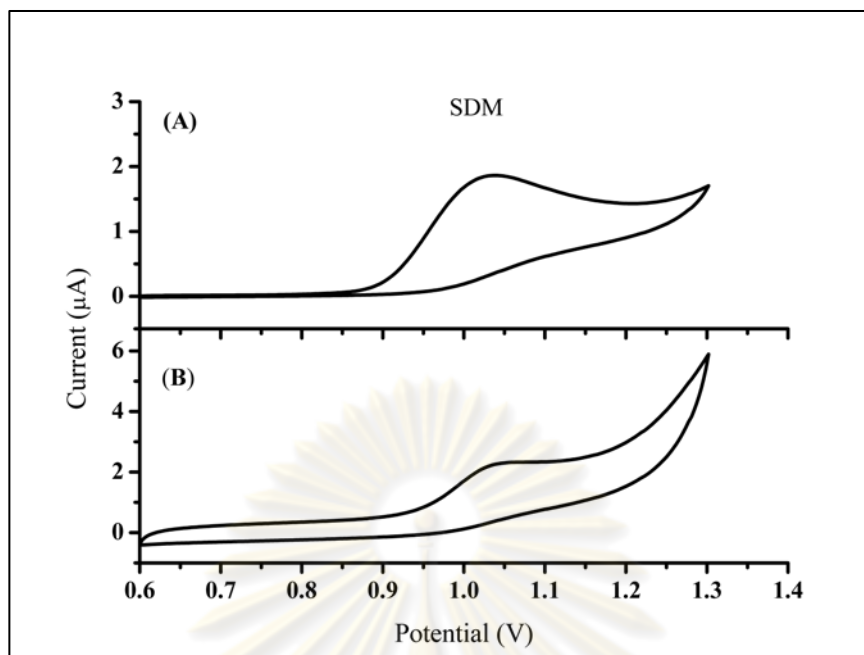


**Figure 4.9** Cyclic voltammogram of 0.1 mM SDM in phosphate buffer solution pH 3 at (A) BDD and (B) GC electrode. The scan rate was  $50 \text{ mV s}^{-1}$ .

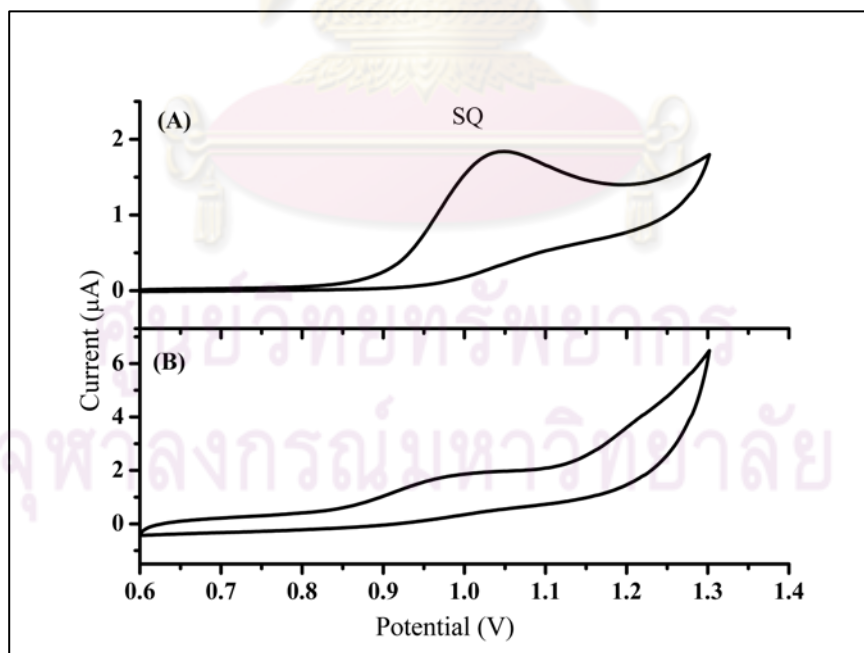


**Figure 4.10** Cyclic voltammogram of 0.1 mM SQ in phosphate buffer solution pH 3 at (A) BDD and (B) GC electrode. The scan rate was  $50 \text{ mV s}^{-1}$ .

**Table 4.1** The electrochemical data obtained from cyclic voltammograms of 0.1 mM seven SAs in phosphate buffer solution pH 3 at the BDD and GC electrode. The scan rate was 50 mV s<sup>-1</sup>.

Analyte	BDD electrode		GC electrode	
	Potential (V)	Current (μA)	Potential (V)	Current (μA)
SG	0.994	1.950	0.997	1.107
SDZ	1.015	2.647	1.012	1.613
SMZ	0.984	1.588	0.981	1.141
SMM	1.061	1.621	1.015	1.264
SMX	1.021	2.359	1.042	1.825
SDM	1.036	1.802	1.046	1.495
SQ	1.046	1.688	1.006	1.119

#### 4.1.4 The Scan Rate Dependence Study

The effect of the scan rate on the electrochemical behaviors of SG, SDZ, SMZ, SMM, SMX, SDM and SQ were investigated by varying the scan rate from 25 to 200 mV s<sup>-1</sup>. The relationship between the current and the square root of the scan rate were observed. It can be seen that the current response is directly proportional to the square root of the scan rate. From these results, it can be concluded that the reaction of these analytes is controlled by diffusion process. Figure 4.11 to 4.17 showed cyclic voltammogram of seven SAs at scan rate 25, 50, 100, 150, 200 mV s<sup>-1</sup> and the relationship between the current response and the square root of scan rate was shown inset. The equation used for explanation the relationship between the current responses and square root of scan rate for the irreversible reaction is shown below.

$$I_p(\text{diffusion}) = (2.686 \times 10^5) n^{3/2} ACD^{1/2} \nu^{1/2}$$

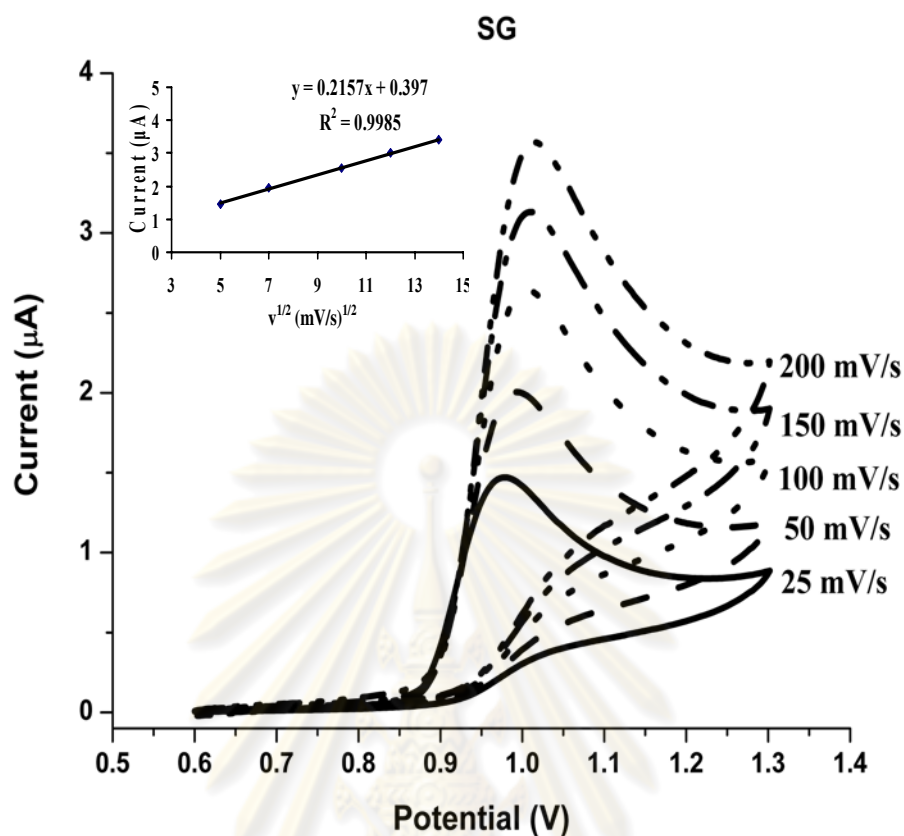


**Figure 4.11** Cyclic voltammogram of 0.1 mM SG in phosphate buffer solution (pH 3) at the BDD electrode. The scan rate was varied from 25 to 200  $\text{mV s}^{-1}$ . The relationship of the current signal to the square root of the scan rate is shown in inset.

ศูนย์วิทยทรัพยากร  
จุฬาลงกรณ์มหาวิทยาลัย

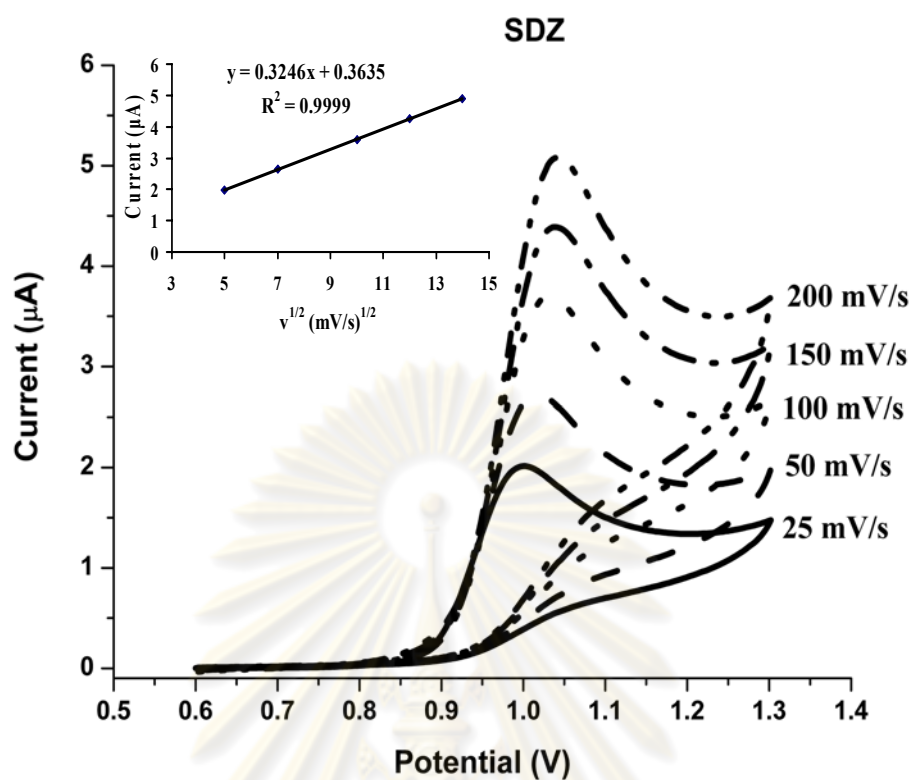


**Figure 4.12** Cyclic voltammogram of 0.1 mM SDZ in phosphate buffer solution (pH 3) at the BDD electrode. The scan rate was varied from 25 to 200  $\text{mV s}^{-1}$ . The relationship of the current signal to the square root of the scan rate is shown in inset.

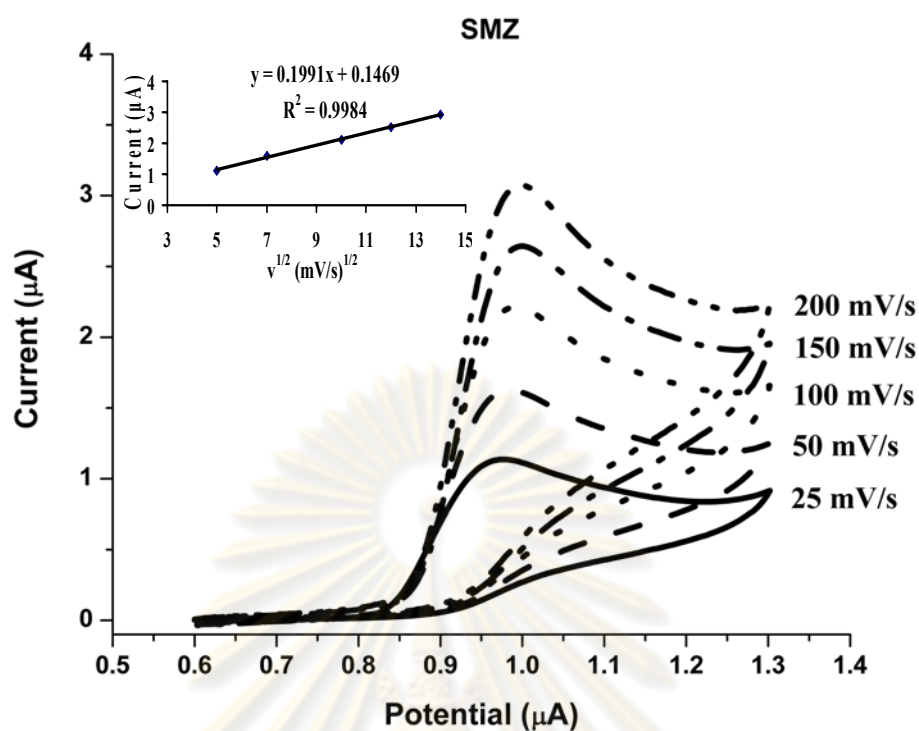


**Figure 4.13** Cyclic voltammogram of 0.1 mM SMZ in phosphate buffer solution (pH 3) at the BDD electrode. The scan rate was varied from 25 to 200  $\text{mV s}^{-1}$ . The relationship of the current signal to the square root of the scan rate is shown in inset.

ศูนย์วิทยทรัพยากร  
จุฬาลงกรณ์มหาวิทยาลัย

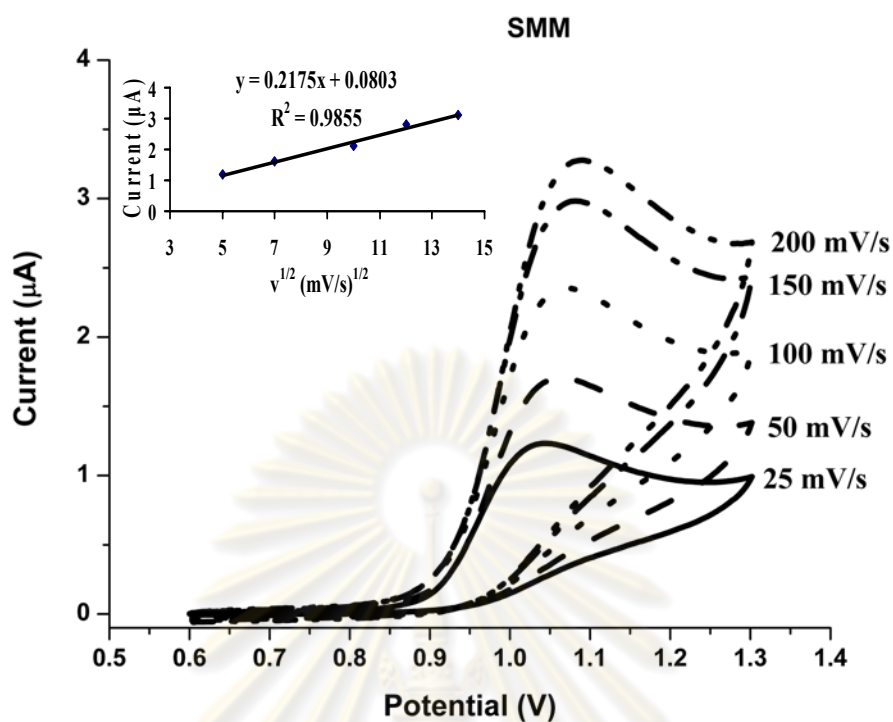


**Figure 4.14** Cyclic voltammogram of 0.1 mM SMM in phosphate buffer solution (pH 3) at the BDD electrode. The scan rate was varied from 25 to 200  $\text{mV s}^{-1}$ . The relationship of the current signal to the square root of the scan rate is shown in inset.

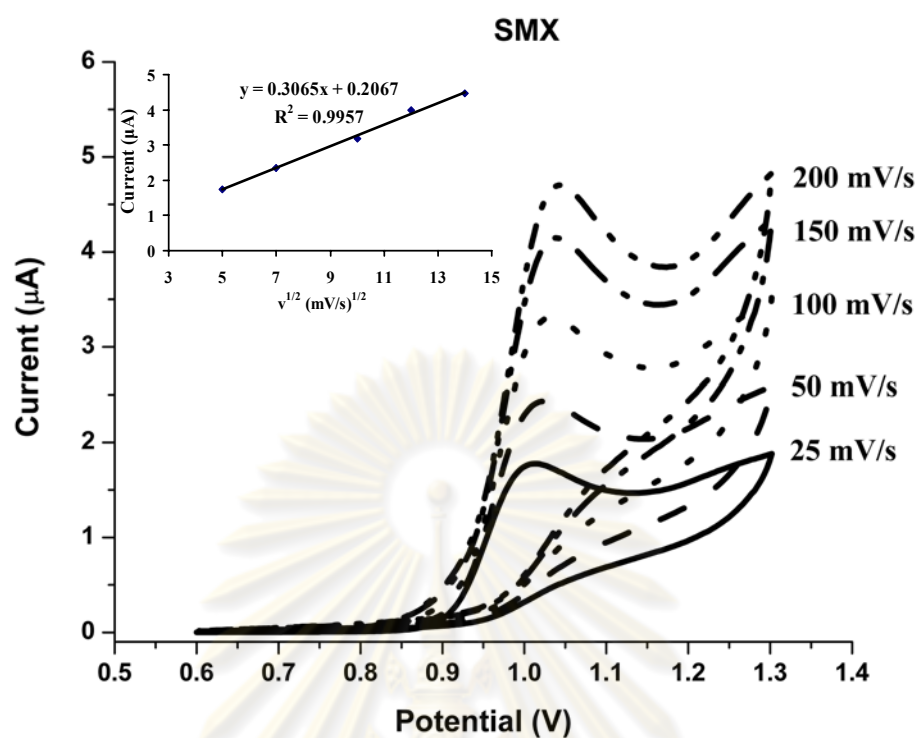


**Figure 4.15** Cyclic voltammogram of 0.1 mM SMX in phosphate buffer solution (pH 3) at the BDD electrode. The scan rate was varied from 25 to 200  $\text{mV s}^{-1}$ . The relationship of the current signal to the square root of the scan rate is shown in inset.

ศูนย์วิทยทรัพยากร  
จุฬาลงกรณ์มหาวิทยาลัย

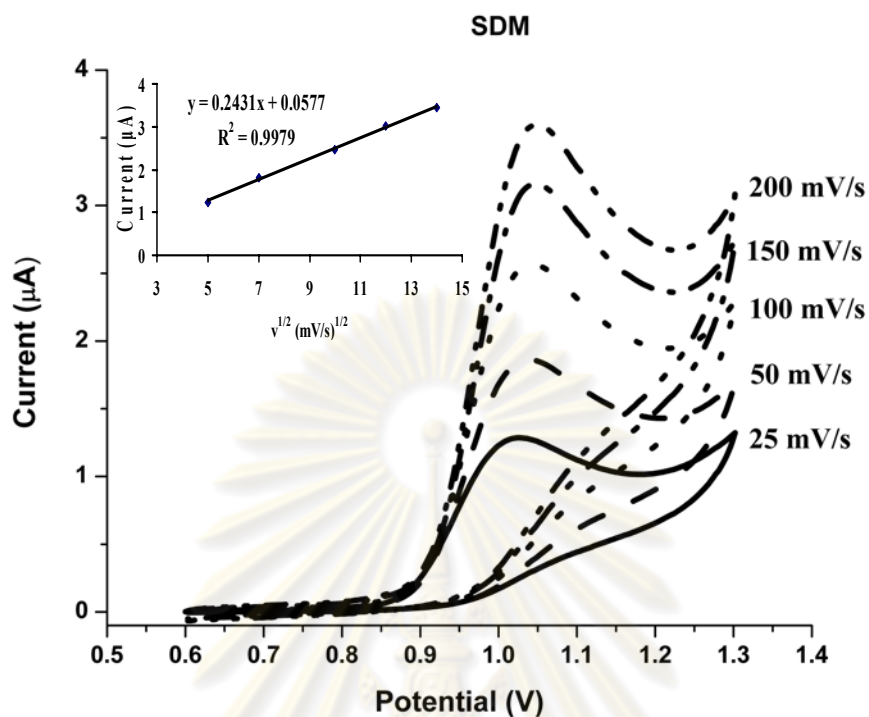


**Figure 4.16** Cyclic voltammogram of 0.1 mM SDM in phosphate buffer solution (pH 3) at the BDD electrode. The scan rate was varied from 25 to 200  $\text{mV s}^{-1}$ . The relationship of the current signal to the square root of the scan rate is shown in inset.

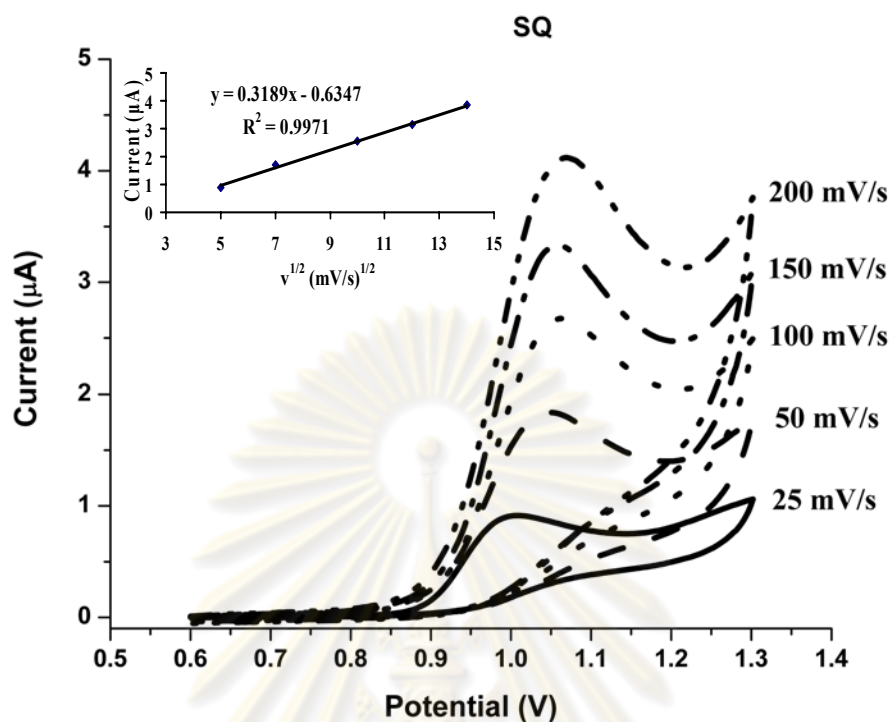


**Figure 4.17** Cyclic voltammogram of 0.1 mM SQ in phosphate buffer solution (pH 3) at the BDD electrode. The scan rate was varied from 25 to 200  $\text{mV s}^{-1}$ . The relationship of the current signal to the square root of the scan rate is shown in inset.

#### 4.1.5 The Concentration Dependence Study

The relation between voltammetric responses and concentration of SG, SDZ, SMZ, SMM, SMX, SDM and SQ were investigated by varying the concentration of these analyte. The results were shown in Figure 4.18 to 4.24. Cyclic voltammograms illustrated that the current signal increased with increasing concentrations of seven SAs. It was found that the peak current was linearly proportional to the concentration ranging from 0.02 to 0.10 mM. The linear regression analysis yields  $R^2 > 0.995$ .

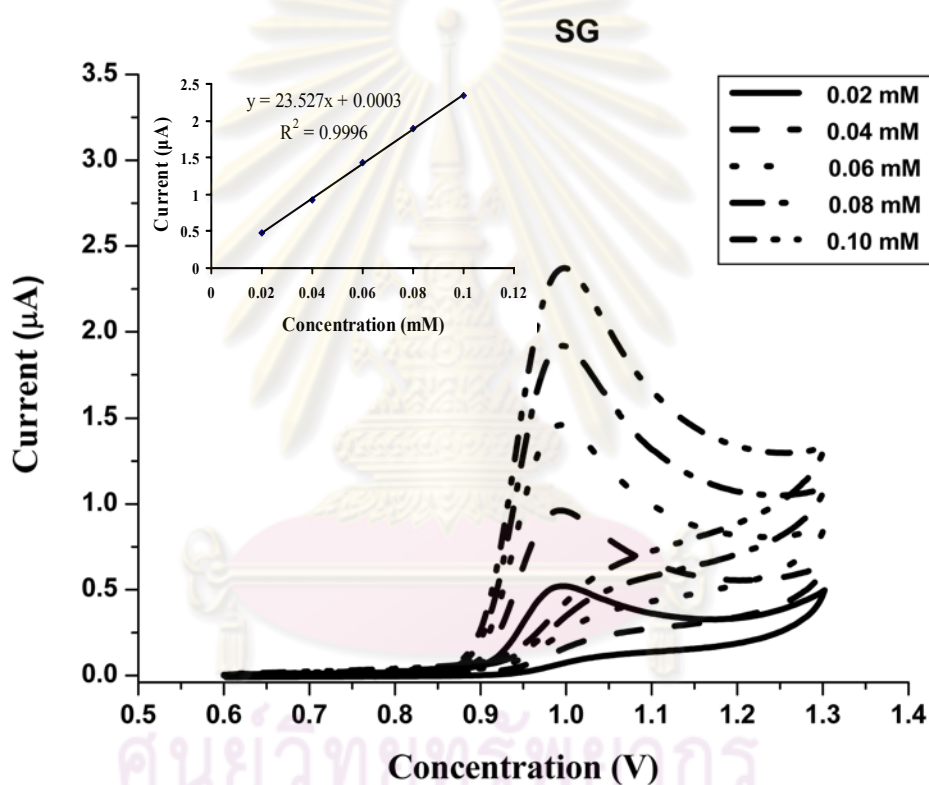


**Figure 4.18** Cyclic voltammogram of SG in phosphate buffer solution (pH 3) at the BDD electrode. The concentration was increased from 0.02 to 0.10 mM. The relationship of the current signal to the concentration is shown in inset.

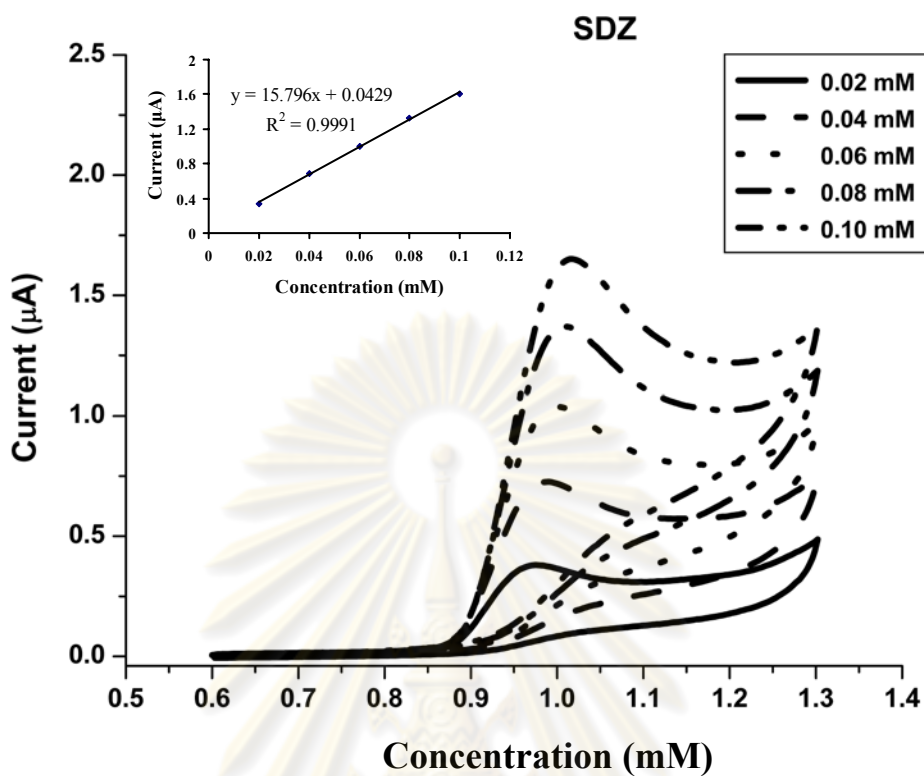


**Figure 4.19** Cyclic voltammogram of SDZ in phosphate buffer solution (pH 3) at the BDD electrode. The concentration was increased from 0.02 to 0.10 mM. The relationship of the current signal to the concentration is shown in inset.

ศูนย์วิทยทรัพยากร  
จุฬาลงกรณ์มหาวิทยาลัย

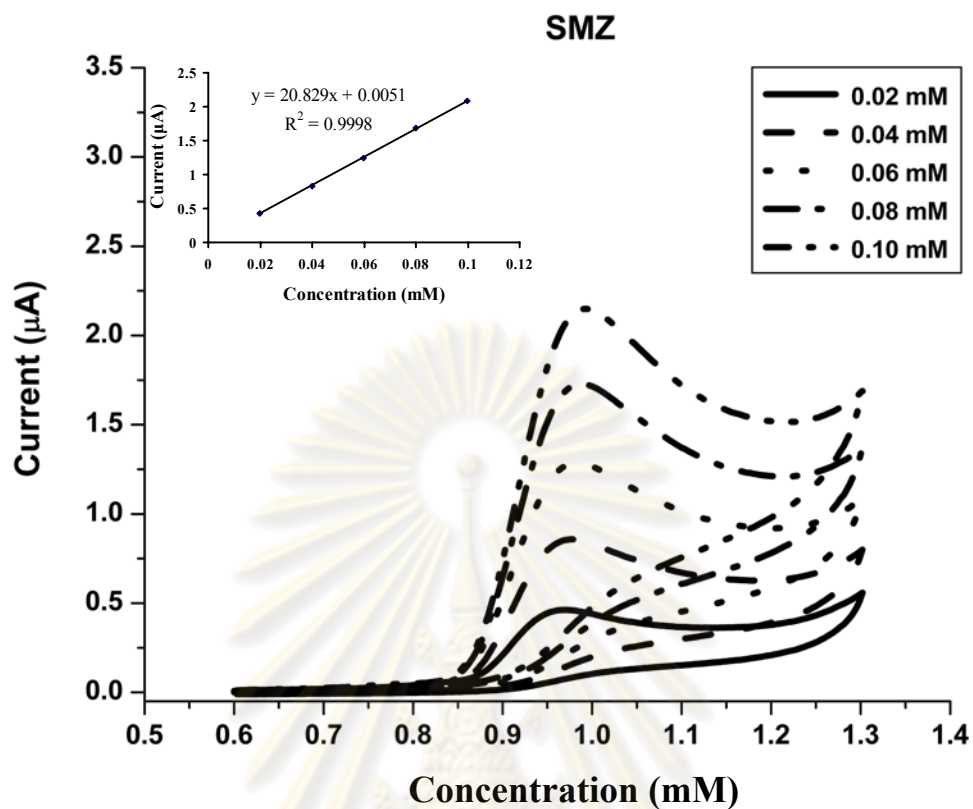


**Figure 4.20** Cyclic voltammogram of SMZ in phosphate buffer solution (pH 3) at the BDD electrode. The concentration was increased from 0.02 to 0.10 mM. The relationship of the current signal to the concentration is shown in inset.

ศูนย์วิทยทรัพยากร  
จุฬาลงกรณ์มหาวิทยาลัย

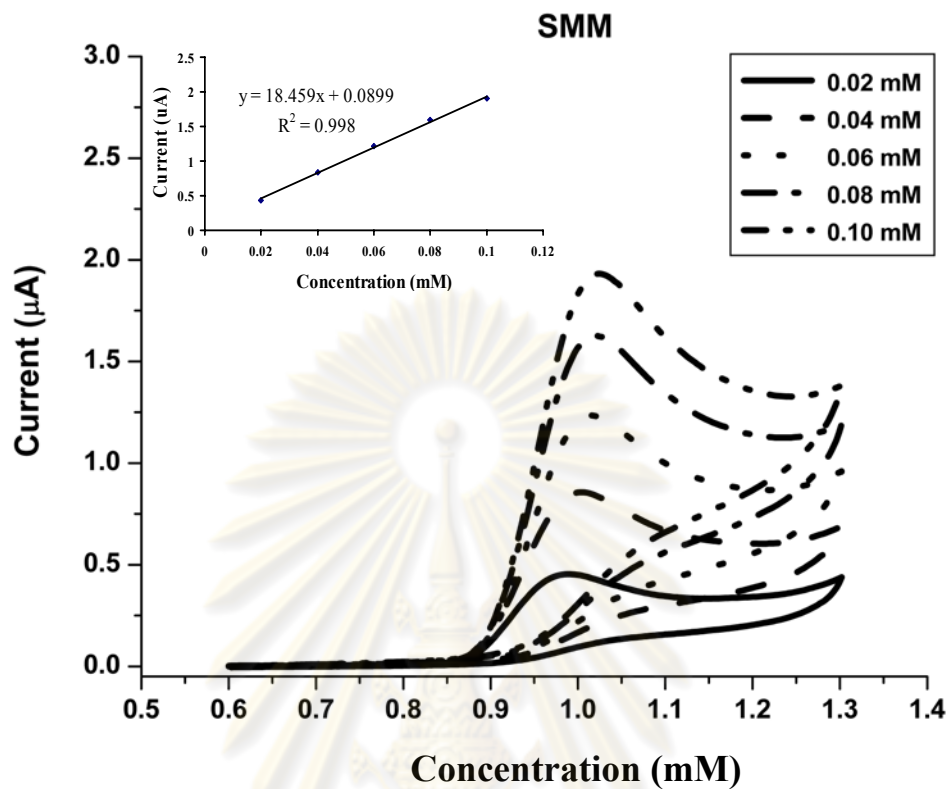


**Figure 4.21** Cyclic voltammogram of SMM in phosphate buffer solution (pH 3) at the BDD electrode. The concentration was increased from 0.02 to 0.10 mM. The relationship of the current signal to the concentration is shown in inset.

ศูนย์วิทยทรัพยากร  
จุฬาลงกรณ์มหาวิทยาลัย

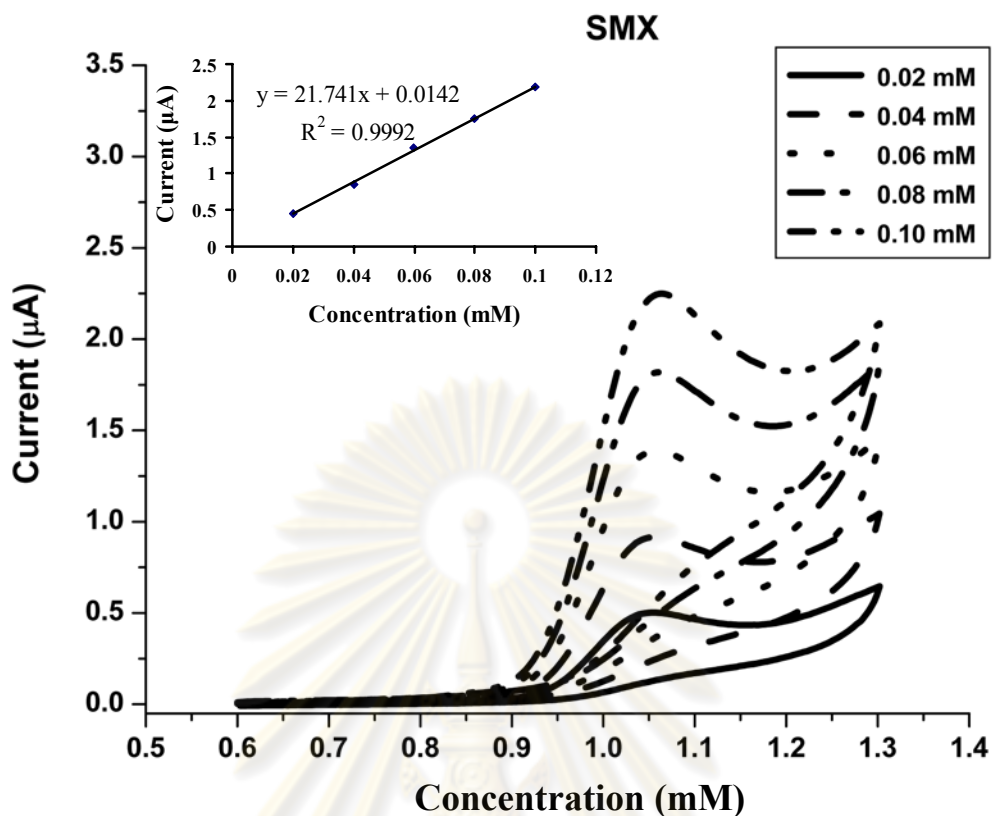


**Figure 4.22** Cyclic voltammogram of SMX in phosphate buffer solution (pH 3) at the BDD electrode. The concentration was increased from 0.02 to 0.10 mM. The relationship of the current signal to the concentration is shown in inset.

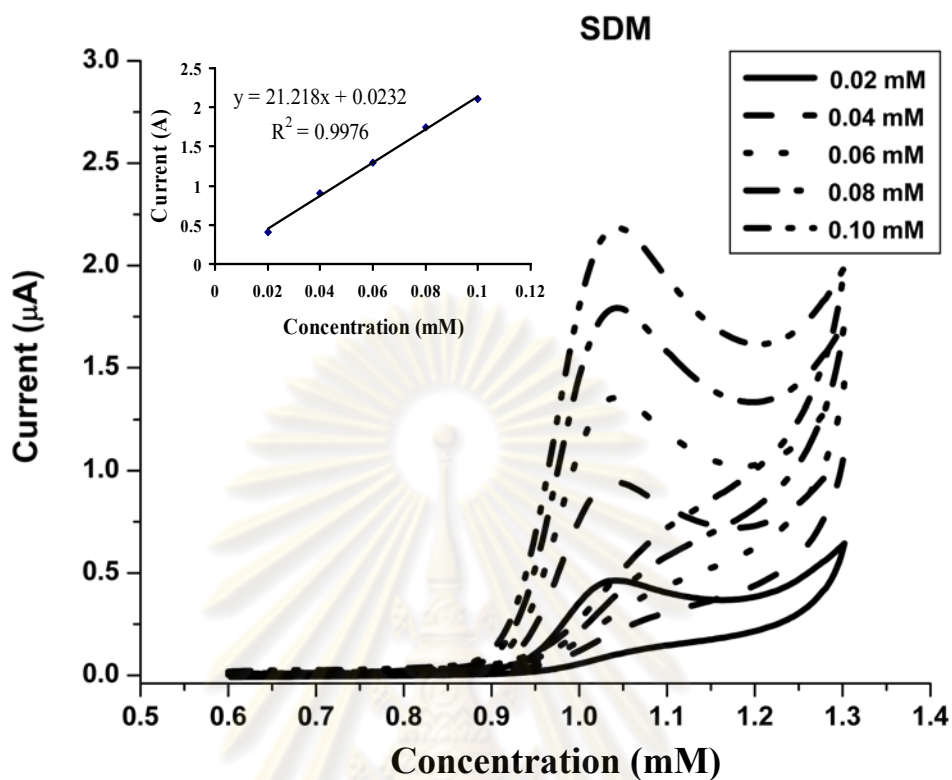


**Figure 4.23** Cyclic voltammogram of SDM in phosphate buffer solution (pH 3) at the BDD electrode. The concentration was increased from 0.02 to 0.10 mM. The relationship of the current signal to the concentration is shown in inset.

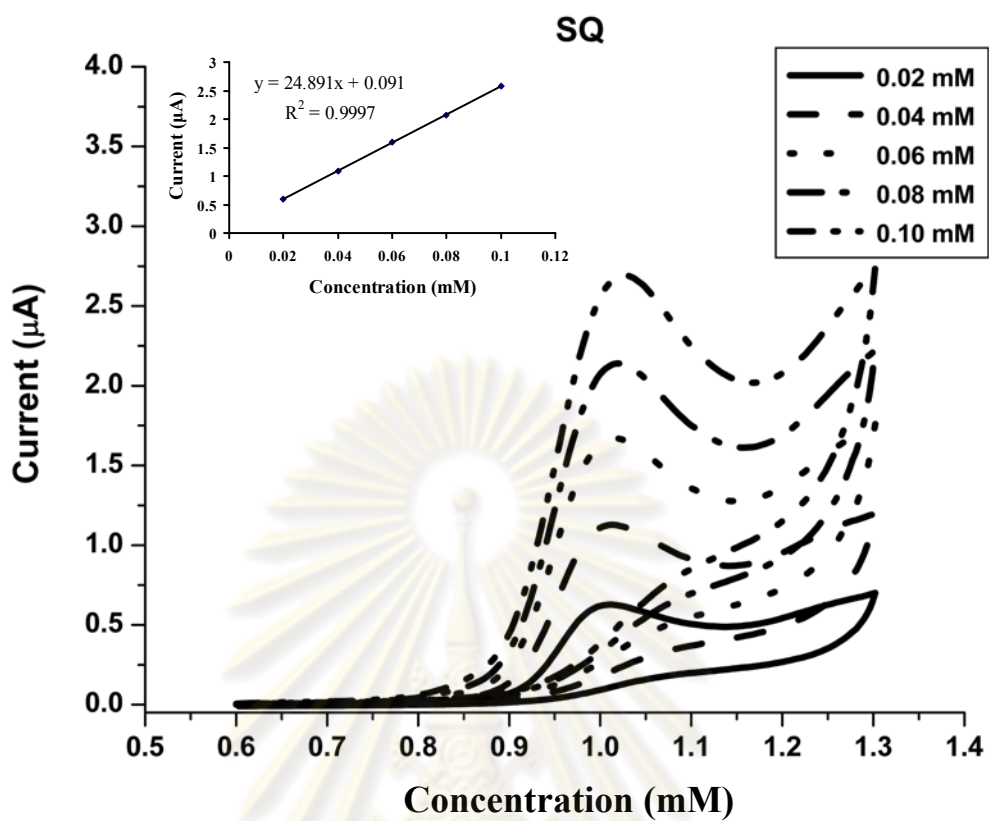


**Figure 4.24** Cyclic voltammogram of SQ in phosphate buffer solution (pH 3) at the BDD electrode. The concentration was increased from 0.02 to 0.10 mM. The relationship of the current signal to the concentration is shown in inset.

ศูนย์วิทยทรัพยากร  
จุฬาลงกรณ์มหาวิทยาลัย

## 4.2 High Performance Liquid Chromatography-Electrochemical Detection

In order to enhance the performance of separation, the monolithic column (Chromolith® Performance RP-18e silica-based 100 mm x 4.6 mm i.d.) was used to separate SG, SDZ, SMZ, SMM, SMX, SDM, SQ and detected by amperometry. The time for separation and detection was less than 8 min. The optimal condition of HPLC-EC was applied to determine seven SAs in a fresh shrimp.

### 4.2.1 Optimal Potential of Amperometry

Hydrodynamic voltammetry was employed to obtain the optimal the detection potential for SA detection. The detection potential ranging from 1.0 V to 1.3 V versus Ag/AgCl was investigated. The hydrodynamic voltammogram obtained was an average of three 20  $\mu\text{L}$ -injections of a 10  $\mu\text{g mL}^{-1}$  SA standard mixture at the BDD electrode. Figure 4.25(A) showed the hydrodynamic voltammetric i-E curve of seven SAs and the background current at each potential. The oxidation current of the SAs and the background current were significantly affected by the detection potentials. Therefore, the ratio between current and background (S/B) was considered. Figure 4.25(B) showed S/B ratios versus the potential detection. The signals increased when the potential increased up to 1.2 V versus Ag/AgCl for SMX, SDM and SQ. These three SAs had lower oxidation signals than the rest of the SAs. In order to compromise the highly sensitive detection of seven SAs in one injection, a detection potential at 1.2 V versus Ag/AgCl was selected as the optimal potential for the amperometric detection of SAs following their HPLC separation.

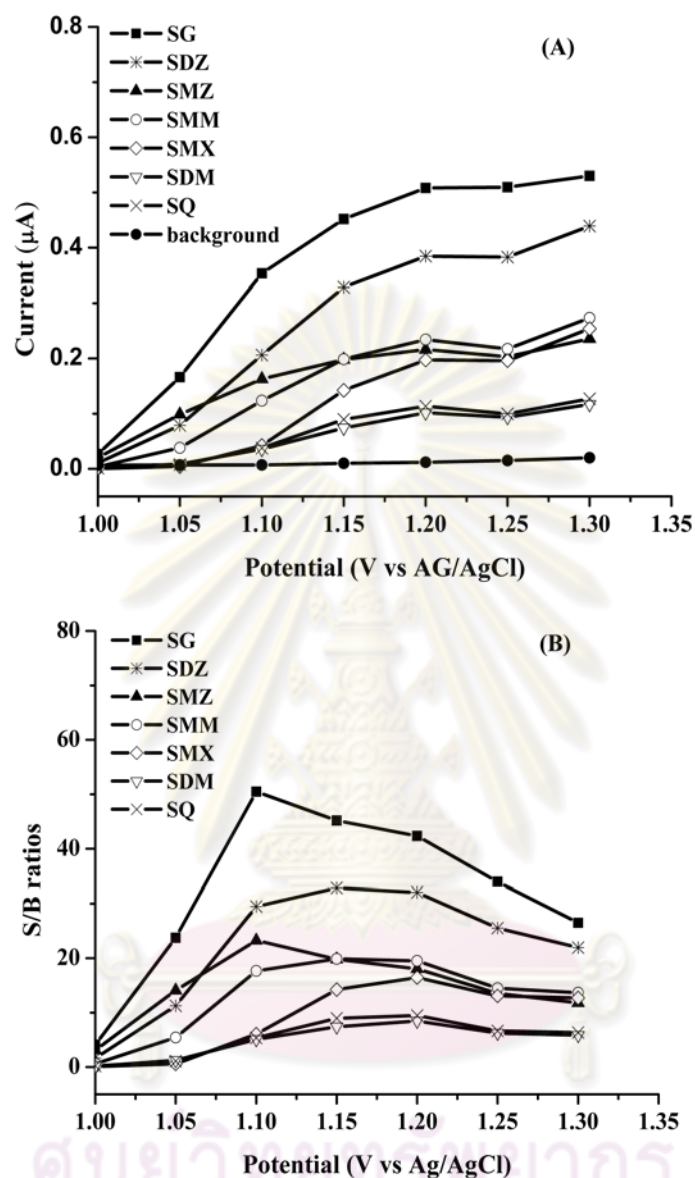


**Figure 4.25** Hydrodynamic voltammetric results for a  $10 \mu\text{g mL}^{-1}$  mixture of seven SAs at BDD electrode. (A) (■) : SG, (\*) : SDZ, (▲) : SMZ, (○) : SMM, (◇) : SMX, (▽) : SDM, (×) : SQ, (●) : background; (B) hydrodynamic voltammogram of signal-to-background ratios. The mobile phase was phosphate buffer (0.05 M, pH 3), acetonitrile and ethanol in the ratio of 80:15:5 (v/v/v). The injection volume was  $20 \mu\text{L}$ , and the flow rate was  $1.5 \text{ mL min}^{-1}$ .

#### 4.2.2 Optimal Flow Rate of Mobile Phase

The flow rate of mobile phase (phosphate buffer (0.05 M, pH 3), acetonitrile and ethanol in the ratio of 80:15:5 (v/v/v)) for carrying SAs to a thin-layer flow cell was studied in the range from 0.5 to 2.0 mL s<sup>-1</sup>. The 10 µg mL<sup>-1</sup> of seven SAs standard mixture was used to study the optimal flow rate. Figure 4.26 showed HPLC-EC chromatogram of a 10 µg mL<sup>-1</sup> of seven SAs standard mixture at various flow rate of mobile phase. As expected, the analysis time decreased when increasing the flow rate of mobile phase. The flow rate of 1.5 mL min<sup>-1</sup> was selected for the HPLC-EC experiment due to good separation, short analysis time and low reagent consumption.



ศูนย์วิทยทรัพยากร  
จุฬาลงกรณ์มหาวิทยาลัย

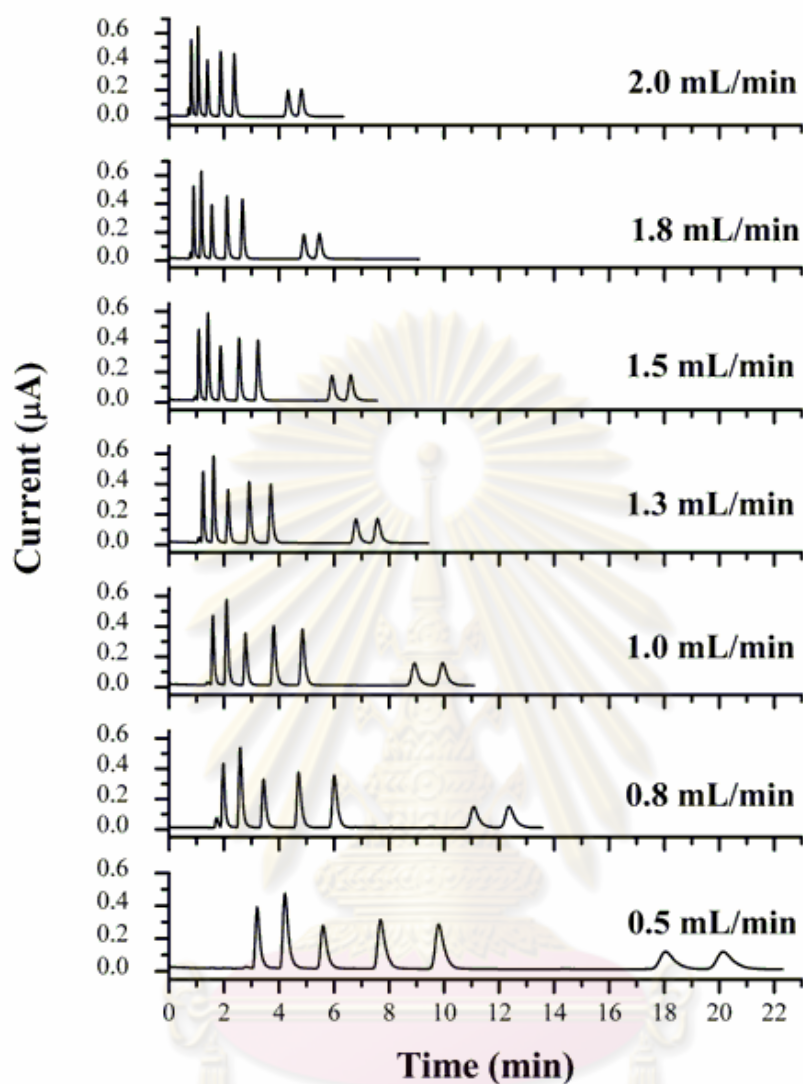


**Figure 4.26** HPLC-EC chromatograms of a  $10 \mu\text{g mL}^{-1}$  mixture of seven standard SAs at various flow rate of mobile phase

### 4.2.3 Optimal Conditions of HPLC-EC

The optimal conditions in HPLC-EC (Table 4.2) was utilized for separation of SG, SDZ, SMZ, SMM, SMX, SDM and SQ using monolithic column. The analysis time for separation and determination was less than 8 min. The chromatogram for the separation of a standard solution of seven SAs was presented in Figure 4.27. The retention times were 1.15, 1.52, 2.01, 2.79, 3.56, 6.59 and 7.35 min for SG, SDZ, SMZ, SMM, SMX, SDM and SQ, respectively. The proposed method was rapid because of the monolithic column has a total porosity higher than 80% thus it could use a higher flow rate, which leads to a faster mass transfer between the stationary and mobile phases.

**Table 4.2** The HPLC-EC conditions for the detection of seven SAs

HPLC parameters	HPLC conditions
Column	Chromolith <sup>®</sup> Performance RP-18e silica-based (100 mm x 4.6 mm i.d.)
Mobile phase	Phosphate buffer (pH 3):acetonitrile: ethanol (80:15:5, v/v/v)
Flow rate	1.5 mL/min
Injection volume	20 $\mu$ L
Temperature	25 <sup>0</sup> C
Detector	Amperometric detection at 1.2 V

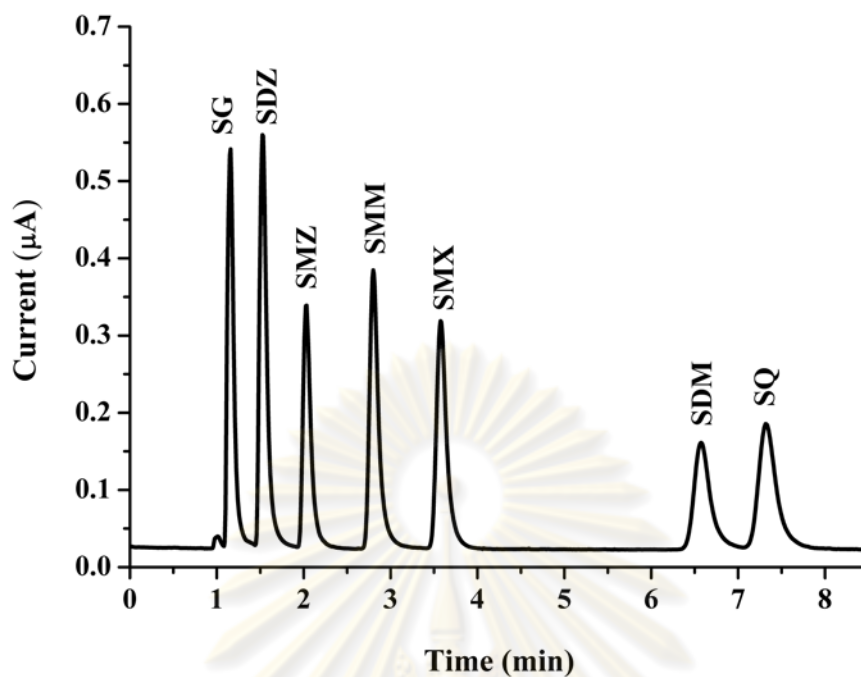


**Figure 4.27** HPLC-EC chromatogram of a  $10 \mu\text{g mL}^{-1}$  mixture of seven standard SAs separated on a monolithic column at flow rate  $1.5 \text{ mL min}^{-1}$ . The detection potential was  $1.2 \text{ V vs. Ag/AgCl}$  using a BDD electrode.

ศูนย์วิทยทรัพยากร  
จุฬาลงกรณ์มหาวิทยาลัย

#### 4.2.4 Comparison column between particles packed column and monolithic column

The  $10 \mu\text{g mL}^{-1}$  of seven SAs standard mixture were separated by Inertsil C4 (particles packed column, 4.6x150 mm.) and Chromolith® Performance RP-18e silica-based (monolithic column, 4.6x100 mm.). The optimal conditions for monolithic column were followed by Table 4.2. The best condition for Inertsil C4 column was 0.05 M phosphate buffer solution (pH 3): acetonitrile in a ratio of 82: 18 (v/v) and flow rate was  $1.0 \text{ mL min}^{-1}$ . The amperometric detection was set at 1.2 V vs Ag/AgCl at BDD electrode. Figure 4.28 illustrated HPLC-EC chromatogram of a  $10 \mu\text{g mL}^{-1}$  mixture of seven standard SAs using a particles packed column and a monolithic column. It can be observed that the use of monolithic column provided faster analysis time when compared to these of particles packed column. The analysis time was reduced from  $\sim 28 \text{ min}$  to  $\sim 8 \text{ min}$  because the low back-pressure at elevated flow rates for monolithic column was found.

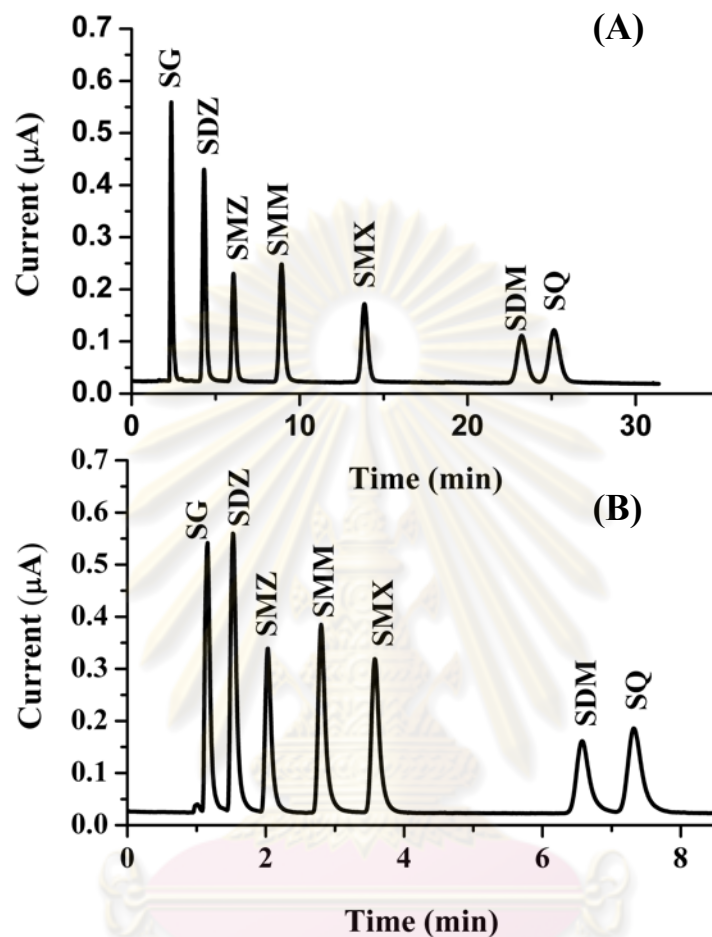


**Figure 4.28** HPLC-EC chromatogram of a  $10 \mu\text{g mL}^{-1}$  mixture of seven standard SAs separated on (A) a particles packed column and (B) monolithic column at flow rate  $1.0, 1.5 \text{ mL min}^{-1}$ , respectively. The detection potential was  $1.2 \text{ V vs. Ag/AgCl}$  using a BDD electrode.

#### 4.2.5 Calibration and Linearity

The calibration of the peak areas against concentrations was plotted. The linearities for all of the SAs within a range between 0.01 and 120  $\mu\text{g mL}^{-1}$  were observed. The coefficients ( $R^2$ ) were higher than 0.99. These calibration curves of seven SAs, shown in Figures 4.28, were obtained from triplicate analyses of each SA. The slope and y-axis intercept together with correlation coefficient of each SA were calculated according to a regression equation,  $y = mx + b$ , and was shown in Table 4.3.

**Table 4.3** Calibration characteristics of SG, SDZ, SMZ, SMM, SMX, SDM and SQ by optimal conditions of HPLC-EC at BDD electrode

Analyte	Linear dynamic range ( $\mu\text{g mL}^{-1}$ )	Slope (peak areas units/ $\mu\text{g mL}^{-1}$ )	Intercept ( $\mu\text{A}$ )	$R^2$
SG	0.01- 50	0.1964	0.0638	0.9982
SDZ	0.01- 50	0.2616	0.0659	0.9988
SMZ	0.01-100	0.1761	0.1348	0.9977
SMM	0.01-100	0.2239	0.2375	0.9961
SMX	0.01- 50	0.2285	0.0448	0.9995
SDM	0.01-120	0.1582	0.1413	0.9985
SQ	0.01-120	0.1925	0.2244	0.9980

ศูนย์วิทยทรัพยากร  
จุฬาลงกรณ์มหาวิทยาลัย

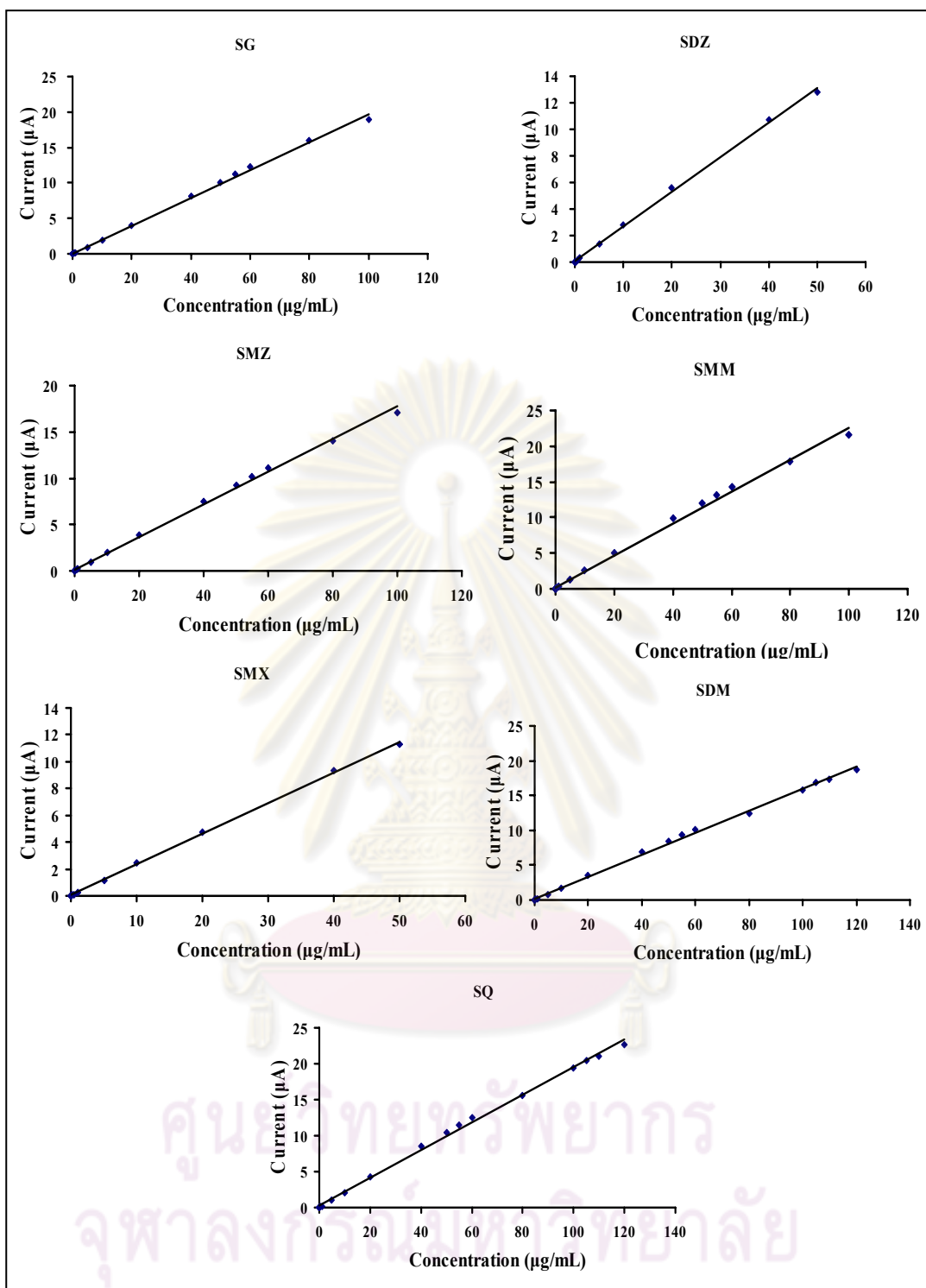


**Figure 4.29** Linearity of seven standard SAs by HPLC-EC using BDD electrode

#### 4.2.6 LOD and LOQ

The limits of detection (LOD) and limits of quantitation (LOQ) were calculated from  $3S_{bl}/S$  and  $10S_{bl}/S$ , where  $S_{bl}$  is the standard deviation of the blank measurement ( $n=10$ ) and  $S$  is the sensitivity of the method or the slope of the linearity. The slope of the linearity was obtained from Table 4.3. The LOD and LOQ were summarized in Table 4.4.

**Table 4.4** LOD and LOQ of seven standard SAs at BDD electrode.

Analyte	LOD (ng mL <sup>-1</sup> )	LOQ (ng mL <sup>-1</sup> )
SG	3.4	11.3
SDZ	1.9	6.2
SMZ	2.2	7.3
SMM	1.4	4.6
SMX	1.2	4.1
SDM	2.0	6.8
SQ	1.9	6.4

### 4.3 Application to Real Sample

The optimal conditions of HPLC-EC was applied to determine SG, SDZ, SMZ, SMM, SMX, SDM and SQ in shrimp after sample preparation by solid-phase extraction. The Na<sub>2</sub>EDTA-McIlvaine buffer solution (pH 4) was used to extract SAs in shrimp and Oasis HLB SPE was employed in cleanup step.

#### 4.3.1 pH of Extracting Solution

Na<sub>2</sub>EDTA-McIlvaine buffer solution is a popular extracting solution employed for extraction of residual SAs in animal tissues due to its enhancement the percentage recoveries. EDTA, within the Na<sub>2</sub>EDTA-McIlvaine buffer solution, acts as a chelating agent that binds with metals and cations in the matrix sample. This binding is useful for the prevention between metals/cations and the SPE cartridges, which also results in the improvement of the extraction efficiency [7, 53]. The optimal pH

of the Na<sub>2</sub>EDTA-McIlvaine buffer solution for the extraction of seven SA residues in shrimp was studied over the range of pH 3 to 7. At pH values higher than pH 5, the mixture was a jelly-like solution. It may be concern high protein and lipid concentrations in the shrimp samples. Moreover, the sample cannot be deprotonated or eluted through the SPE cartridges when using the Na<sub>2</sub>EDTA-McIlvaine buffer solution at high pH extraction. The highest percentage recoveries of the seven SAs were obtained at pH 4. At this pH, the seven SAs were kept in their neutral form because the pH of the extracting solution was lower than the pK<sub>a</sub> values of the SAs (SG: 11.3, SDZ: 6.4, SMZ: 7.5, SMM: 6.5, SMX: 5.6, SDM: 6.0 and SQ: 5.5), and had enhanced retention on the Oasis HLB cartridges. Therefore, the Na<sub>2</sub>EDTA-McIlvaine buffer solution at pH 4 was selected as the optimal pH for the extraction of seven SAs contaminated in shrimp.

#### 4.3.2 Comparison of SPE

Typically, SPE materials significantly affected the recovery. Thus, the C18 and Oasis HLB SPE cartridges were compared. The conditions of the use of SPE procedure were 5 mL of methanol, equilibrated with 5 mL of Milli-Q water and 5 mL of Na<sub>2</sub>EDTA-McIlvaine buffer solution, pH 4. Then, 10 mL of a 10 µg ml<sup>-1</sup> SA standard mixture solution, prepared in a Na<sub>2</sub>EDTA-McIlvaine buffer solution, was loaded and 7 mL of methanol was used to elute the SAs from the SPE cartridge. Figure 4.29 demonstrated the percentage recoveries obtained from the C18 and Oasis HLB cartridges for seven SAs. The Oasis HLB and C18 cartridges provided high recoveries of SMZ, SMM, SMX, SDM and SQ. For SG and SDZ, the C18 cartridges provided lower percentage recoveries than Oasis HLB cartridges, which can be explained by the polarity differences of SG and SDZ. Because of SG and SDZ are more polar than SMZ, SMM, SMX, SDM and SQ, the C18 cartridges were not suitable. In contrast, Oasis HLB can be used for a wider polarity range of analytes because it contains a mixture of hydrophilic N-vinylpyrrolidone and lipophilic divinylbenzene in its structure. Therefore, Oasis HLB cartridges were used for sample preparation in order to maximize the sensitivity.

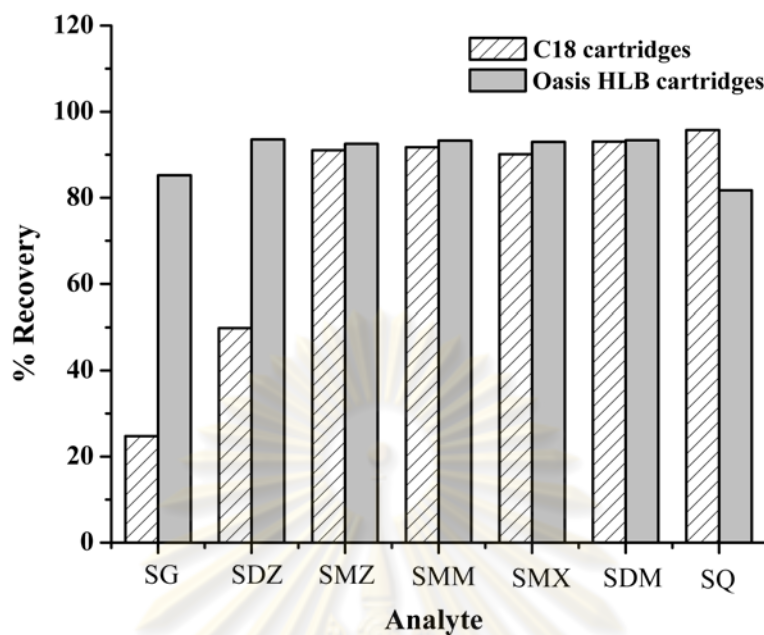


**Figure 4.30** Recoveries obtained of a  $10 \mu\text{g mL}^{-1}$  standard mixture of seven SAs using C18 and Oasis HLB cartridges.

### 4.3.3 Determination of SAs in Shrimp

To assess the applicability of the proposed method, shrimp samples from local supermarkets were investigated by standard addition. The typical chromatogram obtained from the analysis of a shrimp sample was illustrated in Figure 4.30 (B). The peaks were identified by comparison with the retention times of the reference compounds, which were determined by the injection of standard solutions (Figure 4.30(A)). The method can be used to determine SDZ, SMZ, SMM, SMX, SDM and SQ, but SG overlapped with interferences. It can be explained that protein and lipid contents in shrimp were very high although we have used  $\text{Na}_2\text{EDTA}$ -McIlvaine buffer solution and SPE for sample preparation.

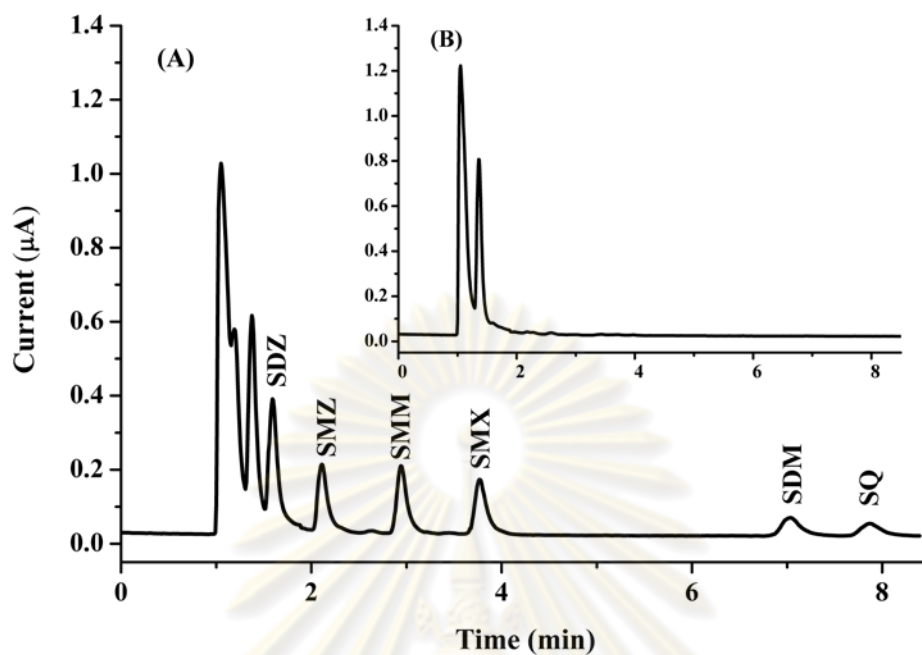
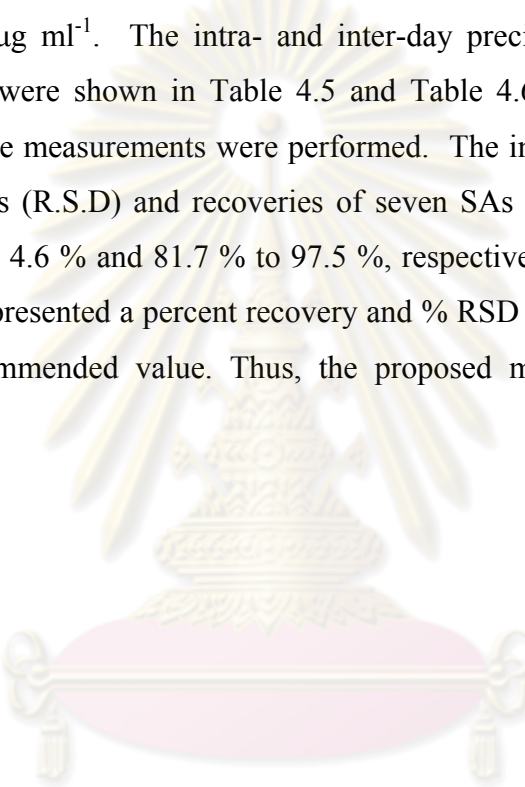


**Figure 4.31** HPLC-EC chromatogram of (A) a shrimp sample spiked with  $10 \mu\text{g mL}^{-1}$  of standard mixture of seven SAs; (B) a blank shrimp sample separated on a monolithic column ( $100 \text{ mm} \times 4.6 \text{ mm i.d.}$ ) at flow rate  $1.5 \text{ mL min}^{-1}$ . The detection potential was  $1.2 \text{ V}$  vs.  $\text{Ag/AgCl}$  using a BDD electrode.

ศูนย์วิทยทรัพยากร  
จุฬาลงกรณ์มหาวิทยาลัย

#### 4.3.4 Method Accuracy and Precision

The precision of the analytical process was calculated by determining the relative standard deviation for the repeated injection of solutions containing the complete set of standard compounds. To evaluate the repeatability of the analytical process, three concentrations (1.5, 5 and 10  $\mu\text{g ml}^{-1}$ ) were studied. These three concentration representative of low, medium and high level were investigated. The accuracy of method was calculated from the percent recovery of spiking blank shrimp at 1.5, 5 and 10  $\mu\text{g ml}^{-1}$ . The intra- and inter-day precision and recovery of the proposed method were shown in Table 4.5 and Table 4.6, respectively. For each concentration, three measurements were performed. The intra- and inter-day relative standard deviations (R.S.D) and recoveries of seven SAs were determined over the ranges of 1.0 % to 4.6 % and 81.7 % to 97.5 %, respectively. It can be seen that the proposed method presented a percent recovery and % RSD value less than the AOAC International recommended value. Thus, the proposed method was accuracy and precision.



ศูนย์วิทยทรัพยากร  
จุฬาลงกรณ์มหาวิทยาลัย

**Table 4.5** Intra-day precisions and recoveries of spiked level 1.5, 5, and 10  $\mu\text{g mL}^{-1}$  by proposed method

Analyte	Spiked level ( $\mu\text{g g}^{-1}$ )	Recovery of Intra-day (%)				
		1	2	3	mean $\pm$ SD <sup>a</sup>	R.S.D (%)
SDZ	1.5	84.8	85.9	83.9	84.8 $\pm$ 1.0	1.1
	5	80.9	81.5	83.8	82.0 $\pm$ 1.5	1.8
	10	82.4	84.4	83.2	83.3 $\pm$ 1.0	1.2
SMZ	1.5	95.9	94.4	93.8	94.6 $\pm$ 1.1	1.1
	5	87.3	90.4	88.6	88.7 $\pm$ 1.5	1.7
	10	81.5	82.2	83.5	82.3 $\pm$ 1.0	1.2
SMM	1.5	92.9	94.8	93.3	93.6 $\pm$ 1.0	1.0
	5	84.5	85.7	88.9	86.3 $\pm$ 2.3	2.6
	10	83.7	83.3	86.0	84.3 $\pm$ 1.4	1.7
SMX	1.5	91.2	89.5	91.7	90.7 $\pm$ 1.3	1.3
	5	85.5	90.1	88.2	87.9 $\pm$ 2.3	2.6
	10	85.9	83.5	83.7	84.3 $\pm$ 1.3	1.5
SDM	1.5	98.4	95.7	98.6	97.5 $\pm$ 1.6	1.6
	5	96.7	94.6	95.9	95.7 $\pm$ 1.0	1.0
	10	95.2	93.0	94.1	94.1 $\pm$ 1.6	1.1
SQ	1.5	93.7	96.7	96.2	95.5 $\pm$ 1.6	1.6
	5	95.6	92.7	97.1	95.1 $\pm$ 2.2	2.3
	10	93.6	95.9	96.9	95.0 $\pm$ 1.6	1.7

<sup>a</sup> mean of recovery (%)  $\pm$  standard deviation of triplicate measurements.

**Table 4.6** Inter-day precisions and recoveries of spiked level 1.5, 5, and 10.0  $\mu\text{g mL}^{-1}$  by proposed method

Analyte	Spiked level ( $\mu\text{g g}^{-1}$ )	Recovery of Inter-day (%)				
		1	2	3	mean $\pm$ SD <sup>a</sup>	R.S.D (%)
SDZ	1.5	89.4	85.9	84.9	86.7 $\pm$ 2.3	2.7
	5	87.9	82.0	86.1	85.3 $\pm$ 3.0	3.5
	10	85.1	81.7	83.3	83.3 $\pm$ 1.6	2.0
SMZ	1.5	94.2	96.1	94.7	94.9 $\pm$ 0.9	1.0
	5	87.2	88.8	91.0	88.9 $\pm$ 1.9	2.1
	10	82.5	80.3	82.4	81.7 $\pm$ 1.2	1.5
SMM	1.5	96.8	95.2	93.7	95.2 $\pm$ 1.5	1.6
	5	89.7	86.4	88.9	88.3 $\pm$ 1.7	1.9
	10	86.9	87.4	84.3	86.2 $\pm$ 1.6	1.9
SMX	1.5	86.9	89.7	90.8	89.1 $\pm$ 1.9	2.2
	5	91.9	87.9	96.6	92.1 $\pm$ 4.3	4.6
	10	88.5	84.1	84.4	85.6 $\pm$ 2.5	2.9
SDM	1.5	93.9	95.0	97.6	95.4 $\pm$ 1.8	1.9
	5	98.3	95.8	97.8	97.3 $\pm$ 1.3	1.4
	10	90.5	92.1	94.1	92.2 $\pm$ 1.8	1.9
SQ	1.5	97.3	94.3	95.5	95.7 $\pm$ 1.5	1.5
	5	98.6	95.2	98.2	97.3 $\pm$ 1.8	1.9
	10	92.1	91.6	95.5	93.0 $\pm$ 2.1	2.2

<sup>a</sup> mean of recovery (%)  $\pm$  standard deviation of triplicate measurements.

#### 4.3.5 Comparison of Methods between the HPLC-EC and HPLC-MS

The proposed method using monolithic column coupled with amperometric detection (HPLC-EC) for determination SDZ, SMZ, SMM, SMX, SDM and SQ of fresh shrimp in local supermarket. The optimal conditions of HPLC-EC in Table 4.2 were used to detect SAs in shrimp. The results of the proposed method was compared to those of HPLC-MS from LCFA. Three shrimp sample (blank shrimp, shrimp spiked SAs at 5 and 10  $\mu\text{g g}^{-1}$ ) were determined SAs for comparison of both methods. The results obtained by both methods are shown in Table 4.7. For comparison, a paired *t*-test at the 95% confidence interval was performed on the results obtained from shrimp spiking at level 5, 10  $\mu\text{g g}^{-1}$  ( $n=3$ ). The statistical *t*-value (4.303) was significantly higher than the experimental *t*-values between the two pairs of assays. The experimental *t*-values obtained by the proposed method were 0.710, 2.737, 0.306, 1.106, 2.722 and 0.702 for spiked concentrations at 5  $\mu\text{g g}^{-1}$  and 0.550, 0.262, 3.051, 0.055, 0.577 and 0.169 for spiked concentrations at 10  $\mu\text{g g}^{-1}$  of SDZ, SMZ, SMM, SMX, SDM and SQ, respectively. Table 4.8 summarized value of SAs concentration and *t*-test for both methods. It was successfully found that there is no significant difference between the two sets of results obtained from the proposed methodology as compared with HPLC-MS, suggesting that these results are acceptable.

ศูนย์วิทยทรัพยากร  
จุฬาลงกรณ์มหาวิทยาลัย

**Table 4.7** Comparisons results of two methods in shrimp sample

Analyte	Concentration of SAs found <sup>a</sup>	
	HPLC-EC	HPLC-MS <sup>b</sup>
<b>Blank shrimp</b>		
SDZ	ND <sup>c</sup>	ND <sup>c</sup>
SMZ	ND <sup>c</sup>	ND <sup>c</sup>
SMM	ND <sup>c</sup>	ND <sup>c</sup>
SMX	ND <sup>c</sup>	ND <sup>c</sup>
SDM	ND <sup>c</sup>	ND <sup>c</sup>
SQ	ND <sup>c</sup>	ND <sup>c</sup>
<b>Spiking at level 5 µg g<sup>-1</sup></b>		
SDZ	4.76 ± 0.36	4.60 ± 0.41
SMZ	4.71 ± 0.31	4.95 ± 0.25
SMM	4.92 ± 0.39	4.88 ± 0.48
SMX	4.76 ± 0.33	4.69 ± 0.46
SDM	4.93 ± 0.14	5.12 ± 0.20
SQ	5.04 ± 0.21	5.01 ± 0.16
<b>Spiking at level 10 µg g<sup>-1</sup></b>		
SDZ	8.82 ± 0.62	8.78 ± 0.61
SMZ	9.09 ± 0.96	9.07 ± 1.06
SMM	8.94 ± 0.22	8.83 ± 0.25
SMX	8.83 ± 0.70	8.84 ± 0.76
SDM	8.99 ± 0.27	8.88 ± 0.37
SQ	8.66 ± 0.53	8.68 ± 0.69

<sup>a</sup> Mean ± standard deviation (n=3)

<sup>b</sup> Result of Laboratory Center for Food and Agricultural product Company Limited (LCFA)

<sup>c</sup> Not detected

**Table 4.8** *t*-test values of comparison two method

Analyte	Sample	Concentration of SAs found <sup>a</sup> (5 µg g <sup>-1</sup> )		<i>t</i> -test	Concentration of SAs found <sup>a</sup> (10 µg g <sup>-1</sup> )		<i>t</i> -test
		HPLC-EC	HPLC-MS		HPLC-EC	HPLC-MS	
Sulfadiazine	Shrimp 1	4.39 ± 0.10	4.12 ± 0.24	0.710	8.17 ± 0.22	8.20 ± 0.60	0.550
	Shrimp 2	4.75 ± 0.10	4.83 ± 0.32		9.39 ± 0.32	9.42 ± 0.30	
	Shrimp 3	5.12 ± 0.22	4.85 ± 0.31		8.89 ± 0.32	8.72 ± 0.29	
Sulfamethazine	Shrimp 1	4.36 ± 0.18	4.66 ± 0.28	2.737	8.03 ± 0.13	7.98 ± 0.27	0.262
	Shrimp 2	4.95 ± 0.23	5.06 ± 0.16		9.94 ± 0.17	10.1 ± 0.26	
	Shrimp 3	4.83 ± 0.16	5.12 ± 0.19		9.31 ± 0.17	9.12 ± 0.29	
Sulfamonomethoxine	Shrimp 1	4.49 ± 0.02	4.38 ± 0.37	0.306	8.74 ± 0.23	8.65 ± 0.42	3.051
	Shrimp 2	5.04 ± 0.24	5.34 ± 0.31		9.17 ± 0.08	9.11 ± 0.24	
	Shrimp 3	5.24 ± 0.28	4.92 ± 0.49		8.90 ± 0.22	8.72 ± 0.23	
Sulfamethoxazole	Shrimp 1	4.59 ± 0.17	4.42 ± 0.13	1.106	8.41 ± 0.30	8.60 ± 1.87	0.055
	Shrimp 2	5.15 ± 0.06	5.22 ± 0.26		9.64 ± 0.09	9.69 ± 0.26	
	Shrimp 3	4.54 ± 0.15	4.44 ± 0.35		8.45 ± 0.29	8.23 ± 0.26	
Sulfadimethoxine	Shrimp 1	4.92 ± 0.13	5.18 ± 0.13	2.722	9.21 ± 0.16	9.28 ± 1.36	0.577
	Shrimp 2	5.08 ± 0.14	5.28 ± 0.22		9.06 ± 0.12	9.06 ± 0.27	
	Shrimp 3	4.79 ± 0.22	4.89 ± 0.40		8.68 ± 0.15	8.68 ± 0.27	
Sulfaquinoxaline	Shrimp 1	4.93 ± 0.21	5.03 ± 0.28	0.702	9.16 ± 0.27	9.28 ± 0.82	0.169
	Shrimp 2	4.92 ± 0.24	4.84 ± 0.20		8.11 ± 0.26	7.93 ± 0.26	
	Shrimp 3	5.28 ± 0.23	5.16 ± 0.33		8.71 ± 0.15	8.82 ± 0.26	

## CHAPTER V

### CONCLUSIONS

#### 5.1 Conclusions

A monolithic column (100x 4.6 mm) and a boron-doped diamond electrode were used to determine sulfaguanidine, sulfadiazine, sulfamethazine, sulfamonomethoxine, sulfamethoxazole, sulfadimethoxine and sulfaquinoxaline in fresh shrimp. This work demonstrated that the method was rapid, highly selective, highly sensitive, and low detection limit due to the advantages of a monolithic column and BDD electrode. A monolithic column had high porous more than 80% that can be used high flow rate leading to fast mass transfer of analytes between mobile and stationary phase and low back-pressure. Thus, the analysis time was less than 8 min that it was faster than Inertsil C4 packed column about 20 min for separation of seven SAs standard. Comparison results of seven SAs using cyclic voltammetry found that the BDD electrode provided higher signal than GC electrode. Owing to the background current obtained from the BDD electrode was smaller than that obtained from the GC electrode. Thus, BDD electrode offered the higher sensitivity.

To obtain the optimal HPLC-EC conditions, the mobile phase of phosphate buffer (0.05 M, pH3): acetonitrile: ethanol in a ratio of 80:15:5 (v/v/v) on a monolithic column at a flow rate of 1.5 mL min<sup>-1</sup> at 25 °C was set. The potential of 1.2 V versus Ag/AgCl was selected as the optimal value for SAs determination. For the validation of this method, the linearity was in the range of 0.01-50 µg mL<sup>-1</sup> for SDZ, and SMX, 0.01-100 µg mL<sup>-1</sup> for SG, SMZ, and SMM, 0.01-120 µg mL<sup>-1</sup> for SDM, and SQ. The correlation coefficient of seven SAs was > 0.995. The LOD and LOQ of this method were in the range of 1.2-3.4 and 4.1-11.3 ng mL<sup>-1</sup>, respectively. The limits of detection obtained from this method were lower than previous research as well as a maximum residue limit of EU. The recoveries of the sulfonamides in spiked shrimp samples at 1.5, 5, 10 µg g<sup>-1</sup> were in the range of 81.7 to 97.5 % with % RSD of intra-day between 1.0 and 2.6 % and % RSD of inter-day between 1.0 and 4.6 %. The percentage recoveries and RSD of proposed method were corresponding

to AOAC International. It was found that the method provided good accuracy and precision.

The proposed method using HPLC-EC and HPLC-MS of Laboratory Center for Food and Agricultural Products Company Limited (LCFA) were compared for the quantitative analysis of SDZ, SMZ, SMM, SMX, SDM, and SQ in fresh shrimp. The *t*-test method was used to compare the results obtained from both methods. The experimental *t*-test values were smaller than the statistical *t*-test. This indicated that there was no significant difference between the results obtained by the proposed method and HPLC-MS. Therefore, the proposed method could be used as an alternative method of conventional procedure.

## 5.2 Suggestion for Further Work

In this study, the real samples studied were only shrimp samples. Other samples such as milk, meat and animal feed should be of particular interest for this study as well. Moreover, the proposed method can be developed for determination of other antibiotic groups, such as chloramphenicol, nitrofurans, and tetracycline.

ศูนย์วิทยทรัพยากร  
จุฬาลงกรณ์มหาวิทยาลัย

## REFERENCES

- [1] Gehring, T. A.; Griffin, B.; Williams, R.; Geiseker, C.; Rushing, L. G.; and Siitonen, P. H. Multiresidue determination of sulfonamides in edible catfish, shrimp and salmon tissues by high-performance liquid chromatography with postcolumn derivatization and fluorescence detection. **Journal of Chromatography B** 840 (2006): 132-138.
- [2] Fang, G.; He, J.; and Wang, S. Multiwalled carbon nanotubes as sorbent for on-line coupling of solid-phase extraction to high-performance liquid chromatography for simultaneous determination of 10 sulfonamides in eggs and pork. **Journal of Chromatography A** 1127 (2006): 12-17.
- [3] Commission of the European Community. **The rules governing medical products in the European Community IV**. Brussels:1991.
- [4] Chang, H.; Hu, J.; Asami, M.; and Kunikane, S. Simultaneous analysis of 16 sulfonamide and trimethoprim antibiotics in environmental waters by liquid chromatography-electrospray tandem mass spectrometry. **Journal of Chromatography A** 1190 (2008): 390-393.
- [5] McClure, E. L.; and Wong, C. S. Solid phase microextraction of macrolide, trimethoprim, and sulfonamide antibiotics in wastewaters. **Journal of Chromatography A** 1169 (2007): 53-62.
- [6] Sheridan, R.; Policastro, B.; Thomas, S.; and Rice, D. Analysis and occurrence of 14 sulfonamide antibacterials and chloramphenicol in honey by solid-phase extraction followed by LC/MS/MS analysis. **Journal of Agricultural and Food Chemistry** 56 (2008): 3509-3516.
- [7] Koesukwiwat, U.; Jayanta, S.; and Leepipatpiboon, N. Solid-phase extraction for multiresidue determination of sulfonamides, tetracyclines, and pyrimethamine in Bovine's milk. **Journal of Chromatography A** 1149 (2007): 102-111.
- [8] Díaz-Cruz, M. S.; García-Galán, M. J.; and Barceló, D. Highly sensitive simultaneous determination of sulfonamide antibiotics and one metabolite in environmental waters by liquid chromatography-quadrupole linear ion trap-mass spectrometry. **Journal of Chromatography A** 1193 (2008): 50-59.

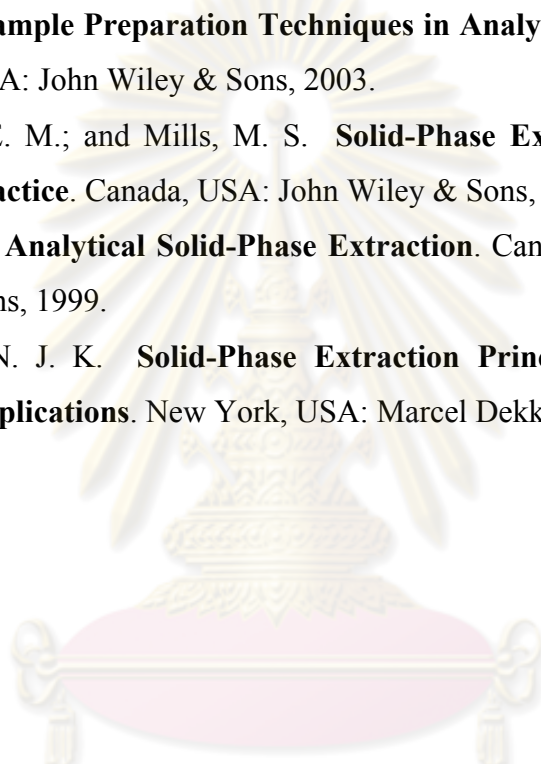
- [9] Li, H.; Kijak, P. J.; Turnipseed, S. B.; and Cui, W. Analysis of veterinary drug residues in shrimp: A multi-class method by liquid chromatography-quadrupole ion trap mass spectrometry. **Journal of Chromatography B** 836 (2006): 22-38.
- [10] Ye, Z. Q.; Weinberg, H. S.; and Meyer, M. T. Trace analysis of trimethoprim and sulfonamide, macrolide, quinolone, and tetracycline antibiotics in chlorinated drinking water using liquid chromatography electrospray tandem mass spectrometry. **Analytical Chemistry** 79 (2007): 1135-1144.
- [11] Choi, K. J.; Kim, S. G.; Kim, C. W.; and Kim, S. H. Determination of antibiotic compounds in water by on-line SPE-LC/MSD. **Chemosphere** 66 (2007): 977-984.
- [12] You, T.; Yang, X.; and Wang, E. Determination of sulfadiazine and sulfamethoxazole by capillary electrophoresis with end-column electrochemical detection. **The analyst** 123 (1998): 2357-2360.
- [13] Fuh, M. S.; and Chu, S. Quantitative determination of sulfonamide in meat by solid-phase extraction and capillary electrophoresis. **Analytica Chimica Acta** 499 (2003): 215-221.
- [14] Wang, X. L.; Li, K.; Shi, D. S., et al. Development of an immunochromatographic lateral-flow test strip for rapid detection of sulfonamides in eggs and chicken muscles. **Journal of Agricultural and Food Chemistry** 55 (2007): 2072-2078.
- [15] Furusawa, N. Rapid high-performance liquid chromatographic determining technique of sulfamonomethoxine, sulfadimethoxine, and sulfaquinoxaline in eggs without use of organic solvents. **Analytica Chimica Acta** 481 (2003): 255-259.
- [16] Granja, R. M.; Niño, A. M.; Rabone, F.; and Salerno, A. G. A reliable high-performance liquid chromatography with ultraviolet detection for the determination of sulfonamides in honey. **Analytica Chimica Acta** 613 (2008): 116-119.
- [17] Gratacós-Cubarsí, M.; Castellari, M.; Valero, A.; and García-Regueiro, J. A. A simplified LC-DAD method with an RP-C12 column for routine monitoring of three sulfonamides in edible calf and pig tissue. **Anal Bioanal Chem** 385 (2006): 1218-1224.

- [18] He, J. X.; Wang, S.; Fang, G. Z.; Zhu, H. P.; and Zhang, Y. Molecularly imprinted polymer online solid-phase extraction coupled with high-performance liquid chromatography-UV for the determination of three Sulfonamides in pork and chicken. **Journal of Agricultural and Food Chemistry** 56 (2008): 2919-2925.
- [19] Roybal, J. E.; Pfenning, A. P.; Turnipseed, S. B.; and Gonzales, S. A. Application of size-exclusion chromatography to the analysis of shrimp for sulfonamide residues. **Analytica Chimica Acta** 483 (2003): 147-152.
- [20] Wen, Y.; Zhang, M.; Zhao, Q.; and Feng, Y. Q. Monitoring of five sulfonamide antibacterial residues in milk by in-tube solid-phase microextraction coupled to high-performance liquid chromatography. **Journal of Agricultural and Food Chemistry** 53 (2005): 8468-8473.
- [21] Niu, H.; Cai, Y.; Shi, Y., et al. Evaluation of carbon nanotubes as a solid-phase extraction adsorbent for the extraction of cephalosporins antibiotics, sulfonamides and phenolic compounds from aqueous solution. **Analytica Chimica Acta** 594 (2007): 81-92.
- [22] Roudaut, B.; and Garnier, M. Sulphonamide residues in eggs following drug administration via the drinking water. **Food Additives & Contaminants: Part A** 19 (2002): 373 - 378.
- [23] Maudens, K. E.; Zhang, G. F.; and Lambert, W. E. Quantitative analysis of twelve sulfonamides in honey after acidic hydrolysis by high-performance liquid chromatography with post-column derivatization and fluorescence detection. **Journal of Chromatography A** 1047 (2004): 85-92.
- [24] Preechaworapun, A.; Chuanwatanakul, S.; Einaga, Y.; Grudpan, K.; Motomizu, S.; and Chailapakul, O. Electroanalysis of sulfonamides by flow injection system/high-performance liquid chromatography coupled with amperometric detection using boron-doped diamond electrode. **Talanta** 68 (2006): 1726-1731.
- [25] Rao, T. N.; Sarada, B. V.; Tryk, D. A.; and Fujishima, A. Electroanalytical study of sulfa drugs at diamond electrodes and their determination by HPLC with amperometric detection. **Journal of Electroanalytical Chemistry** 491 (2000): 175-181.

- [26] Guiochon, G. Monolithic columns in high-performance liquid chromatography. **Journal of Chromatography A** 1168 (2007): 101-168.
- [27] Unger, K. K.; Skudas, R.; and Schulte, M. M. Particle packed columns and monolithic columns in high-performance liquid chromatography-comparison and critical appraisal. **Journal of Chromatography A** 1184 (2008): 393-415.
- [28] Tanaka, N.; and Kobayashi, H. Monolithic columns for liquid chromatography. **Analytical and Bioanalytical Chemistry** 376 (2003): 298-301.
- [29] Hosoya, K.; Hira, N.; Yamamoto, K.; Nishimura, M.; and Tanaka, N. High-performance polymer-based monolithic capillary column. **Analytical Chemistry** 78 (2006): 5729-5735.
- [30] Núñez, O.; Nakanishi, K.; and Tanaka, N. Preparation of monolithic silica columns for high-performance liquid chromatography. **Journal of Chromatography A** 1191 (2008): 231-252.
- [31] Barbero, G. F.; Liazid, A.; Palma, M.; and Barroso, C. G. Fast determination of capsaicinoids from peppers by high-performance liquid chromatography using a reversed phase monolithic column. **Food Chemistry** 107 (2008): 1276-1282.
- [32] Tzanavaras, P. D.; and Themelis, D. G. Development and validation of a high-throughput high-performance liquid chromatographic assay for the determination of caffeine in food samples using a monolithic column. **Analytica Chimica Acta** 581 (2007): 89-94.
- [33] Muñiz -Valencia, R.; Gonzalo-Lumbreras, R.; Santos-Montes, A.; and Izquierdo-Hornillos, R. Liquid chromatographic method development for anabolic androgenic steroids using a monolithic column: Application to animal feed samples. **Analytica Chimica Acta** 611 (2008): 103-112.
- [34] Viñas, P.; Soler-Romera, M. J.; and Hernández-Córdoba, M. Liquid chromatographic determination of phenol, thymol and carvacrol in honey using fluorimetric detection. **Talanta** 69 (2006): 1063-1067.

- [35] García-Jiménez, J. F.; Valencia, M. C.; and Capitán-Vallvey, L. F. Simultaneous determination of antioxidants, preservatives and sweetener additives in food and cosmetics by flow injection analysis coupled to a monolithic column. **Analytica Chimica Acta** 594 (2007): 226-233.
- [36] Samanidou, V. F.; Ioannou, A. S.; and Papadoyannis, I. N. The use of a monolithic column to improve the simultaneous determination of four cephalosporin antibiotics in pharmaceuticals and body fluids by HPLC after solid phase extraction--a comparison with a conventional reversed-phase silica-based column. **Journal of Chromatography B** 809 (2004): 175-182.
- [37] Deeb, S. E.; Preu, L.; and Wätzig, H. Evaluation of monolithic HPLC columns for various pharmaceutical separations: Method transfer from conventional phases and batch to batch repeatability. **Journal of Pharmaceutical and Biomedical Analysis** 44 (2007): 85-95.
- [38] Seifrtová, M.; Pena, A.; Lino, C.; and Solich, P. Determination of fluoroquinolone antibiotics in hospital and municipal wastewaters in Coimbra by liquid chromatography with a monolithic column and fluorescence detection. **Analytical and Bioanalytical Chemistry** 391 (2008): 799-805.
- [39] Kishida, K.; and Furusawa, N. Matrix solid-phase dispersion extraction and high-performance liquid chromatographic determination of residual sulfonamides in chicken. **Journal of Chromatography A** 937 (2001): 49-55.
- [40] Skoog, D. A.; West, D. M.; and Holler, F. J. **Fundamentals of Analytical Chemistry**. 7th ed. New York, USA: Saunders College Publishing 1996.
- [41] Harvey, D. **Modern Analytical Chemistry**. USA: The McGraw-Hill, 1976.
- [42] Christian, G. D.; and O'Reilly, J. E. **Instrument Analysis**. 2nd ed: Allyn and Eacon, Inc, 1978.
- [43] Poole, F. C. **The essence of chromatography**. Danvers, USA: Clearance center, Inc., 2003.
- [44] Plambeck, J. A. **Electroanalytical Chemistry Basic Principles and Applications**. New York, USA: John Wiley, 1982.

- [45] Skoog, D. A.; Holler, F. J.; and Nieman, T. A. **Principles of Instrument Analysis**. New York, USA: Harcourt Brace College Publishers, 1998.
- [46] Braun, R. D. **Introduction to Instrumental Analysis**. Singapore: McGraw-Hill Book 1987.
- [47] Harris, D. C. **Quantitative chemical analysis**. 7th ed. California, USA: W.H. Freeman and company
- [48] Settle, F. A. **Handbook of Instrumental Techniques for Analytical Chemistry**. New Jersey, USA: Prentice Hall PTR, 1997.
- [49] Mitra, S. **Sample Preparation Techniques in Analytical Chemistry**. Canada, USA: John Wiley & Sons, 2003.
- [50] Thurman, E. M.; and Mills, M. S. **Solid-Phase Extraction Principles and Practice**. Canada, USA: John Wiley & Sons, 1998.
- [51] Fritz, J. S. **Analytical Solid-Phase Extraction**. Canada, USA: John Wiley & Sons, 1999.
- [52] Simpson, N. J. K. **Solid-Phase Extraction Principles, Techniques, and Applications**. New York, USA: Marcel Dekker, 2000.



ศูนย์วิทยทรัพยากร  
จุฬาลงกรณ์มหาวิทยาลัย



**APPENDICES**

ศูนย์วิทยทรัพยากร  
จุฬาลงกรณ์มหาวิทยาลัย

## APPENDIX A

## The Scan Rate Dependence Study at GC Electrode

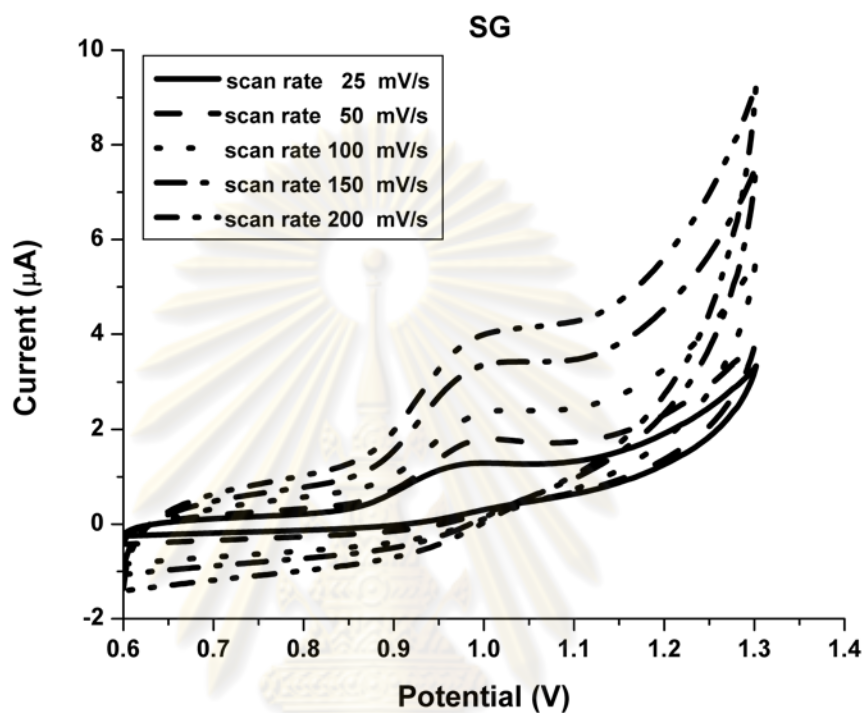


**Figure A1** Cyclic voltammogram of 0.1 mM SG in phosphate buffer solution (pH 3) at the GC electrode. The scan rate was from 25 to 200  $\text{mV s}^{-1}$ .

ศูนย์วิทยทรัพยากร  
จุฬาลงกรณ์มหาวิทยาลัย

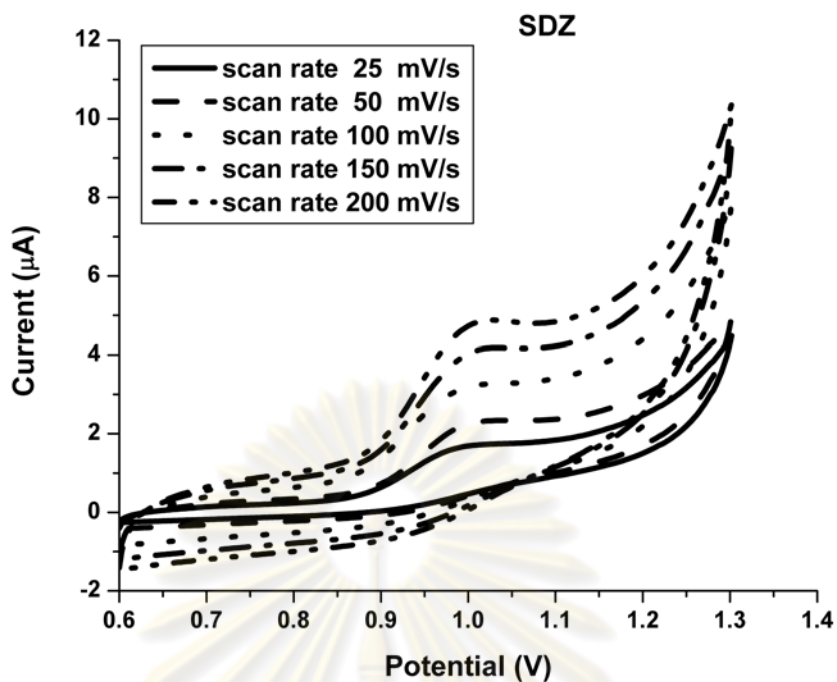


**Figure A2** Cyclic voltammogram of 0.1 mM SDZ in phosphate buffer solution (pH 3) at the GC electrode. The scan rate was from 25 to 200  $\text{mV s}^{-1}$ .

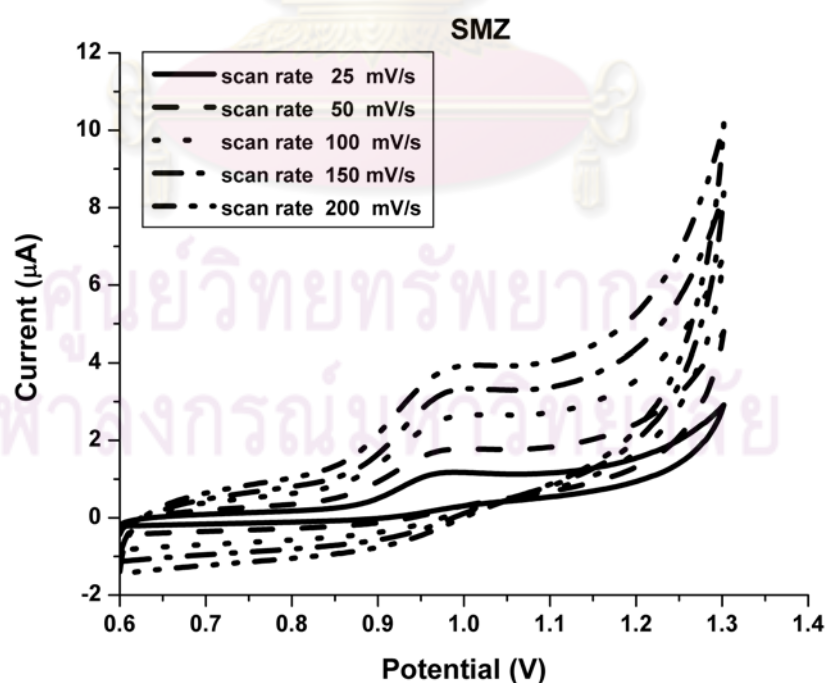


**Figure A3** Cyclic voltammogram of 0.1 mM SMZ in phosphate buffer solution (pH 3) at the GC electrode. The scan rate was from 25 to 200  $\text{mV s}^{-1}$ .

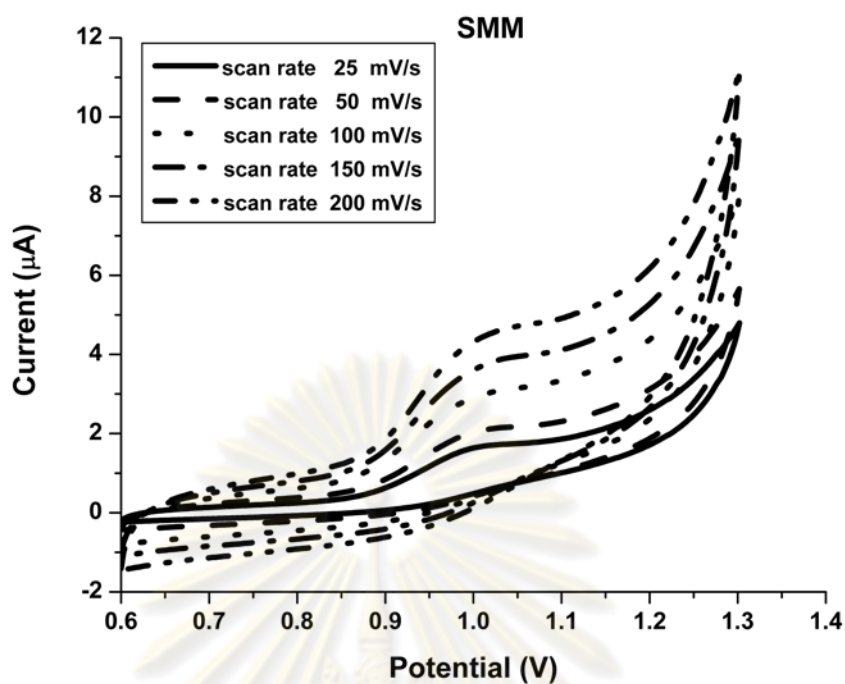


**Figure A4** Cyclic voltammogram of 0.1 mM SMM in phosphate buffer solution (pH 3) at the GC electrode. The scan rate was from 25 to 200  $\text{mV s}^{-1}$ .

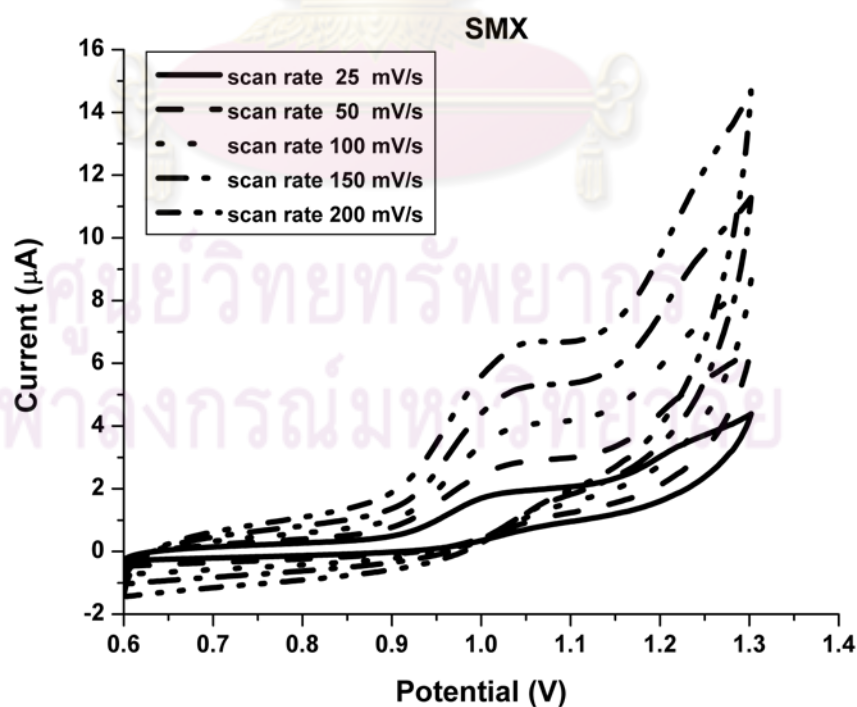


**Figure A5** Cyclic voltammogram of 0.1 mM SMX in phosphate buffer solution (pH 3) at the GC electrode. The scan rate was from 25 to 200  $\text{mV s}^{-1}$ .

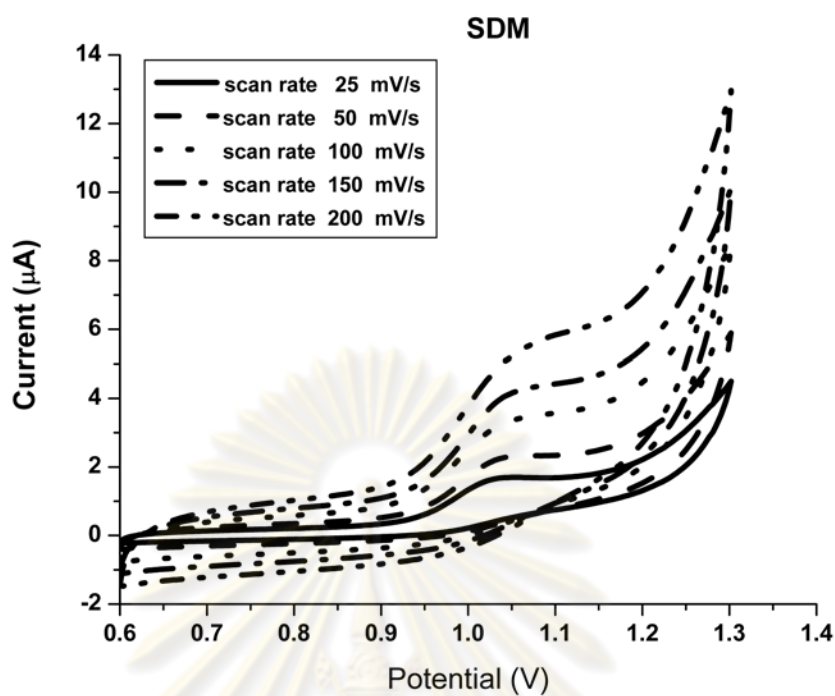


**Figure A6** Cyclic voltammogram of 0.1 mM SDM in phosphate buffer solution (pH 3) at the GC electrode. The scan rate was from 25 to 200  $\text{mV s}^{-1}$ .

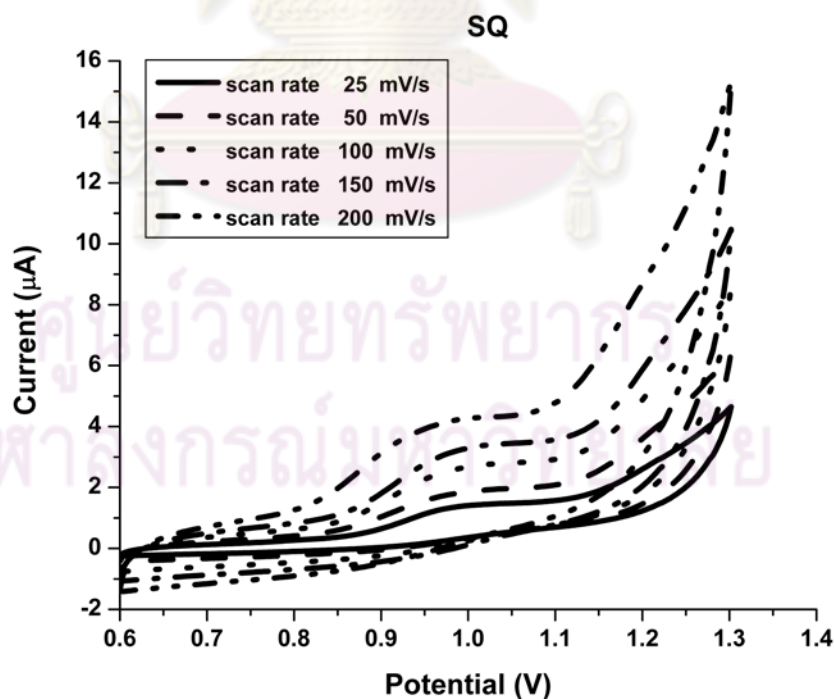


**Figure A7** Cyclic voltammogram of 0.1 mM SQ in phosphate buffer solution (pH 3) at the GC electrode. The scan rate was from 25 to 200  $\text{mV s}^{-1}$ .

**Table A1** Linear equation of relation between current response and scan rate at GC electrode of 0.1 mM SAs

Analyte	Linear equation <sup>a</sup> of relation between current and scan rate	R <sup>2</sup>
SG	$y = 0.1453x + 0.0989$	0.9879
SDZ	$y = 0.1870x + 0.2459$	0.9834
SMZ	$y = 0.1473x + 0.0904$	0.9890
SMM	$y = 0.1512x + 0.2636$	0.9849
SMX	$y = 0.3016x - 0.3256$	0.9978
SDM	$y = 0.2065x + 0.0790$	0.9849
SQ	$y = 0.1390x + 0.1749$	0.9964

<sup>a</sup> y is current response and x is concentration of SA

ศูนย์วิทยทรัพยากร  
จุฬาลงกรณ์มหาวิทยาลัย

## APPENDIX B

## Results for various volume of methanol in elute step of solid-phase extraction

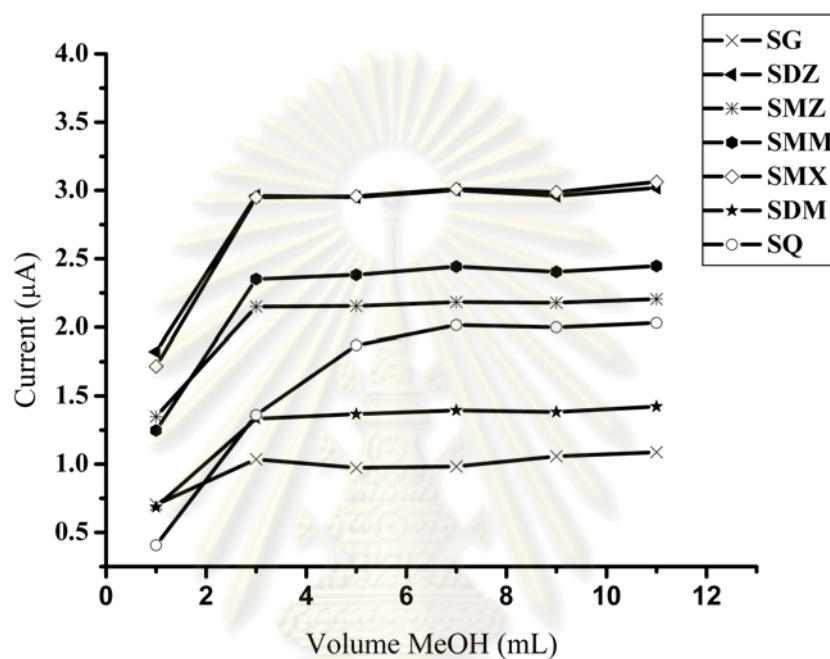


**Figure B1** Volume of methanol in elute step by using  $10 \mu\text{g mL}^{-1}$  seven standard mixture of SA for loading step at Oasis HLB SPE

ศูนย์วิทยทรัพยากร  
จุฬาลงกรณ์มหาวิทยาลัย

## APPENDIX C

### Precision and Accuracy

**Table C1** Acceptable RSD values according to AOAC International

Analyte %	Analyte ratio	Unit	RSD (%)
100	1	100%	1.3
10	10-1	10%	2.8
1	10-2	1%	2.7
0.1	10-3	0.1 %	3.7
0.01	10-4	100 ppm	5.3
0.001	10-5	10 ppm	7.3
0.0001	10-6	1 ppm	11
0.00001	10-7	100 ppb	15
0.000001	10-8	10 ppb	21
0.0000001	10-9	1 ppb	30

**Table C2** Acceptable recovery percentages as a function of the analyte concentration

Analyte %	Analyte ratio	Unit	Mean recovery (%)
100	1	100%	98-102
10	10-1	10%	98-102
1	10-2	1%	97-103
0.1	10-3	0.1 %	95-105
0.01	10-4	100 ppm	90-107
0.001	10-5	10 ppm	80-110
0.0001	10-6	1 ppm	80-110
0.00001	10-7	100 ppb	80-110
0.000001	10-8	10 ppb	60-115
0.0000001	10-9	1 ppb	40-120

## VITAE

**NAME** : Miss Haruthai Sangjarusvichai  
**ADDRESS** : 220 Moo 5, Thamakham, Amphur Muang, Saengchuto  
Road, Kanchanaburi 71000  
**E-mail** : [turtle\\_winner@hotmail.com](mailto:turtle_winner@hotmail.com)

### PERSONAL INFORMATION

Date of Birth: October 2, 1983                      Race: Thai  
Nationality: Thai                                      Religion: Buddhism  
Domicile/Habitation: Kanchanaburi

### EDUCATION

2006 – 2009 : Chulalongkorn University  
Master of Science Program in Analytical Chemistry  
2002 – 2005 : Suan Sunandha Rajabhat University  
Bachelor of Science Program in Chemistry (Second class honour)  
1999 – 2001 : Kanjananukroh School, Thailand, High School

### PUBLICATION

February, 2009 “Rapid separation and highly sensitive detection methodology for sulfonamides in shrimp using a monolithic column coupled with BDD amperometric detection” accepted in Talanta.